ON PERFORMANCE OF PI CONTROLLERS DESIGNED FOR A COUPLED TANKS SYSTEM WITH UNCERTAIN TIME-VARYING TIME-DELAY

Adham ALBANNA

MASTER DEGREE Thesis

Department of Electrical and Electronic Engineering

Programme in Control Systems

Supervisor: Assist. Prof. Dr Hakkı Ulaş ÜNAL

Eskişehir

Eskişehir Technical University

Institute of Graduate Programs

August 2021

ABSTRACT

ON PERFORMANCE OF PI CONTROLLERS DESIGNED FOR A COUPLED TANKS SYSTEM WITH UNCERTAIN TIME-VARYING TIME-DELAY

Adham ALBANNA

Department of Electrical and Electronic Engineering

Program in Control Systems

Eskişehir Technical University, Institute of Graduate Programs, August 2021

Supervisor: Assist. Prof. Dr Hakkı Ulaş ÜNAL

PI controllers are widely used in numerous process control applications in industry because of its simplicity and providing satisfactory performance. This performance may degrade if delays in the process dynamics are not taken into account. Since delays in process control applications may not be measured previously and they may vary during the process, designed PI controller should be robust in presence of uncertain time-varying time-delays. There exist numerous PI controller design approaches for systems having uncertain delays, however, in most of these approaches they are assumed to be time-invariant.

In this thesis, a sufficient condition is given for the presence of a controller which stabilizes the given feedback system against the uncertain time-varying time-delays. Then, by utilizing this condition, a robust PI controller design technique for a coupled tanks, whose input is subjecting to uncertain time-varying time-delay, is presented. In addition, Smith-Predictor and delay-based PI controller design techniques are proposed for the same system. Then, in order to examine the effect of uncertain time-varying time-delays in performance of these controllers, several simulation studies are done for the considered coupled tanks system.

Keywords: Uncertain time-varying time-delays, PI controller, Smith predictor.

ÖZET

ZAMAN İLE DEĞİŞEN BELİRSİZ ZAMAN GECİKMELİ BAGLI TANKLAR SİSTEMİNDEKİ PI DENETLEYİCİLERİN PERFORMANSI

Adham ALBANNA

Elektrik ve Elektronik Mühendisliği Anabilim Dalı

Kontrol Kumanda Sistem Bilim Dalı

Eskişehir Teknik Üniversitesi, Lisansüstü Eğitim Enstitüsü, Ağustos 2021

Danışman: Dr. Öğr. Üyesi Hakkı Ulaş ÜNAL

Endustrideki süreç denetimi uygulamalarının birçoğunda basit ve tatmin edici performans gösteren oransal integrator (PI) denetleyiciler kullanılmaktadır. Fakat, süreç içinde var olan zaman gecikmeleri denetleyici tasarımda ihmal edilirse, tasarlanan denetleyicinin performansı bozulabilir. Zaman gecikmeleri süreç başlamadan önce belirlenemeyebilir ve süreç boyunca değişiklik gösterebilir. Dolayısıyla, tasarlanacak PI denetleyicilerin zaman ile değişen belirsiz zaman gecikmelerine karşılık dayanıklı olması gerekir. Belirsiz zaman-gecikmeli sistemler için literatürde oldukça fazla çalışma bulunmaktadır, fakat bu çalışmaların çoğunda zaman ile değişmeyen belirsiz zaman gecikmeleri ele alınmıştır.

Bu tezde, bir geri-besleme sistemi, sistemdeki zaman ile değişen belirsiz zaman gecikmelerine karşı kararlı kılacak bir denetleyicinin varlığı için yeterli koşul sunulmuştur. Bu koşulları kullanarak, girişi zaman ile değişen belirsiz zaman gecikmesine maruz kalan bağıl tanklar sistemi için dayanıklı PI denetleyici tasarım tekniği verilmiştir. Ayrıca aynı sistem için Smith-Predictor ve zaman-gecikmeli PI denetleyici tasarımları da verilmiştir. Ardından, zaman ile değişen zaman-gecikmelerinin bu denetleyicilerin performansına etkisini anlamak için çeşitli bağıl tank sistemlerini ele alarak benzetim çalışmaları yapılmıştır.

Anahtar Sözcükler: Değişen belirsiz zaman gecikmeleri, PI kontrolör, Smith öngörücü..

ACKNOWLEDGEMENTS

I would like to thank my supervisor, Assist. Prof. Dr. Hakkı Ulaş ÜNAL for providing guidance and feedback throughout working on this thesis. Thanks also to my family for helping me to pass the difficult situations throughout studying. Also I am thankful to my friends who motivated me and supported me when it was required. This thesis has been supported by the project 19ADP057 which is approved by the SRP Committee

.

Adham ALBANNA

31/08/2021

STATEMENT OF COMPLIANCE WITH ETHICAL PRINCIPLES AND RULES

I hereby truthfully declare that this thesis is an original work prepared by me; that I have behaved in accordance with the scientific ethical principles and rules throughout the stages of preparation, data collection, analysis and presentation of my work; that I have cited the sources of all the data and information that could be obtained within the scope of this study, and included these sources in the references section; and that this study has been scanned for plagiarism with "scientific plagiarism detection program" used by Eskişehir Technical University, and that "it does not have any plagiarism" whatsoever. I also declare that, if a case contrary to my declaration is detected in my work at any time, I hereby express my consent to all the ethical and legal consequences that are involved.

Adham ALBANNA

CONTENTS

Page

HEADER PAGE .... İ

FINAL APPROVAL FOR THESIS .... İİ

ABSTRACT .... İİİ

ÖZET .... İV

ACKNOWLEDGEMENTS V

STATEMENT OF COMPLIANCE WITH ETHICAL PRINCIPLES AND RULES .... Vİ

CONTENTS .... Vİİ

LIST OF TABLES .... İX

LIST OF FIGURES ....ERROR! BOOKMARK NOT DEFINED.

1. INTRODUCTION 1

2. MATHEMATICAL MODEL OF THE COUPLED TANK WITH UNCERTAIN TIME-VARYING TIME-DELAY. 3

2.1 Mathematical Model 4

2.2. Dynamic model linearization 7

3. $\mathcal{H}\infty$ CONTROLLER DESIGN FOR SISO SYSTEMS WITH UNCERTAIN-TIME-VARYING-DELAY 13

4. CONTROLLER DESIGN AND SIMULATIONS 19

4.1 PI controller design approach for a nominal plant 20

4.2 Smith-Predictor -based PI controller 24

4.3 Delay-(nominal) based PI controller 37

4.4 Robust PI controller 50

5. CONCLUSION 65

REFERENCES 66

APPENDIX 70

LIST OF TABLES

Page

Table 2.1. The values of variables of Coupled Tanks system [29]. 12
Table 4.1. Design Parameter where b=2. 51

LIST OF FIGURES

Page

Figure 2.1. A schematic representation of the model 3
Figure 2.2. The input and output mass in a tank 4
Figure 3.1. The feedback system of an actual plant 14
Figure 3.2. Uncertainty representation 14
Figure 3.3. Uncertain part 15
Figure 3.4. Input Multiplicative Uncertainty Repsentation. 18
Figure 4.1. The set of K_p and K_i ensuring design objectives (see Code 4.1) ... 19
Figure 4.2. Simulation result for (Kp, Ki) = (0.63, 0.04) and $\tau(t) = 0$ 19
Figure 4.3. Simulation result for (Kp, Ki) = (0.63, 0.04) and $\tau(t) = 12$ 20
Figure 4.4. Simulation result for (Kp, Ki) = (0.63, 0.04) and $\tau(t) = 12 + 10$ 21
Figure 4.5. Simulation result for (Kp, Ki) = (0.63, 0.04) and $\tau(t) = 12 + 10\sin(2\pi/400t)$ 21
Figure 4.6. Simulation result for (Kp, Ki) = (0.63, 0.04) and $\tau(t) = 12 + 10\sin(2\pi 2/00t)$ 21
Figure 4.7. Simulation result for (Kp, Ki) = (0.63, 0.04) and $\tau(t) = 12 + 10\sin(2\pi/10t)$ 22
Figure 4.8. Simulation result for (Kp, Ki) = (0.63, 0.04) and $\tau(t) = 12 + 10\sin(2\pi t)$ 22
Figure 4.9. Simulation result for (Kp, Ki) = (0.63, 0.04) and $\tau(t) = 12 + 5\sin(2\pi/400t)$ 22
Figure 4.10. Simulation result for (Kp, Ki) = (0.63, 0.04) and $\tau(t) = 12 + 5\sin(2\pi/200t)$ 23
Figure 4.11. Simulation result for (Kp, Ki) = (0.63, 0.04) and $\tau(t) = 12 + 5\sin(2\pi/10t)$ 23
Figure 4.12. Simulation result for (Kp, Ki) = (0.63, 0.04) and $\tau(t) = 12 + 5\sin(2\pi t)$ 23
Figure 4.14. Simulation result for (Kp, Ki) = (0.63, 0.04) and h = 1 25
Figure 4.15. Simulation result for (Kp, Ki) = (0.63, 0.04) and h = 15 25
Figure 4.16. Simulation result for (Kp, Ki) = (0.63, 0.04) and h = 23.5 25
Figure 4.17. Simulation result for (Kp, Ki) = (0.63, 0.04) and h = 50. 26
Figure 4.18. Simulation result for (Kp, Ki) = (0.63, 0.04) and $\tau(t) = 12$ 26

Figure 4.19. Simulation result for (Kp, Ki) = (0.63, 0.04) and $\tau(t) = 12 + 5$...26
Figure 4.20. Simulation result for (Kp, Ki) = (0.63, 0.04) and $\tau(t) = 12 + 10$.27
Figure 4.21. Simulation result for (Kp, Ki) = (0.63, 0.04) and $\tau(t) = 12 + 5 + 5\sin(2\pi/200t)$ ...27
Figure 4.22. Simulation result for (Kp, Ki) = (0.63, 0.04) and $\tau(t) = 12 + 5 + 5\sin(2\pi t)$ ...27
Figure 4.23. Simulation result for (Kp, Ki) = (0.63, 0.04) and $\tau(t) = 12 + 10\sin(2\pi/200t)$ ...28
Figure 4.24. Simulation result for (Kp, Ki) = (0.63, 0.04) and $\tau(t) = 12 + 5\sin(2\pi/200t)$ ...28
Figure 4.25. Simulation result for (Kp, Ki) = (0.63, 0.04) and $\tau(t) = 12 + 5\sin(2\pi/10t)$...28
Figure 4.26. Simulation result for (Kp, Ki) = (0.63, 0.04) and $\tau(t) = 12 + 5\sin(2\pi t)$...29
Figure 4.27. Simulation result for (Kp, Ki) = (0.63, 0.04) and $\tau(t) = 30$...29
Figure 4.28. Simulation result for (Kp, Ki) = (0.63, 0.04) and $\tau(t) = 30 + 5$...29
Figure 4.29. Simulation result for (Kp, Ki) = (0.63, 0.04) and $\tau(t) = 30 + 10$.30
Figure 4.30. Simulation result for (Kp, Ki) = (0.63, 0.04) and $\tau(t) = 30 + 10 + 10\sin(2\pi/400t)$ ...30
Figure 4.31. Simulation result for (Kp, Ki) = (0.63, 0.04) and $\tau(t) = 30 + 10 + 10\sin(2\pi/200t)$ ...30
Figure 4.32. Simulation result for (Kp, Ki) = (0.63, 0.04) and $\tau(t) = 30 + 10 + 10\sin(2\pi/10t)$ ...31
Figure 4.33. Simulation result for (Kp, Ki) = (0.63, 0.04) and $\tau(t) = 30 + 10 + 10\sin(2\pi t)$...31
Figure 4.34. Simulation result for (Kp, Ki) = (0.63, 0.04) and $\tau(t) = 30 + 5 + 10\sin(2\pi/200t)$ ...31
Figure 4.35. Simulation result for (Kp, Ki) = (0.63, 0.04) and $\tau(t) = 30 + 5 + 10\sin(2\pi/10t)$ ...32
Figure 4.36. Simulation result for (Kp, Ki) = (0.63, 0.04) and $\tau(t) = 30 + 5 + 10\sin(2\pi t)$...32

Figure 4.37. Simulation result for (Kp, Ki) = (0.63, 0.04) and $\tau(t) = 30 + 10\sin(2\pi/200t)$ 32
Figure 4.38. Simulation result for (Kp, Ki) = (0.63, 0.04) and $\tau(t) = 30 + 10\sin(2\pi/10t)$ 33
Figure 4.39. Simulation result for (Kp, Ki) = (0.63, 0.04) and $\tau(t) = 30 + 10\sin(2\pi t)$ 33
Figure 4.40. Simulation result for (Kp, Ki) = (0.63, 0.04) and $\tau(t) = 30 + 5in(2\pi/200t)$ 33
Figure 4.41. Simulation result for (Kp, Ki) = (0.63, 0.04) and $\tau(t) = 30 + 5\sin(2\pi/10t)$ 34
Figure 4.42. Simulation result for (Kp, Ki) = (0.63, 0.04) and $\tau(t) = 30 + 5\sin(2\pi t)$ 34
Figure 4.43. Simulation result for (Kp, Ki) = (0.63, 0.04) and $\tau(t) = 30 + 5 + 5\sin(2\pi/400t)$ 34
Figure 4.44. Simulation result for (Kp, Ki) = (0.63, 0.04) and $\tau(t) = 30 + 5 + 5\sin(2\pi/200t)$ 35
Figure 4.45. Simulation result for (Kp, Ki) = (0.63, 0.04) and $\tau(t) = 30 + 5 + 5\sin(2\pi/10t)$ 35
Figure 4.46. Simulation result for (Kp, Ki) = (0.63, 0.04) and $\tau(t) = 30 + 5 + 5\sin(2\pi t)$. 35
Figure 4.47. The set of K_p and K_i ensuring design objectives for h=20 and ensures Q4. 37
Figure 4.48. The set of K_p and K_i ensuring design objectives for h=30 and ensures Q4. 37
Figure 4.49. Simulation results for (Kp, Ki) = (0.3, 0.009) and $\tau(t) = 12$ 37
Figure 4.50. Simulation results for (Kp, Ki) = (0.3, 0.009) and $\tau(t) = 12 + 5$ 38
Figure 4.51. Simulation results for (Kp, Ki) = (0.3, 0.009) and $\tau(t) = 12 + 10$ 38
Figure 4.52. Simulation results for (Kp, Ki) = (0.3, 0.009) and $\tau(t) = 12 + 5 + 5\sin(2\pi/400t)$ 38
Figure 4.53. Simulation results for (Kp, Ki) = (0.3, 0.009) and $\tau(t) = 12 + 5 + 5\sin(2\pi/10t)$ 39

Figure 4.54. Simulation results for (Kp, Ki) = (0.3, 0.009) and $\tau(t) = 12 + 5 + 5\sin(2\pi t)$ 39
Figure 4.55. Simulation results for (Kp, Ki) = (0.3, 0.009) and $\tau(t) = 12 + 10\sin(2\pi/400t)$ 39
Figure 4.56. Simulation results for (Kp, Ki) = (0.3, 0.009) and $\tau(t) = 12 + 10\sin(2\pi/200t)$ 40
Figure 4.57. Simulation results for (Kp, Ki) = (0.3, 0.009) and $\tau(t) = 12 + 10\sin(2\pi/10t)$ 40
Figure 4.58. Simulation results for (Kp, Ki) = (0.3, 0.009) and $\tau(t) = 12 + 10\sin(2\pi t)$ 40
Figure 4.59. Simulation results for (Kp, Ki) = (0.3, 0.009) and $\tau(t) = 12 + 5\sin(2\pi/400t)$ 41
Figure 4.60. Simulation results for $(\mathrm{Kp}, \mathrm{Ki}) = (0.3, 0.009)$ and $\tau(t) = 12 + 5\sin(2\pi/200t)$ 41
Figure 4.61. Simulation results for (Kp, Ki) = (0.3, 0.009) and $\tau(t) = 12 + 5\sin(2\pi/10t)$ 41
Figure 4.62. Simulation results for (Kp, Ki) = $(0.3, 0.006)$ and $\tau(t) = 30$ 42
Figure 4.63. Simulation results for $(\mathrm{Kp}, \mathrm{Ki}) = (0.3, 0.006)$ and $\tau(t) = 30 + 5$ 42
Figure 4.64. Simulation results for (Kp, Ki) = $(0.3, 0.006)$and $\tau(t) = 30 + 10$ 42
Figure 4.65. Simulation results for $(\mathrm{Kp}, \mathrm{Ki}) = (0.3, 0.006)$ and $\tau(t) = 30 + 10 + 10\sin(2\pi/400t)$ 43
Figure 4.66. Simulation results for $(\mathrm{Kp}, \mathrm{Ki}) = (0.3, 0.006)$ and $\tau(t) = 30 + 10 + 10\sin(2\pi/200t)$ 43
Figure 4.67. Simulation results for (Kp, Ki) = $(0.3, 0.006)$ and $\tau(t) = 30 + 10 + 10\sin(2\pi/10t)$ 43
Figure 4.68. Simulation results for (Kp, Ki) = $(0.3, 0.006)$ and $\tau(t) = 30 + 10 + 10\sin(2\pi t)$ 44
Figure 4.69. Simulation results for (Kp, Ki) = $(0.3, 0.006)$ and $\tau(t) = 30 + 5 + 10\sin(2\pi/400t)$ 44

Figure 4.70. Simulation results for (Kp, Ki) = $(0.3, 0.006)$ and $\tau(t) = 30 + 5 + 10\sin(2\pi/200t)$ 44
Figure 4.71. Simulation results for (Kp, Ki) = $(0.3, 0.006)$ and $\tau(t) = 30 + 5 + 10\sin(2\pi/10t)$ 45
Figure 4.72. Simulation results for (Kp, Ki) = $(0.3, 0.006)$ and $\tau(t) = 30 + 5 + 10\sin(2\pi t)$....45
Figure 4.73. Simulation results for (Kp, Ki) = $0.3, 0.006$ and $\tau(t) = 30 + 10\sin(2\pi/400t)$ 45
Figure 4.74. Simulation results for (Kp, Ki) $0.3, 0.006$ and $\tau(t) = 30 + 10\sin(2\pi/200t)$ 46
Figure 4.75. Simulation results for (Kp, Ki) = $(0.3, 0.006)$and $\tau(t) = 30 + 10\sin(2\pi/10t)$ 46
Figure 4.76. Simulation results for (Kp, Ki) = $0.3, 0.006$ and $\tau(t) = 30 + 10\sin(2\pi t)$....46
Figure 4.77. Simulation results for (Kp, Ki) = $(0.3, 0.006)$ and $\tau(t) = 30 + 5\sin(2\pi/400t)$ 47
Figure 4.78. Simulation results for (Kp, Ki) = $(0.3, 0.006)$ and $\tau(t) = 30 + 5\sin(2\pi/200t)$ 47
Figure 4.79. Simulation results for (Kp, Ki) = $(0.3, 0.006)$ and $\tau(t) = 30 + 5\sin(2\pi/10t)$....47
Figure 4.80. Simulation results for (Kp, Ki) = $(0.3, 0.006)$ and $\tau(t) = 30 + 5\sin(2\pi t)$ 48
Figure 4.81. Simulation results for (Kp, Ki) = $(0.3, 0.006)$ and $\tau(t) = 30 + 5 + 5\sin(2\pi/400t)$ 48
Figure 4.82. Simulation results for (Kp, Ki) = $(0.3, 0.006)$ and $\tau(t) = 30 + 5 + 5\sin(2\pi/200t)$ 48
Figure 4.83. Simulation results for (Kp, Ki) = $(0.3, 0.006)$ and $\tau(t) = 30 + 5 + 5\sin(2\pi/10t)$....49
Figure 4.84. Simulation results for (Kp, Ki) = $(0.3, 0.006)$ and $\tau(t) = 30 + 5 + 5\sin(2\pi t)$ 49
Figure 4.85. The set of K_p and K_i ensuring design objectives for case 1 and case 2,....51

Figure 4.86. The set of K_p and K_i ensuring design objectives for case 3, ...51
Figure 4.87. The set of K_p and K_i ensuring design objectives for case 4, ...51
Figure 4.88. Simulation results for $\tau(t) = 10 + 1/8 + 7/8 \sin(2\pi 200t)$...........52
Figure 4.89. Simulation results for $\tau(t) = 10 + 1/8 + 7/8 \sin(2\pi/10t)$...........52
Figure 4.90. Simulation results for $\tau(t) = 10 + 5$ 52
Figure 4.91. Simulation results for $\tau(t) = 10 + 5/2 + 5/2 \sin(2\pi/40t)$...........53
Figure 4.92. Simulation results for $\tau(t) = 10 + 5/2 + 5/2 \sin(2\pi/200t)$.........53
Figure 4.93. Simulation results for $\tau(t) = 10 + 1/8 + 368 \sin(2\pi/200t)$ 53
Figure 4.94. Simulation results for $\tau(t) = 10 + 1/8 + 36/8 \sin(2\pi/40t)$.........54
Figure 4.95. Simulation results for $\tau(t) = 25 + 5$ 54
Figure 4.96. Simulation results for $\tau(t) = 25 + 5/2 + 5/2 \sin(2\pi/20t)$...........54
Figure 4.97. Simulation results for $\tau(t) = 25 + 5/2 + 5/2 \sin(2\pi/200t)$.........55
Figure 4.98. Simulation results for $\tau(t) = 25 + 1/8 + 36/8 \sin(2\pi/200t)$ 55
Figure 4.99. Simulation results for $\tau(t) = 25 + 1/8 + 36/8 \sin(2\pi/50t)$.........55
Figure 4.100. Simulation results for $\tau(t) = 40 + 10$..56
Figure 4.101. Simulation results for $\tau(t) = 40 + 9 + 1/2 \sin(2\pi/20t)$ 56
Figure 4.102. Simulation results for $\tau(t) = 40 + 9 + 1/2 \sin(2\pi/200t)$...........56
Figure 4.103. Simulation results for $\tau(t) = 40 + 1/8 + 8 \sin(2\pi/200t)$...........57
Figure 4.104. Simulation results for $\tau(t) = 40 + 1/8 + 8 \sin(2\pi 40t)$ 57
Figure 4.105. Simulation results for $\tau t(t) = 10 + 1/8 + 78 \sin(2\pi/200t)$ 58
Figure 4.106. Simulation results for $\tau(t) = 10 + 1/8 + 7/8 \sin(2\pi/10t)$.........58
Figure 4.107. Simulation results for $\tau(t) = 10 + 5$ 58
Figure 4.108. Simulation results for $\tau(t) = 10 + 5/2 + 5/2 \sin(2\pi/40t)$.........59
Figure 4.109. Simulation results for $\tau(t) = 10 + 5/2 + 5/2 \sin(2\pi/200t)$.......59
Figure 4.110. Simulation results for $\tau(t) = 10 + 1/8 + 36/8 \sin(2\pi/200t)$ 59
Figure 4.111. Simulation results for $\tau(t) = 10 + 1/8 + 36/8 \sin(2\pi/40t)$.......60
Figure 4.112. Simulation results for $\tau(t) = 25 + 5$ 60
Figure 4.113. Simulation results for $\tau(t) = 25 + 5/2 + 5/2 \sin(2\pi/20t)$.........60
Figure 4.114. Simulation results for $\tau(t) = 25 + 5/2 + 5/2 \sin(2\pi/200t)$.......61
Figure 4.115. Simulation results for $\tau(t) = 25 + 1/8 + 36/8 \sin(2\pi/200t)$ 61
Figure 4.116. Simulation results for $\tau(t) = 25 + 1/8 + 36/8 \sin(2\pi/50t)$.......61
Figure 4.117. Simulation results for $\tau(t) = 40 + 10$..62

Figure 4.118. Simulation results for $\tau(t) = 40 + 9 + 1/2\sin(2\pi/20t)$ 62
Figure 4.119. Simulation results for $\tau(t) = 40 + 9 + 1/2\sin(2\pi/200t)$ 62
Figure 4.120. Simulation results for $\tau(t) = 40 + 1/8 + 8\sin(2\pi/200t)$ 63
Figure 4.121. Simulation results for $\tau(t) = 40 + 1/8 + 8\sin(2\pi/40t)$ 63

1. INTRODUCTION

A time-delay system is common in various engineering processes. It is typically used in biological processes, chemical processes, and mechanical systems [30, 32]. The occurrence of delays is considered to be one of the major causes of system instability and degradation. Dealing with delays in a control system is a difficult and long-standing problem because systems with time delays are in a class of infinite-dimensional systems [31]. In addition, delay may result in unexpected behavior, such as small delays may yield unstable behavior in some systems whereas large delays may require to stabilize some certain systems [32]. Due to the presence of such complex behaviors, delays should be taken into account while we model a dynamic system. Note, due to the discrepancy with the actual physical system and its mathematical model, which is to be used to design controller satisfying design objectives, it is more realistic to consider the delay as uncertain time-varying time-delay.

In order to design a controller, which stabilizes the physical plant and meets the design specifications against uncertainties, robust control tools can be used. H^{∞} control is one of the powerful robust control methods, since it utilizes the magnitude of the plant uncertainties in a proper way by the small-gain theorem which verifies the internal stability of the feedback interconnected stable causal systems [33]. For designing a stabilizing controller for a system with uncertain delay, one of the approaches is to take the known nominal time-delay outside the generalized plant [13, 14]. Therefore, if there exists uncertainty in the actual time-delay, then, it will be seen in the uncertainty block of the generalized framework. However in this case, the uncertainty block may become non-causal and the small-gain theorem, may not be used. So, since the H^{∞} controller design is based on the small-gain theorem, the stabilizing H^{∞} controller cannot be designed unless uncertainty block is made causal by introducing some constraints on the uncertain part of the actual time-delays [4, 23, 24].

In this work, we will consider the performance of various PI controllers designed for level control of a coupled tanks, where their inputs subjecting uncertain time-delays. Level control is one of the design objectives in many process control applications which includes coupled tanks such as food processing, water purification, and etc [5, 18, 19]. In order to keep the liquid level in a tank around the desired level, PI controllers are often preferred because of their simplicity and ensuring satisfactory performance [2, 3]. There exist numerous delay-based PI controller design approaches proposed in the literature, see, for instance, [7, 11, 16] and references therein. In most of these works time- delays are assumed to be time-invariant, however, from the practical point of view, it may be better to design PI controllers in presence of uncertain time-varying time-delays. In order to achieve this, H^∞ based PI controller design will be considered. In order to understand the effect of uncertain time-varying time-delays, we will compare the performance of the controller designed by the proposed approach with two different controllers. One of these controllers is classical Smith-predictor based PI-controller and the second one is delay-based PI controller, which is obtained by searching a PI parameter set, which stabilizes the feedback system and guarantee the design objectives for a given fixed-delay. In fact, it is expected to obtain better performance from the H^∞-based controller, however, due to the conservativeness of H^∞-controller design approach, such a comparison may give us interesting results. In addition, the plant to be considered is non-linear whereas the controller design approaches are proposed for linear system. Furthermore, the input of the physical system is restricted to be positive. Hence, performance comparison is also meaningful from the practical point of view [20, 26].

Our coupled tanks plant is a two-tank module consisting of a pump with a water basin and two tanks. Due to the transportation phenomena, the pump does not provide water to the tanks whenever a voltage applied to it, therefore, there exists a dead-time in the dynamics of the coupled tanks. In addition, the pump is bidirectional, hence, it pushes liquid to the tanks if the applied voltage is non-negative.

In Chapter 2, we are going to describe our coupled tanks system and explain the mathematical modeling for the system. in Chapter 3, we will present the uncertainty representation of the actual plant. In Chapter 4, considered PI controller design approaches will be explained and simulation works will be presented.

2. MATHEMATICAL MODEL OF THE COUPLED TANK WITH UNCERTAIN TIME-VARYING TIME-DELAY.

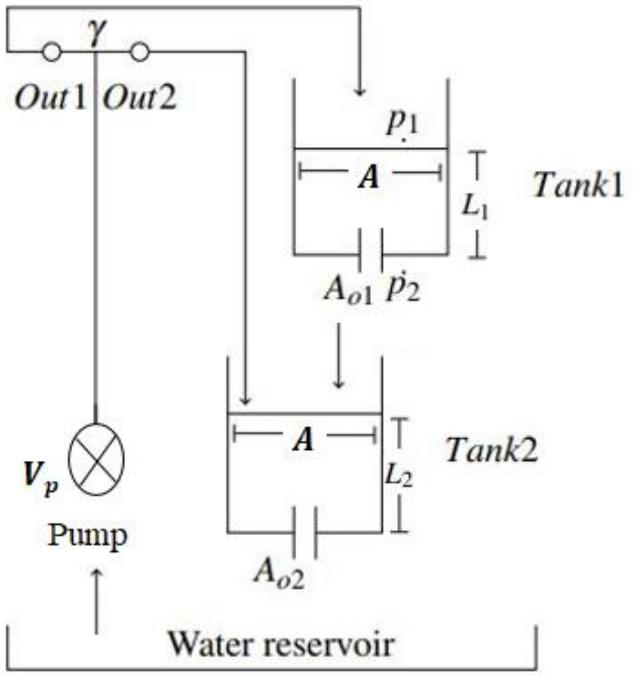

Figure 2.1. *A schematic representation of the model*

Consider a schematic representation of coupled tanks system which is given in Figure 2.1. It is consisted of two tanks and a pump with a water basin. The two tanks are constructed in the way such that the flow from Tank 1 can flow through an outlet orifice located at the bottom of the tank into the Tank 2. The outlet orifice of the Tank 2 flows to the main water reservoir below. The pump thrusts water vertically to two quick-connect orifices Out1 and Out2, such that in Figure 2.1, one of them feeds Tank 1 and the other feeds Tank 2. The water levels in the two tanks assumed to be measured by pressure sensors and available for feedback. In the figure, L_1 (cm) corresponds to the water level in Tank 1, L_2 (cm) corresponds to the water level in Tank 2, $A(cm^2)$ corresponds to the cross sectional of the two tanks, V_p (V) corresponds to the applied voltage to the pump, A_{o1} (cm^2) is the area of output orifice of Tank 1, A_{o2} $(cm^2)$is the area of output orifice of Tank 2, p_1 and p_2 are a virtual points to be used in Bernoulli's law latter, and γ is the valve position, whereas our valve has two out orifices which distribute the water to the tanks and the valve position depends on these out orifices and its value between 0 and 1.

2.1 Mathematical Model

In order to explain the modelling of a coupled tank let us consider the system shown in Figure 2.2. In the figure, respectively, $m_{in}(t)$ and $m_{out}(t)$ are the inflow and output flow rates of a liquid in a given tank. The mass balance principle tells us that if we have a tank contains a liquid, then the change of the total accumulated mass m_t in this tank equal the difference between input mass flow rate $\dot{m}_{in}$ and output mass flow rate $\dot{m}_{out}$ in the same tank as in Figure 2.2 [6]. Then, rate of change of mass in the tank boundaries can be written as

$$\frac{dm_t(t)}{dt} = \dot{m}_{in}(t) - \dot{m}_{out}(t), \tag{1}$$

The input and output mass flow rates in the tank shown in Figure 2.2 depend on the liquid density say ρ, and the volumetric inflow and outflow rates in this tank. Since the total accumulated mass in this tank shown as m_t is represented as the multiplication between the volume V and liquid density ρ, at the same tank [6]. Therefore

$$\dot{m}_{in}(t) = \rho F_{in}(t),$$

$$\dot{m}_{out}(t) = \rho F_{out}(t),$$

$$\frac{dm_t(t)}{dt} = \rho \frac{dV(t)}{dt},$$

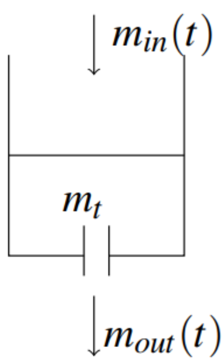

Figure 2.2. *The input and output mass in a tank*

where F_{in} and F_{out} are the volumetric inflow and outflow rates respectively. Then equation (1) can be written as

$$\frac{dV(t)}{dt} = F_{in}(t) - F_{out}(t).$$

We know that the volume V equal height of the tank times cross sectional area. By applying the mass balance principle to the water level on our coupled tanks system, the equation of motion (EOM) of Tank 1 and Tank 2 can be written as

$$A\frac{dL_1(t)}{dt} = F_{in1}(t) - F_{out1}(t),$$

$$A\frac{dL_2(t)}{dt} = F_{in2}(t) - F_{out2}(t),$$

where F_{in1} and F_{out1} are the volumetric inflow and outflow rates corresponding to Tank 1, F_{in2} and F_{out2} are the volumetric inflow and outflow rates rates corresponding to Tank 2, and A (cm^2) is the cross-sectional area of both tanks as shown in Figure 2.1. The volumetric inflow rates in the tanks $F_{in(i)}, i = 1{,}2$ depend on the input voltage supplied to the pump $V_p(t)$, pump constant K_p and the valve's position γ. As shown in Figure 2.1, since we take into account the transmission delay from input of pump to its output, the volumetric inflow rate in Tank 1 can be written as

$$F_{in1}(t) = \gamma K_p V_p(t - \tau(t)), \tag{2}$$

where $\tau(t)$ is the uncertain time-varying time-delay which is applied on the pump that feed Tank1 and Tank 2, therefore, the volumetric infolw rate on Tank 1 and Tank 2 has the same uncertain time-varying time-delay. Since there exists two flows to Tank 2, the volumetric inflow rate to Tank 2 can be written as:

$$F_{in2}(t) = (1-\gamma)K_p V_p\big(t - \tau(t)\big) + F_{out1}(t). \tag{3}$$

In order to obtain volumetric outflow rates of the tanks, one of the ways is to use Bernoulli's law. This law states that the summation of kinetic and potential energy along a streamline is constant [6, 9]. Now, let p_1 be a point on the surface of the water in Tank

1 and v_{p_1} be the velocity of the flowing fluid on this point. Similarly, let p_2 be a point on the bottom of the water in Tank 2 and v_{p_2} be the velocity of the flowing fluid on this point. Note, since the pressure of the water at these points is the air pressure, by Bernoulli's law [18, 22],

$$\frac{v_{p_2}^2}{2} + gL_{p_2} = \frac{v_{p_1}^2}{2} + gL_{p_1}, \tag{4}$$

where L_{p_1} and L_{p_2} are distances of points p_1 and p_2 to the bottom of the basin, respectively, with respect to reference, and g is gravitational acceleration. Note, since the cross sectional area of Tank 1 is much larger than the area of output orifice of the tank that makes the liquid level change on the surface of water is almost stationary, so the kinetic energy is assumed to be zero on the surface of water in Tank 1. Therefore the velocity of the surface of water in Tank 1 v_{p_1} is zero [29],

$$v_{p_2} = v_{o1},$$

where v_{o1} is the outflow velocity for Tank 1. Then, since $L_{p_1} = L_{p_2} + L_1$, from equation (4) it can be shown that

$$g(L_{p_2} + L_1) = \frac{(v_{o1})^2}{2} + gL_{p_2},$$

$$\frac{(v_{o1})^2}{2} = g(L_{p_2} + L_1) - gL_{p_2},$$

$$v_{o1} = \sqrt{2gL_1}. \tag{5}$$

The same for Tank 2:

$$v_{o2} = \sqrt{2gL_2}, \tag{6}$$

where v_{o2} is the outflow velocity for Tank 2. Then volumetric outflow rates of Tank 1 and Tank 2 are given respectively by:

$$F_{out1} = A_{o1}\sqrt{2gL_1}, \tag{7}$$

$$F_{out2} = A_{o2}\sqrt{2gL_2}. \tag{8}$$

Using mass balance equation where constant density is assumed, since the rate of change in liquid level in Tank 1 is given by

$$\frac{dL_1(t)}{dt} = \frac{F_{in1}(t) - F_{out1}(t)}{A}. \tag{9}$$

By substituting (2) and (7) into (9)

$$\frac{dL_1(t)}{dt} = \frac{\gamma K_p V_p(t-\tau(t))}{A} - \frac{A_{o1}\sqrt{2gL_1(t)}}{A}.$$

Similarly, since

$$\frac{dL_2(t)}{dt} = \frac{F_{in2}(t) - F_{out2}(t)}{A}, \tag{10}$$

by substituting (3) and (8) into (10)

$$\frac{dL_2(t)}{dt} = \frac{(1-\gamma) K_p V_p(t-\tau(t))}{A} + \frac{A_{o1}\sqrt{2gL_1(t)}}{A} - \frac{A_{o2}\sqrt{2gL_2(t)}}{A},$$

therefore, the mathematical model of the system can be shown as:

$$\frac{dL_1(t)}{dt} = \frac{\gamma K_p V_p(t-\tau(t))}{A} - \frac{A_{o1}\sqrt{2gL_1(t)}}{A}, \tag{11}$$

$$\frac{dL_2(t)}{dt} = \frac{(1-\gamma) K_p V_p(t-\tau(t))}{A} + \frac{A_{o1}\sqrt{2gL_1(t)}}{A} - \frac{A_{o2}\sqrt{2gL_2(t)}}{A}, \tag{12}$$

where it is assumed that $V_p(t)$, L_1(t) and $L_2(t)$ are assumed to be zero for $t \in (-\max_{t \geq t_0}|\tau(t)|, 0)$.

2.2. Dynamic model linearization

We need to find the delay-free transfer function which will help us to design and implement a level controller for the system. In order to do that we need to linearize our nonlinear dynamic equations given in equations (11, 12) by assuming that $\tau(t) = 0$. As seen in equations (11, 12), the equilibrium points are, L_{10}, which is the desired equilibrium level for Tank 1, $V_{p0,}$ which is the static equilibrium input voltage, which produces the desired level for Tank 1, and L_{20} is the desired equilibrium level for Tank 2 which is produced by L_{10}. Let

$$\Delta_{L_1} = L_1 - L_{10},$$

$$\Delta_{L_2} = L_2 - L_{20,}$$

$$\Delta_{V_p} = V_p - V_{p0},$$

where Δ_{L_1} is the deviation variable between L_1 and L_{10}, and the same for Δ_{L_2} and ΔV_p [22, 1]. We know that the equations of motion for Tank 1 and 2 as follow:

$$\frac{d}{dt} L_1(t) =: f_1\big(V_p(t), L_1(t)\big),$$

$$\frac{d}{dt} L_2(t) =: f_2\left(V_p(t), L_1(t), L_2(t)\right).$$

The obtained linearized equation of motion should be a function of the system's small deviations about its equilibrium point (V_{p0}, L_{10}) for Tank 1, and $(V_{p0}; L_{10}; L_{20})$ for Tank 2. Therefore, based on Taylor series approximation given by the following format [12, 22]:

$$\frac{\partial^2}{\partial V_p \partial L_1} f_1\big(V_p, L_1\big) \cong f_1\big(V_{p0}, L_{10}\big) + \left(\frac{\partial}{\partial V_p} f_1\big(V_p, L_1\big)\right)\big(V_p - V_{p0}\big) + \left(\frac{\partial}{\partial L_1} f_1\big(V_p, L_1\big)\right)(L_1 - L_{10}).$$

Then, from (11)

$$\frac{\partial^2}{\partial V_p \partial L_1} f_1\big(V_p, L_1\big) = \frac{\gamma K_p V_{p0} - A_{o1}\sqrt{2gL_{10}}}{A} + \frac{\gamma K_p}{A}\big(V_p - V_{p0}\big) - \frac{A_{o1}\sqrt{2g}}{2\sqrt{L_{10}}A}(L_1 - L_{10}),$$

we know that the deviation at $L_1 = L_{10}$ is zero it means that:

$$\frac{dL_{10}(t)}{dt} = 0,$$

then

$$\frac{\gamma K_p}{A} V_{p0} - \frac{A_{o1}\sqrt{2gL_{10}}}{A} = 0,$$

then

$$\frac{d\Delta_{L_1}(t)}{dt} = -T_1\Delta_{L_1}(t) + \gamma K_m \Delta_{V_p}(t), \tag{13}$$

where

$$T_1 = \frac{A_{o1}\sqrt{2g}}{2\sqrt{L_{10}}A}, and \;\; K_m = \frac{K_p}{A}.$$

Similarly,

$$\frac{\partial^3}{\partial V_p \partial L_1 \partial L_2} f_2(V_p, L_1, L_2) \cong f_2(V_{p0}, L_{10}, L_{20}) + \left(\frac{\partial}{\partial V_p} f_2(V_p, L_1, L_2)\right)(V_p - V_{p0})$$

$$+ \left(\frac{\partial}{\partial L_1} f_2(V_p, L_1, L_2)\right)(L_1 - L_{10}) + \left(\frac{\partial}{\partial L_2} f_2(V_p, L_1, L_2)\right)$$

$$(L_2 - L_{20}),$$

so the linerized equation for Tank 2 will be:

$$\frac{dL_2(t)}{dt} = \frac{(1-\gamma)K_p V_{p0}}{A} + \frac{A_{o1}\sqrt{2g}L_{10}}{A} - \frac{A_{o2}\sqrt{2g}L_{20}}{A} + \frac{(1-\gamma)K_p}{A}(V_p - V_{p0})$$
$$+ \frac{A_{o1}\sqrt{2g}}{2\sqrt{L_{10}}A}(L_1 - L_{10}) - \frac{A_{o2}\sqrt{2g}}{2\sqrt{L_{20}}A}(L_2 - L_{20}).$$

And it is known that

$$\frac{dL_{20}(t)}{dt} = 0,$$

so we have

$$\frac{(1-\gamma)K_p V_{p0}}{A} + \frac{A_{o1}\sqrt{2g}L_{10}}{A} - \frac{A_{o2}\sqrt{2g}L_{20}}{A} = 0,$$

$$\frac{d\Delta_{L2}(t)}{dt} = T_1\Delta_{L_1}(t) - T_2\Delta_{L_2}(t) + (1-\gamma)K_m\Delta_{V_p}(t), \quad (14)$$

where

$$T_2 = \frac{A_{o2}\sqrt{2g}}{2\sqrt{L_{20}}A}.$$

Now we can find the free delay transfer function between our input V_{p_1} and output L_{21} from the linearized equations (13,14) as follows:

$$\Delta_{L_1}(s) = \frac{\gamma K_m\,\Delta_{V_p}(s)}{(s+T_1)}, \quad (15)$$

$$s\Delta_{L_2}(s) = T_1\Delta_{L_1}(s) - T_2\Delta_{L_2}(s) + (1-\gamma)K_m\,\Delta_{V_p}(s),$$

$$\Delta_{L_2}(s)(s+T_2) = T_1\frac{\gamma K_m\,\Delta_{V_p}(s)}{(s+T_1)} + (1-\gamma)K_m\Delta_{V_p}(s),$$

$$\Delta_{L_2}(s)(s+T_2) = \frac{T_1\gamma K_m\Delta_{V_p}(s) + (s+T_1)(1-\gamma)K_m\Delta_{V_p}(s)}{(s+T_1)},$$

$$\Delta_{L_2}(s) = \frac{T_1\gamma K_m\Delta_{V_p}(s) + (s+T_1)(1-\gamma)K_m\Delta_{V_p}(s)}{(s+T_1)(s+T_2)},$$

$$\Delta_{L_2}(s) = \frac{(T_1+(1-\gamma)s)}{(s+T_1)(s+T_2)}K_m\Delta_{V_p}(s). \quad (16)$$

Now the free delay transfer function for our coupled tanks system will be:

$$P_{\mathrm{o}}(\mathrm{s}) = \frac{\Delta_{L_2}(s)}{\Delta_{V_p}(s)} = \frac{(T_1+(1-\gamma)s)}{(s+T_1)(s+T_2)}K_m. \quad (17)$$

Throughout the thesis, unless otherwise is stated, $P_0(\mathrm{s})$ will be called a nominal plant. Description of the actual model is as shown below. Let O_τ be an operator by τ such that if $u(\mathrm{t}) = O_\tau V_p(t)$, then

$$u(t) = \begin{cases} V_p\big(t-\tau(t)\big), & t-\tau(t) \geq t_0 \\ 0, & t-\tau(t) < t_0 \end{cases}, \ t > t_0. \tag{18}$$

Furthermore, if $\tau(t) = h + \delta(t)$, where h is assumed to be known and non-negative, $\delta(t)$ is uncertain and time-varying. and $\delta(t_0) = 0$, then, $O_\tau = O_h\ O_\delta = O_\delta\ O_h,\ t > t_0$. In addition, it is assumed that $\max\limits_{t \geq t_0}\{-\delta(t)\} \leq \overline{\delta} \leq h$, for some $\overline{\delta} > 0$, and $|\delta(t)| < \hat{\delta}$, $|\dot{\delta}(t)| < \beta$, $t \geq 0$, $\delta(0) = 0$ for some bounds $\hat{\delta} > 0$ and $0 < \beta < 1$. Then,

$$\frac{dL_1(t)}{dt} = -\frac{A_{o1}\sqrt{2gL_1(t)}}{A} + \frac{\gamma K_p}{A}u(t), \tag{19}$$

$$\frac{dL_2(t)}{dt} = \frac{A_{o1}\sqrt{2gL_1(t)}}{A} - \frac{A_{o2}\sqrt{2gL_2(t)}}{A} + \frac{(1-\gamma)K_p}{A}u(t). \tag{20}$$

where

$$u(\mathrm{t}) = O_\tau V_p(t). \tag{21}$$

From physical point of view, since pump is assumed to be unidirectional and the actuator input is bounded

$$0 \leq V_p(t) \leq V_{pmax},\ t > t_0, \tag{22}$$

where V_{pmax} is a some positive number. In addition

$$V_p(t) = 0,\ L_1\ (t) = L_2\ (t) = 0, \quad t \leq t_0. \tag{23}$$

Then, the actual model can be described a set of equations given as in equations (19, 20) under the conditions given in (21, 22, 23).

Table 2.1. The values of variables of Coupled Tanks system [29].

Variable	value	Variable	value
K_p	$4.6\ (\frac{cm^3}{\sec})/Volt$	L_{10}	17.2287(cm)
γ	0.57141	T_1	0.0272
A_{o1}	0.0791 (cm^2)	T_2	0.1094
A_{o2}	0.2424 (cm^2)	K_m	$0.2127(\frac{cm^3}{\sec})/Volt$
g	981 ($\frac{cm}{s}$)	L_{max}	30 (cm)
A	15.5179 (cm^2)	V_{pmax}	12 (V)
L_{20}	10 (cm)		

In order to see the ressults in practice, we will consider the experimental coupled tank of Quanser in [29]. By using the values of the parameters given in Table 2.1, transfer function of the nominal plant is obtained as

$$P_o(s) = \frac{0.127s + 0.008019}{s^2 + 0.1359s + 0.0029}. \tag{24}$$

3. $\mathcal{H}^\infty$ CONTROLLER DESIGN FOR SISO SYSTEMS WITH UNCERTAIN-TIME-VARYING-DELAY

In this section, robust controller design for linear time invariant (LTI) single-input-single-output (SISO). LTI systems whose input or output is subjecting to uncertain time-varying time-delay will be considered. The results of this section will be used to design a PI controller for the system given in Chapter 2. Consider a SISO linear plant Π such that its input is subject to some uncertain time-varying time-delay $\tau(t) = h + \delta(t)$, where h is the assumed to be known and non-negative and $\delta(t)$ is assumed to be uncertain, however, satisfies the following conditions

$$\max_{t \geq t_0}\{-\delta(t)\} \leq \overline{\delta} \leq h,$$

for some $\overline{\delta} > 0$. In addition, $|\delta(t)| < \hat{\delta}$, $|\dot{\delta}(t)| < \beta$, $t \geq 0$, $\delta(0) = 0$ for some bounds $\hat{\delta} > 0$ and $0 < \beta < 1$. Then, $\Pi = P_o O_\tau = P_o O_\delta O_h$, where P_o is a finite-dimensional and LTI nominal plant. $O_h(O_\delta)$ is a delay-operator with respect to h (δ) as described in equation (18). Since the model has some uncertain dynamics, whether it is time-varying or not, these dynamics should be taken into account in case of designing a stabilizing controller for a feedback system given in Figure 3.1. Note, since actual plant can not be modelled perfectly, a set of uncertain plants, which covers the actual plant, should be represented. To model the uncertain part of $P_o O_\delta$ considering the bounds and variations of the uncertain time-varying time-delays, one possible way is to introduce the weighting function $\overline{W}(s)$. As a result, by applying correct weighting functions, we can form the dynamic behavior of the system by imposing certain boundaries on the uncertain parameters, which are dependent on the chosen weighting function, where $\overline{W}(s) := \frac{as+b}{s+c}$, and a, b and c are some positive design parameters [24]. Whereas, we chose positive values for a, b, and c to ensure that $\overline{W}(s)$ and its inverse are stable, avoiding the possibility

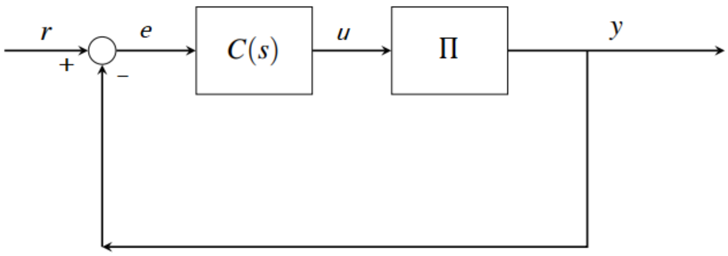

Figure 3.1. *The feedback system of an actual plant*

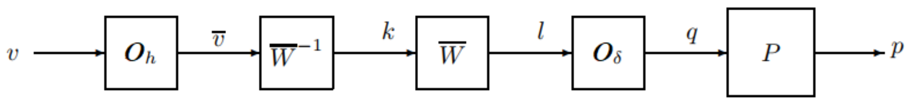

Figure 3.2. *Uncertainty representation*

of unstable zero/pole cancellation. In order to take into account present uncertainties, one of the ways is represent the uncertain model as in Figure 3.2.

From Figure 3.2, state-space representation of the weighting function $\overline{W}$ can be written as

$$\dot{x}(t) = -cx(t) + (b - ac)k(t), \tag{25}$$

$$l(t) = x(t) + ak(t). \tag{26}$$

Then, from Figure 3.2, $q(t) = l(t - \delta(t))$. Note that

$$x(t - \delta(t)) - x(t) = \int_t^{t-\delta(t)} \dot{x}(\zeta)d\zeta, \tag{27}$$

where $x(t) = 0$, $t \in (-\hat{\delta}, 0]$. Therfore from (25, 26)

$$q(t) = x(t) + \int_t^{t-\delta(t)} \dot{x}(\zeta)d\zeta + ak(t - \delta(t)).$$

Then by (27)

$$q(t) = l(t) + \int_t^{t-\delta(t)} \big(-cx(\zeta) + (b - ac)k(\zeta)\big)d\zeta + ak\big(t - \delta(t)\big) - ak(t),$$

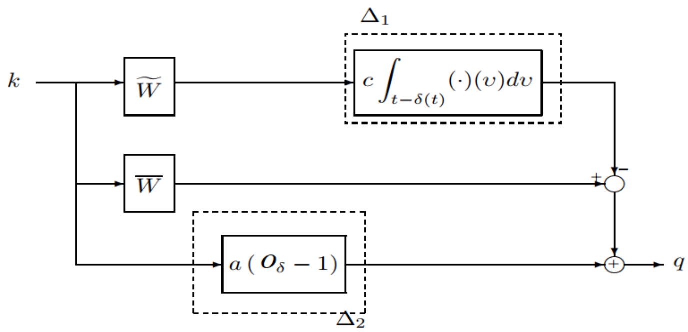

Figure 3.3. *Uncertain part*

$$q(t) = l(t) + \int_{t}^{t-\delta(t)} -cl(\zeta) + bk(\zeta)d\zeta + ak\big(t-\delta(t)\big) - ak(t),$$

$$q(t) = \frac{b}{c}k(t) - r(t) + c\int_{t}^{t-\delta(t)} r(\zeta)d\zeta + ak\big(t-\delta(t)\big) - ak(t),$$

$$q(t) = \tfrac{b}{c}k(t) - r(t) - c\int_{t-\delta(t)}^{t} r(\zeta)d\zeta + ak\big(t-\delta(t)\big) - ak(t). \tag{28}$$

Now let

$$r(t) := \frac{b}{c}k(t) - l(t),$$

$$\widetilde{W}(s) := \frac{s(b+ac)}{c(s+c)},$$

Then, since $r(s) = \widetilde{W}(s)k(s)$, then the mapping from k to q in Figure 3.2 can be shown as in Figure 3.3.

Let

$$v(t) := \int_{t-\delta(t)}^{t} r(v)dv, \tag{29}$$

and $n(t) := |r(t)|$. Then, since

$$|v(t)| \leq \int_{t-\delta(t)}^{t} |r(v)|dv, \tag{30}$$

from equation (29)

$$|v(t)| \leq \begin{cases} |\hat{v}(t)|, & \text{if} \quad \delta(t) \geq 0, \\ |\overline{v}(t)|, & \text{if} \quad \delta(t) \leq 0, \end{cases}$$

where $\hat{v}(t) := \int_{t-\hat{\delta}}^{t} n(v)dv$, and $\overline{v}(t) := \int_{t}^{t+\hat{\delta}} n(v)dv$. By Laplace transformation, since

$$\hat{v}(s) = \frac{e^{\hat{\delta}s}-1}{s} n(s),$$

$$\overline{v}(s) = \frac{e^{-\hat{\delta}s}-1}{s} n(s),$$

then, both

$$\|\hat{v}(t)\|_2 \leq \hat{\delta}\|n(t)\|_2, \tag{31}$$

$$\|\overline{v}(t)\|_2 \leq \hat{\delta}\|n(t)\|_2. \tag{32}$$

Therefore, $\|v(t)\|_2 \leq \hat{\delta}\|n(t)\|_2 = \hat{\delta}\|r(t)\|_2$, since $\int_0^\infty |n(t)|^2 dt = \int_0^\infty |r(t)|^2 dt$. Hence, $\|\Delta_1\|_2 \leq c\hat{\delta}$, where $c = \frac{1}{\sqrt{2}\hat{\delta}}$. Note that same bound also found in [24], however, we let uncertainty block non-causal, which results in less conservative results. To find an upper bound for Δ_2, as in [23, 25], let us define,

$$\lambda := v - \delta(v) =: f(v),$$

$$\frac{d\lambda}{dv} = 1 - \frac{d\delta(v)}{dv} := 1 - g(\lambda).$$

Note, since it is assumed that $\left|\frac{d\delta(v)}{dv}\right| < 1$, therefore, $\frac{df(v)}{dv} > 0$.

The latter inequality implies that $v = f^{-1}(\lambda)$, then, $g(\lambda) = \left|\frac{d\delta(v)}{dv}\right|_{v=f^{-1}}(\lambda)$. Therefore if $d(t) := \emptyset(t - \delta(t))$ then,

$$\int_0^\infty |d(t)|^2 dt = \int_0^\infty |\emptyset(t-\delta(t))|^2 dt = \int_0^\infty |\emptyset(\lambda)|^2 \frac{d\lambda}{1-g(\lambda)}, \tag{33}$$

$$< \frac{1}{1-\beta}\int_0^\infty |\emptyset(\lambda)|^2 d\lambda, \tag{34}$$

hence, $\|\Delta_2\|_2 < \frac{a}{\sqrt{1-\beta}}$, where $a = \sqrt{\frac{1-\beta}{2}}$. As mentioned above, the uncertainty blocks are non-causal due to the non-causal integral and time-advance block. The maximum time-advance in both Δ_1 and Δ_2 is $\max_{t\geq 0}\{-\delta(t)\} > 0$, however, since $\overline{\delta} \leq h$, necessity assumptions in [23,24] are satisfied.

Then, the uncertain plant set can be represented as

$$\Pi = P_o O_h + P_o O_h \widehat{\Delta} \widehat{W}, \tag{35}$$

where $\widehat{\Delta} = [\Delta_1 \quad \Delta_2]$, $\widehat{W} = \begin{bmatrix} W_1 \\ W_2 \end{bmatrix}$, where $W_1 := -\frac{s(b-ac)}{c(as+b)}$, $W_2 := \frac{s+c}{as+b}$. Then, If one replaces Π in Figure 3.1 by (35), the feedback scheme in the figure can be represented as shown in Figure 3.4. Therefore, designing a stabilizing controller for a feedback system in Figure 3.1 can be ensured if a stabilizing controller can be designed for the closed-loop system shown in Figure 3.4. In order to find such a controller, suppose C be a controller stabilizes the feedback system given in Figure 3.4 for $\widehat{\Delta}$ =0. In order to ensure the internal stability of the feedback system for all $\widehat{\Delta}$, where $\|\widehat{\Delta}\|_2 < 1$,

$$G = (1 + CP_0 e^{-hs} + CP_0 e^{-hs}{}_o \Delta_1 W_1 + CP_0 e^{-hs} \Delta_2 W_2)^{-1},$$

should be in $\mathcal{H}^\infty$. Note, since C stabilizes the feedback system for $\widehat{\Delta} = 0$, $S = (1 + CP_0 e^{-hs})^{-1}$ is in $\mathcal{H}^\infty$. Note, since G can be written as

$$G = S(1 + SCP_0 e^{-hs} \Delta_1 W_1 + SCP_0 e^{-hs} \Delta_2 W_2)^{-1},$$

then, C stabilizes the feedback system for all $\widehat{\Delta}$ if

$$G_1 = \left(1 + SCP_0 e^{-hs} [\Delta_1 \quad \Delta_2] \begin{bmatrix} W_1 \\ W_2 \end{bmatrix}\right)^{-1} \text{is stable.}$$

Note, G_1 is stable iff

$$G_2 = \left(1 + [\Delta_1 \quad \Delta_2] \begin{bmatrix} W_1 \\ W_2 \end{bmatrix} SCP_0 e^{-hs}\right)^{-1},$$

is stable. Since we let $\widehat{\Delta}$ to be non- causal, by [23], C stabilizes the feedback system given in Figure 3.4 for all $\widehat{\Delta}$, where $\|\widehat{\Delta}\|_2 < 1$, if

$$\left\| \begin{bmatrix} W_1 \\ W_2 \end{bmatrix} SCP_0 e^{-hs} \right\|_\infty < 1. \tag{36}$$

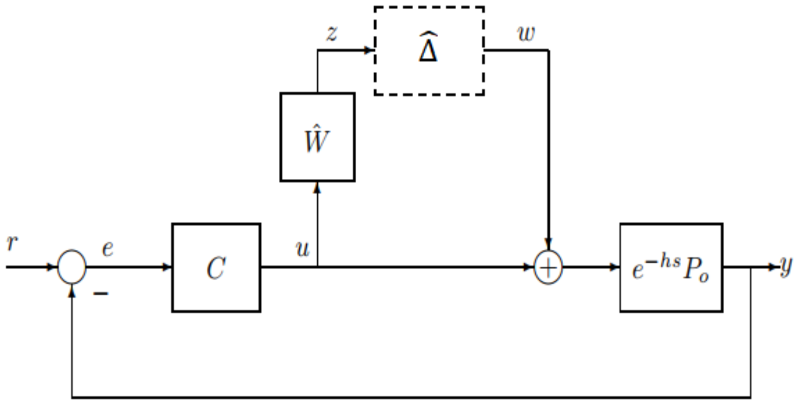

Figure 3.4. *Input Multiplicative Uncertainty Representation.*

4. CONTROLLER DESIGN AND SIMULATIONS

In this Chapter, performance of three different PI controllers designed for a coupled tank whose input is subjecting uncertain time-varying time-delays will be compared. First, we will consider delay-free PI controller. The objective of delay-free controller design is to understand effect of uncertain time-varying time-delays on the performance of the controller. For instance, What is the effect of fast (or slow) varying uncertain delays on the closed-loop system? For the comparison, first, we will design a well-known Smith-Predictor based PI controller. Smith-predictor controller works perfectly when delay is known, however, its response in large delays having uncertain time-varying delays may be interesting [21]. Next, a delay-based PI controller will be considered. Last, H^{∞} based PI controller will be designed by utilizing the results given in the previous Chapter. It is expected a better response in presence of uncertain time-varying time-delay. However, since H^{∞} controller design approaches are conservative because of the small-gain theorem, comparison of these three controllers may provide us a guide.

The first objective of the controller design is to ensure the internal stability of the feedback system. Besides the internal stabilization of the closed-loop system, the controllers are often designed to ensure some performance objectives, which may be perfect tracking or disturbance rejecting under some physical constraints and certain requirements on time-domain behaviour. For instance, in practice, since input(s) and output(s) of actuator are bounded, controller to be designed satisfy the above design objectives under such a physical constraint. Then, by considering Figure 3.1 for $\Pi = P_o(s)$, the design problem can be described as find a stabilizing controller C such as

$$C(s) = K_p + \frac{K_i}{s}. \tag{37}$$

where K_p and K_i are positive, and it achieves the following objectives:

Q1: Ensuring the internal stability.

Q2: The overshoot in the step response has to be less than 15 %.

Q3: The settling time in the step response has to be less than 300 second.

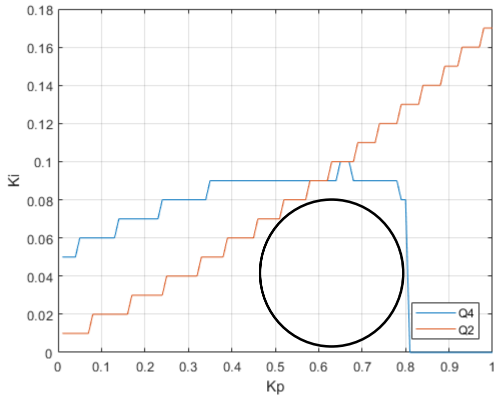

Figure 4.1. *The set of K_p and K_i ensuring design objectives (see Code 4.1)*

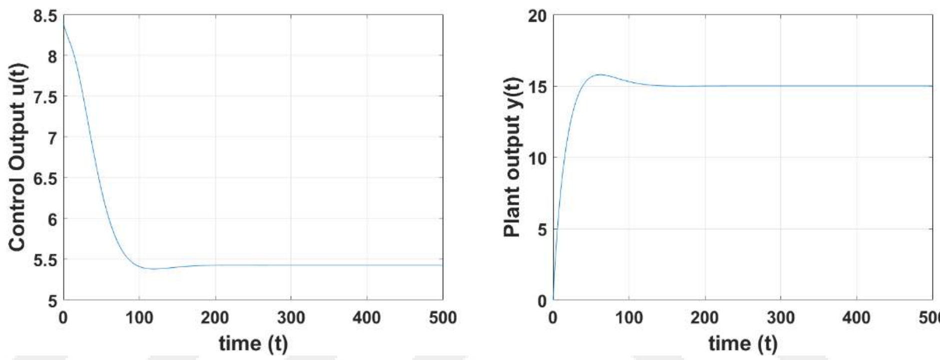

Figure 4.2. *Simulation result for (K_p, K_i) = (0.63, 0.04) and $\tau(t)$ = 0*

Q4: The control signal has to be less than 12V.

4.1 PI controller design approach for a nominal plant

Then, for the free delay (nominal plant) $P_o(s)$ given in (24), since, Q1 hold for all positive K_p and K_i, the set of all PI parameters is shown as given in Figure 4.1. As seen in the figure, there exists infinitely many PI values ensuring the design objectives. The controller parameters are obtained by putting a circle having a largest radius inside the intersection of PI parameter sets shown in Figure 4.1. Then, K_p= 0.63 and K_i = 0.04. Then, By setting r in Figure 3.1 as r=15, and applying K_p and K_i on the free delay (nominal plant) $P_o(s)$, the controller and plant outputs are presented as in Figure 4.2. As shown in the figure the design objectives (Q1, Q2, Q3 and Q4) that mentioned above are satisfied.

In order to understand the effect of time-varying time-delays, we will present some simulation results by considering the free delay (nominal plant) $P_o(s)$ and the actual non linear plant which descriped by (11) and (12), and the controller is the one which is given above. Then, the simulation results for various time-delays are presented as in the Figures 4.3 to 4.12 (see Code 4.2). In these figures, the time-varying time-delay is shown by $\tau(t)$, which is written as $\tau(t) = h + a + b\ sin(2\pi f t)$, where h corresponds to nominal delay, a corresponds to time-invariant part of uncertain time-varying delay, $b\ sin(2\pi f t)$ corresponds to time-varying part of uncertain time-varying delay.

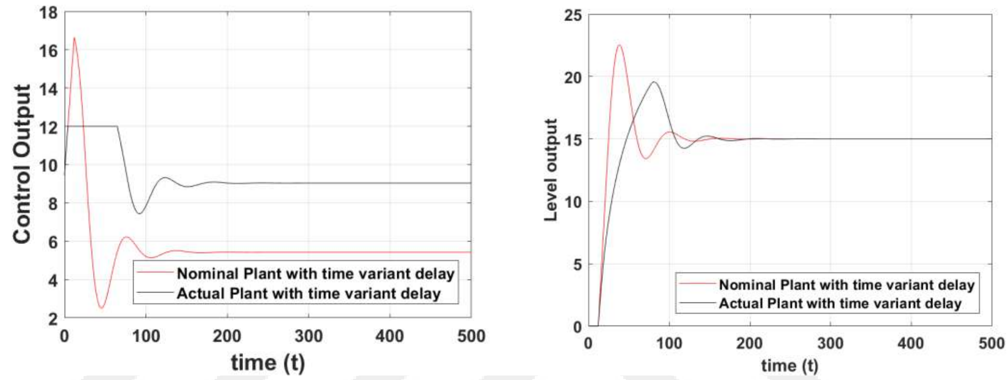

Figure 4.3. *Simulation result for* (K_p, K_i) = *(0.63, 0.04) and* $\tau(t) = 12$

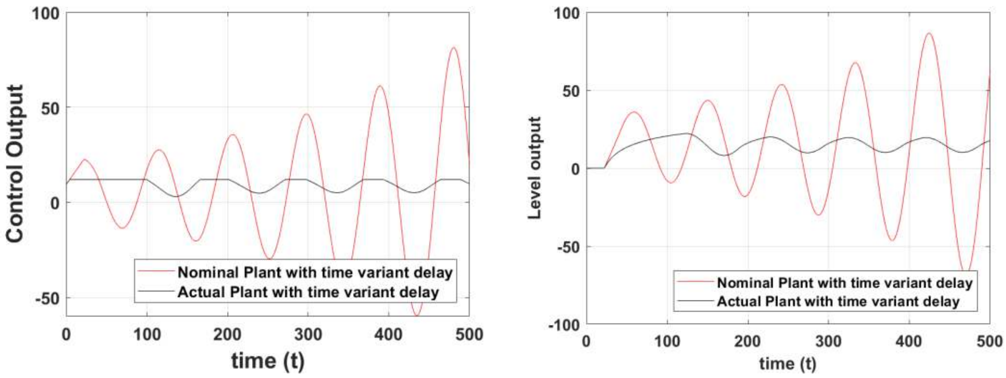

Figure 4.4. *Simulation result for* (K_p, K_i) = *(0.63, 0.04) and* $\tau(t) = 12 + 10$

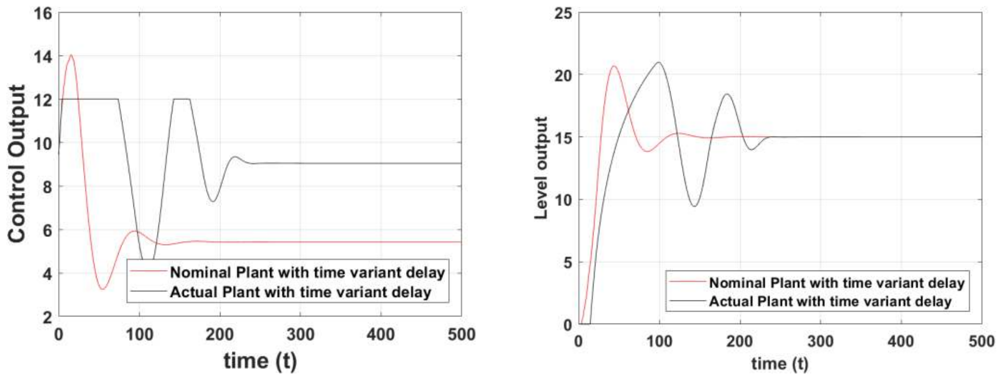

Figure 4.5. *Simulation result for (K_p, K_i) = (0.63, 0.04) and* $\tau(t) = 12 + 10sin(\frac{2\pi}{400}t)$

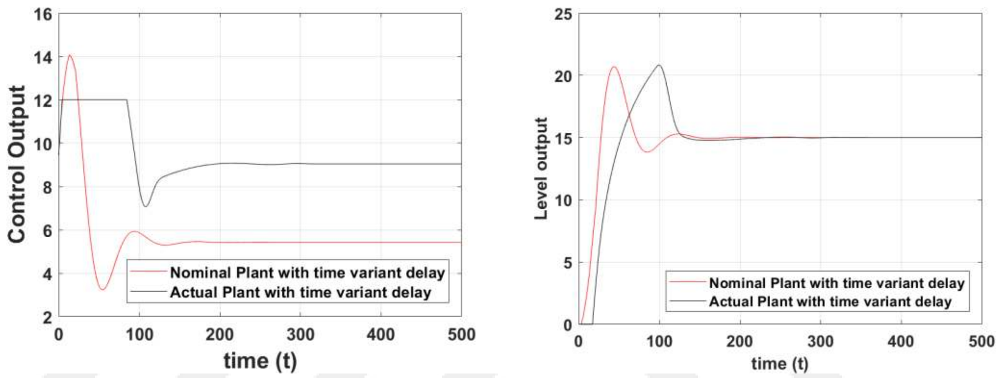

Figure 4.6. *Simulation result for (K_p, K_i) = (0.63, 0.04) and* $\tau(t) = 12 + 10sin(\frac{2\pi}{200}t)$

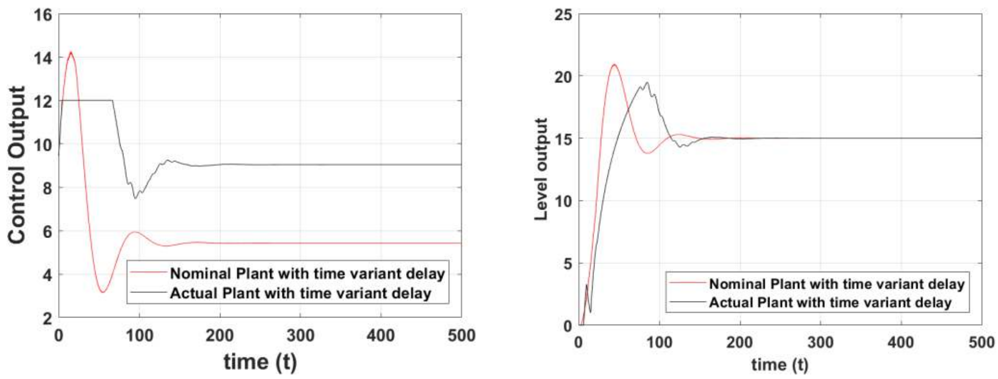

Figure 4.7. *Simulation result for (K_p, K_i) = (0.63, 0.04) and* $\tau(t) = 12 + 10sin(\frac{2\pi}{10}t)$

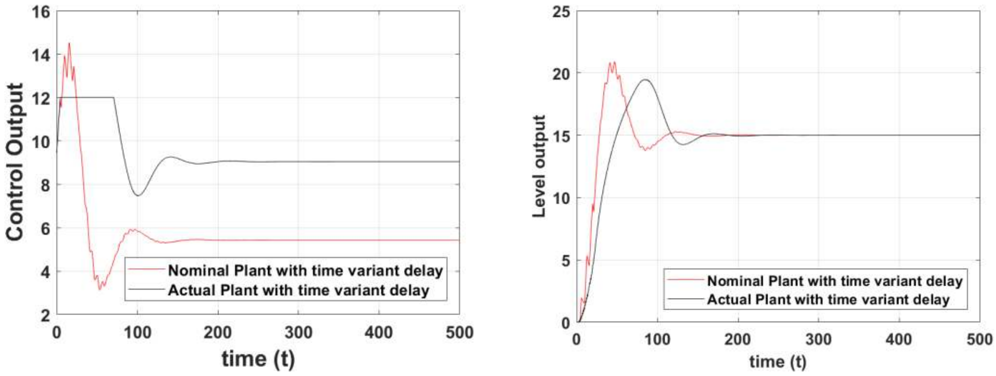

Figure 4.8. *Simulation result for* (K_p, K_i) *= (0.63, 0.04) and* $\tau(t) = 12 + 10sin(\frac{2\pi}{1}t)$

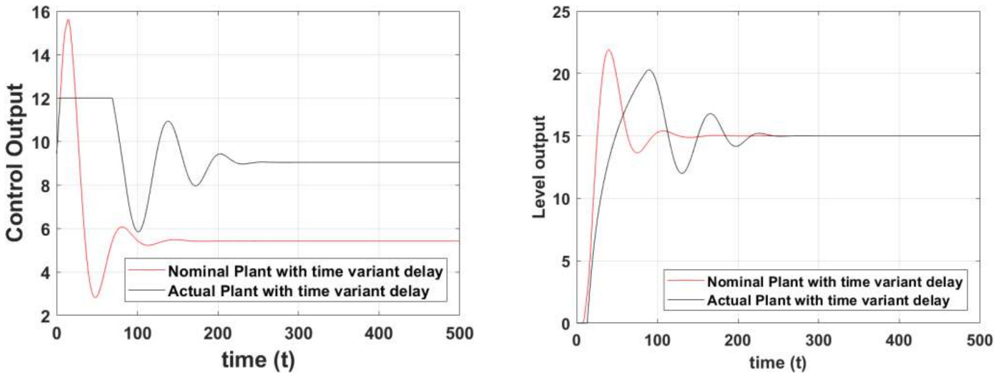

Figure 4.9. *Simulation result for* (K_p, K_i) *= (0.63, 0.04) and* $\tau(t) = 12 + 5\ sin(\frac{2\pi}{400}t)$

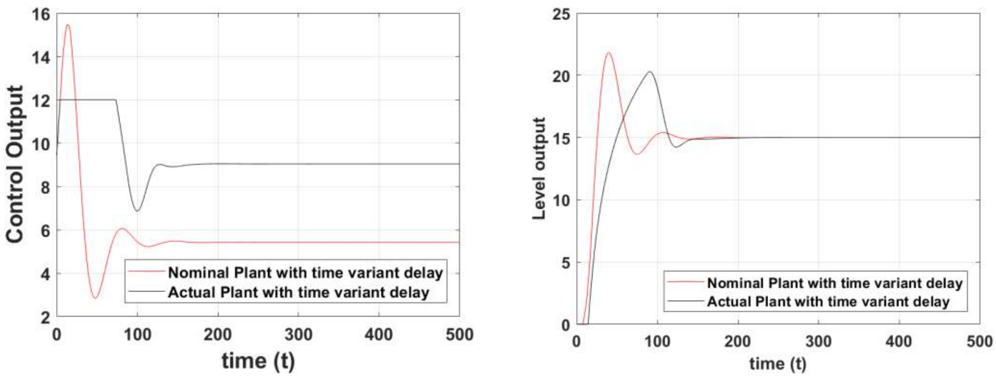

Figure 4.10. *Simulation result for* (K_p, K_i) *= (0.63, 0.04) and* $\tau(t) = 12 + 5sin(\frac{2\pi}{200}t)$

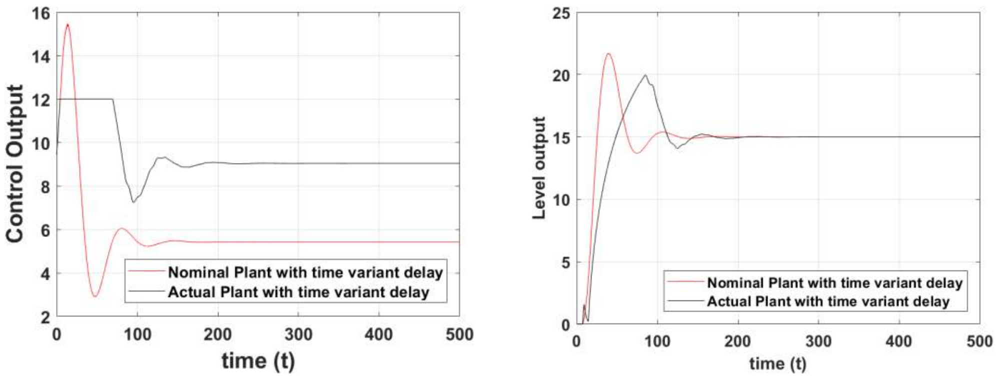

Figure 4.11. *Simulation result for* (K_p, K_i) *= (0.63, 0.04) and* $\tau(t) = 12 + 5sin(\frac{2\pi}{10}t)$

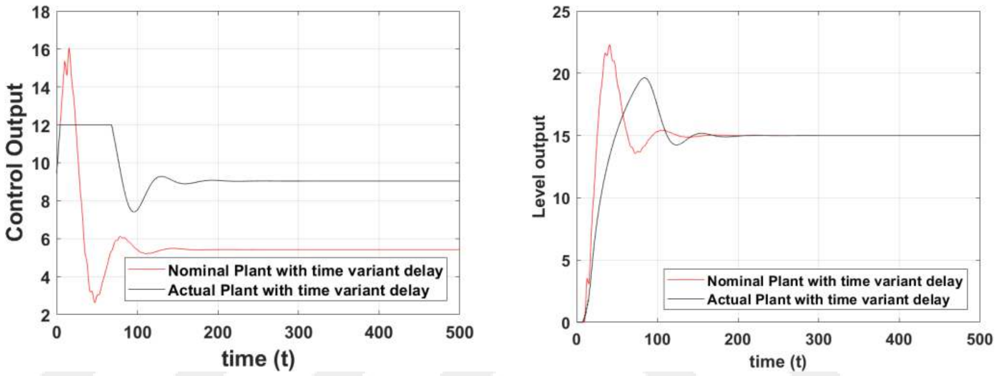

Figure 4.12. *Simulation result for* (K_p, K_i) *= (0.63, 0.04) and* $\tau(t) = 12 + 5sin(\frac{2\pi}{1}t)$

As seen by comparing Figures 4.2 and 4.4, when the actual plant or nominal plant is applied as fixed delay increases, the results become more oscillatory. The effect of time-varying time delays are intresting. As frequency of the variation of delay increases, as seen by comparing Figures 4.4 to 4.12, the contoller output becomes more sharp, which may not be preferred in practice, since presence of sharp changes in the inputs of an actuator may cause unexpected results.

4.2 Smith-Predictor -based PI controller

The structure of Smith predictor as shown in Figure 4.13 consists of two parts the first is the primary controller $C(s)$ and other is the predictor structure. The predictor part consists of the time delay model P_0e^{-hs} and the free delay model P_0. The output of the predictor is compared with the input to the plant, and the difference is compensated through a feedback loop. The aim in Smith predictor is that when the predicted output

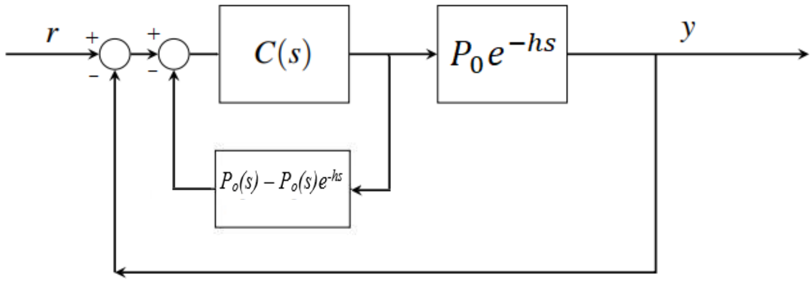

Figure 4.13. *Block diagram of Smith predictor*

equals to the plant output, the signal from the free delay plant can be used for the control, therefore the controller can be designed without considering time delay and the control performance can be significantly improved [21].

In order to see the performance of Smith-predictor (SP) -based PI controller, some simulation results will be presented by considering the closed-loop system given in Figure 4.13 for time-invariant delays and time-varying delays by replacing $P_0 e^{-hs}$ with Π and the controller is the one which is given above (see, Figures 4.19 to 4.46) (see Code 4.4). Note, in these simulations $\tau(t)$ is as described above. Smith-Predictor based controllers work well for fixed delays as seen by comparing Figure 4.2 and Figures 4.14 to 4.18 (see Code 4.3).

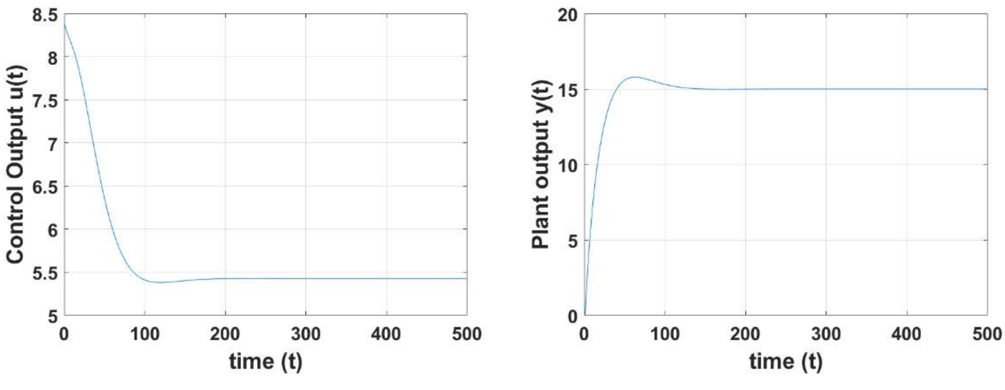

Figure 4.14. *Simulation result for* (K_p, K_i) = *(0.63, 0.04) and* h = *1*

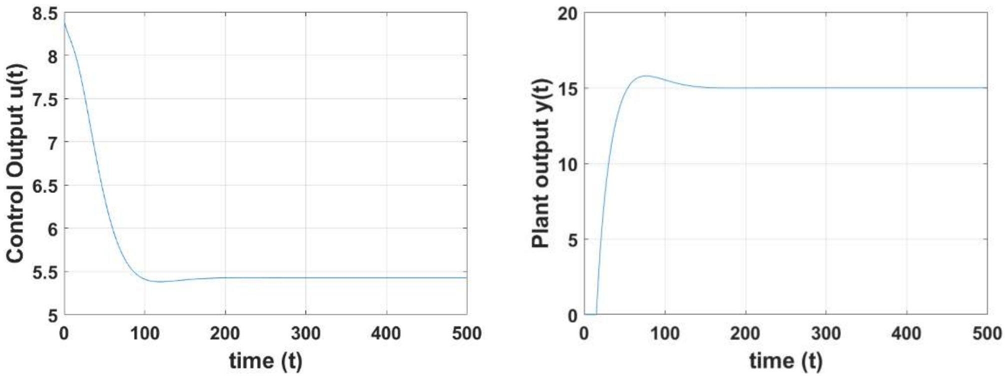

Figure 4.15. *Simulation result for* (K_p, K_i) = *(0.63, 0.04) and* h = *15*

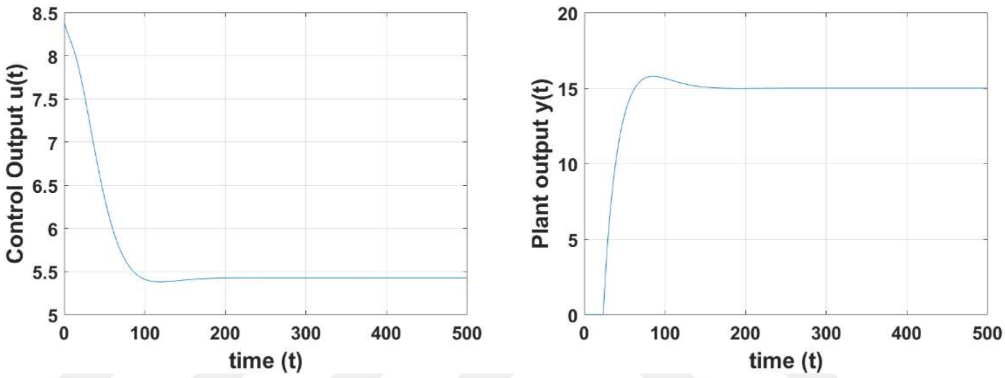

Figure 4.16. *Simulation result for* (K_p, K_i) = *(0.63, 0.04) and* h = *23.5*

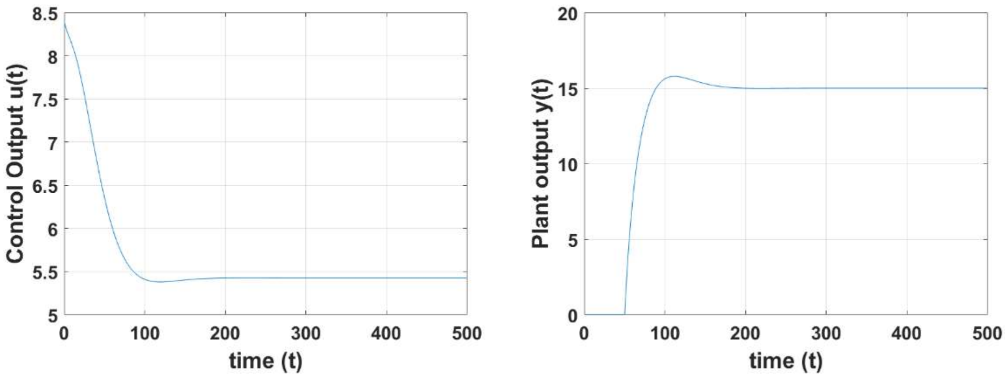

Figure 4.17. *Simulation result for* (K_p, K_i) = *(0.63, 0.04) and* h = *50.*

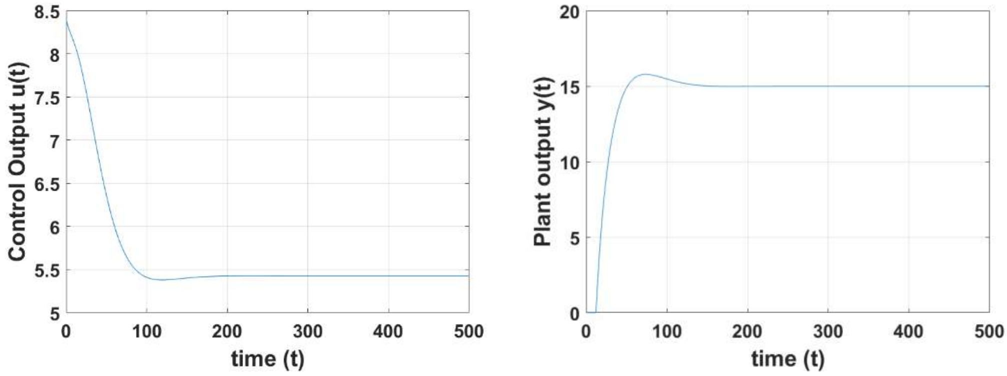

Figure 4.18. *Simulation result for* (K_p, K_i) = *(0.63, 0.04) and* $\tau(t) = 12$

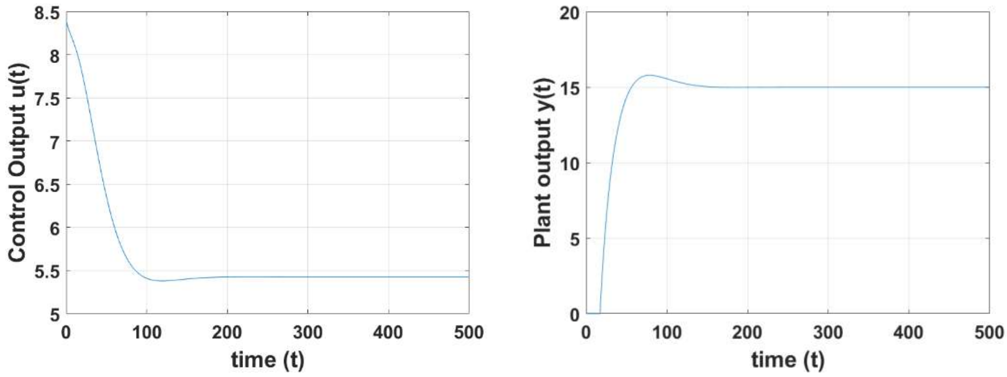

Figure 4.19. *Simulation result for* (K_p, K_i) = *(0.63, 0.04) and* $\tau(t) = 12 + 5$

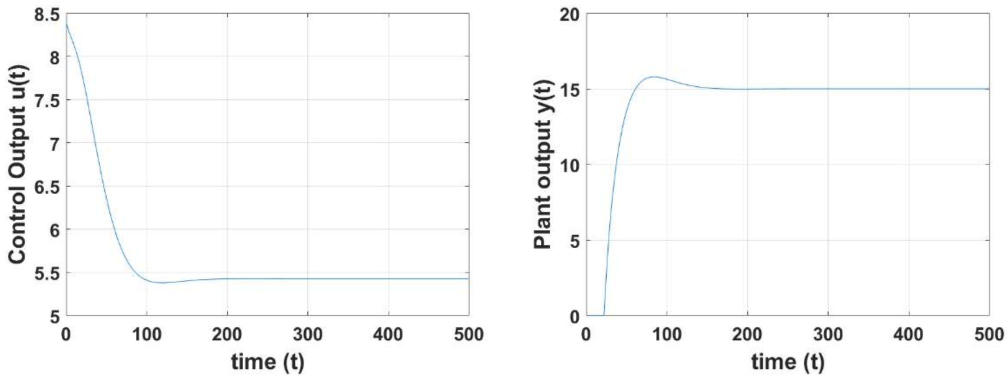

Figure 4.20. *Simulation result for* (K_p, K_i) = *(0.63, 0.04) and* $\tau(t) = 12 + 10$

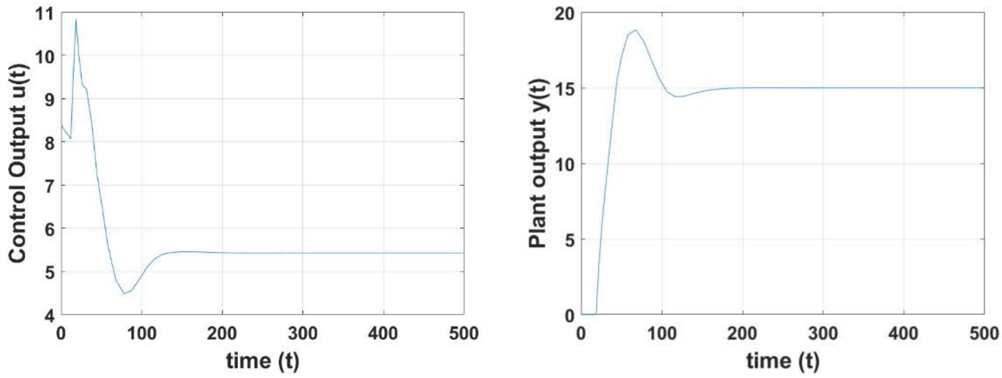

Figure 4.21. *Simulation result for* (K_p, K_i) = *(0.63, 0.04) and* $\tau(t) = 12 + 5 + 5\,sin(\frac{2\pi}{200}t)$

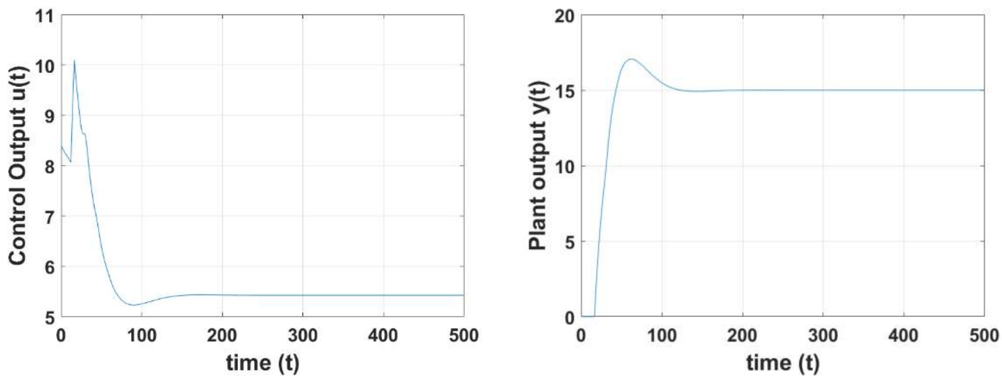

Figure 4.22. *Simulation result for* (K_p, K_i) = *(0.63, 0.04) and* $\tau(t) = 12 + 5 + 5\,sin(\frac{2\pi}{1}t)$

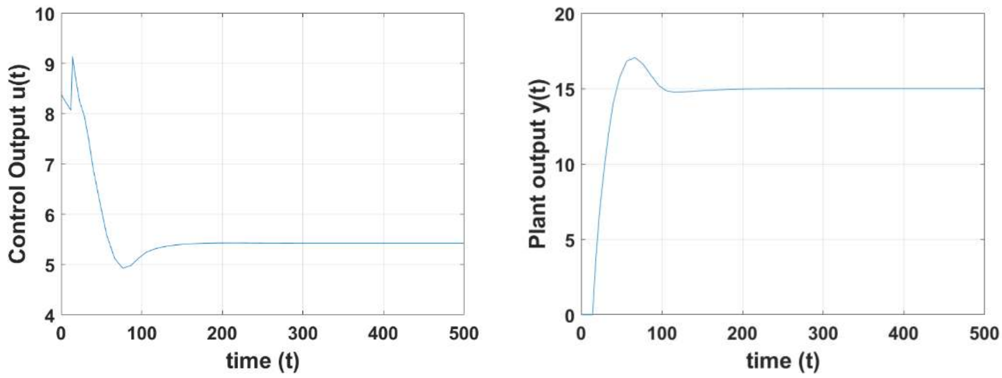

Figure 4.23. *Simulation result for* (K_p, K_i) = *(0.63, 0.04) and* $\tau(t) = 12 + 10sin(\frac{2\pi}{200}t)$

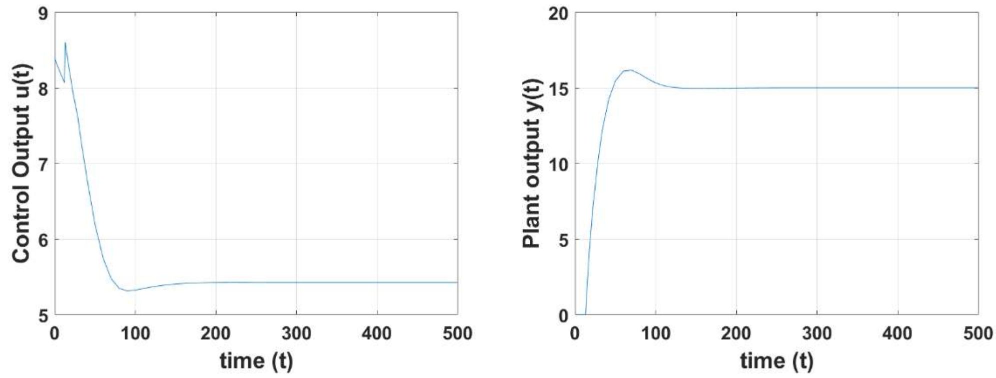

Figure 4.24. *Simulation result for (*K_p*,* K_i*) = (0.63, 0.04) and* $\tau(t) = 12 + 5sin(\frac{2\pi}{200}t)$

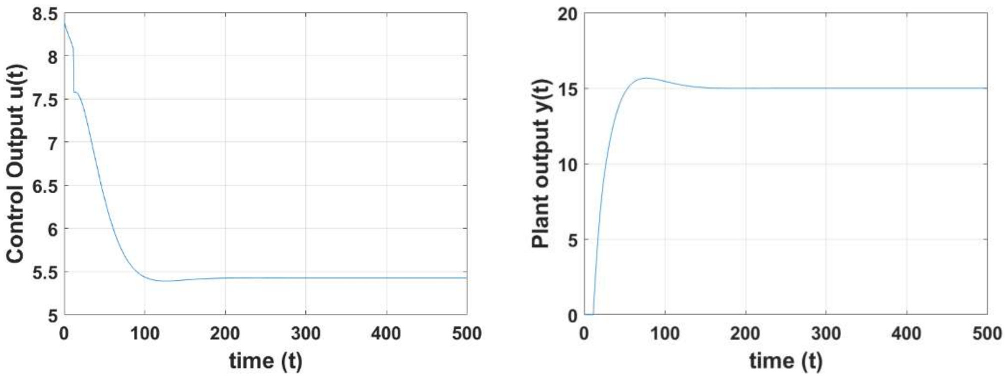

Figure 4.25. *Simulation result for (*K_p*,* K_i*) = (0.63, 0.04) and* $\tau(t) = 12 + 5sin(\frac{2\pi}{10}t)$

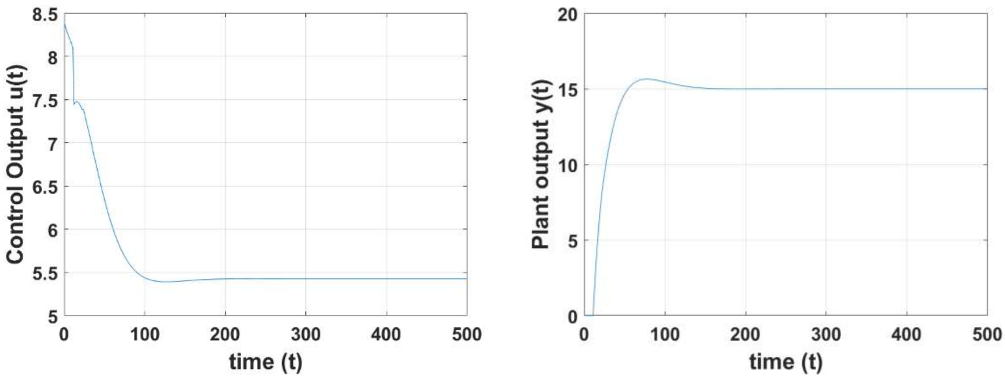

Figure 4.26. *Simulation result for (*K_p*,* K_i*) = (0.63, 0.04) and* $\tau(t) = 12 + 5sin(\frac{2\pi}{1}t)$

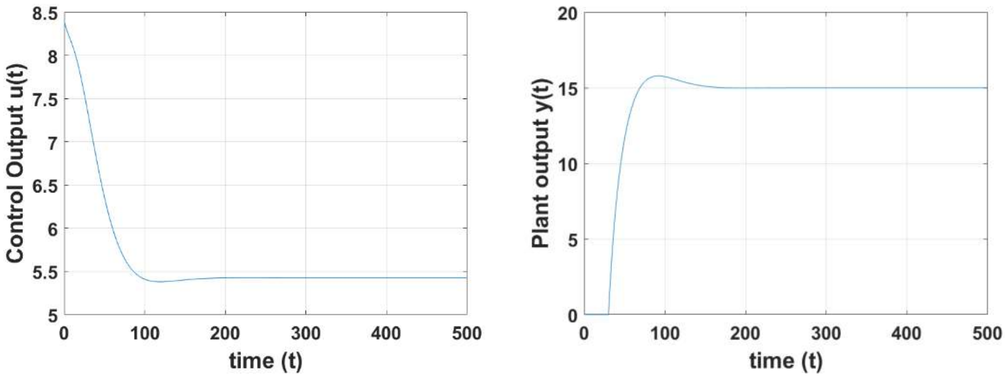

Figure 4.27. *Simulation result for* (K_p, K_i) = *(0.63, 0.04) and* $\tau(t) = 30$

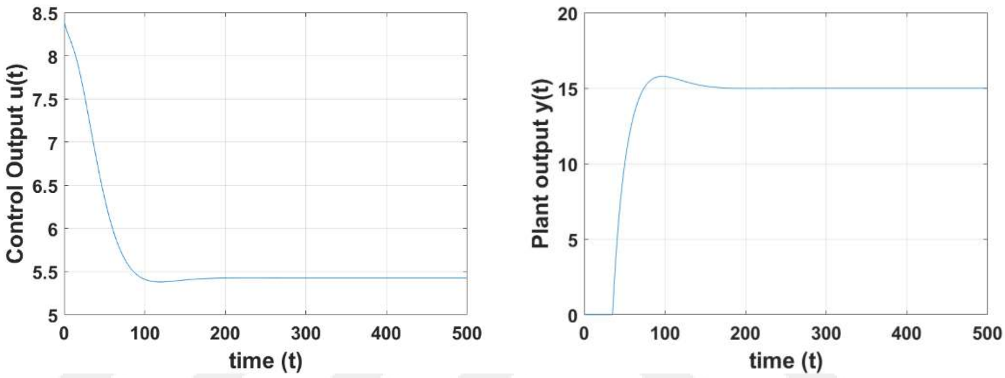

Figure 4.28. *Simulation result for* (K_p, K_i) = *(0.63, 0.04) and* $\tau(t) = 30 + 5$

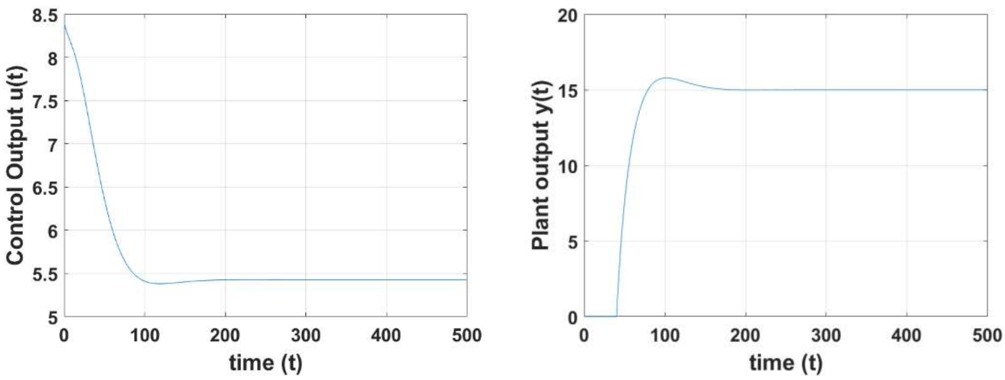

Figure 4.29. *Simulation result for* (K_p, K_i) = *(0.56, 0.037) and* $\tau(t) = 30 + 10$

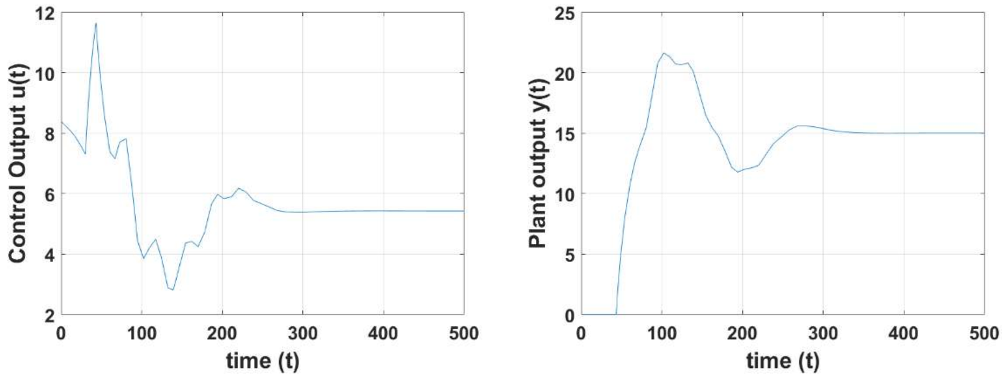

Figure 4.30. *Simulation result for* (K_p, K_i) = *(0.63, 0.04) and* $\tau(t) = 30 + 10 + 10sin(\frac{2\pi}{400}t)$

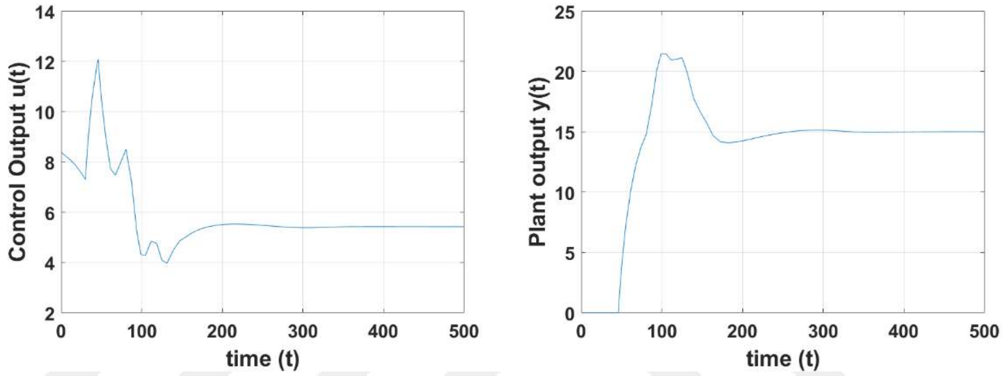

Figure 4.31. *Simulation result for* (K_p, K_i) = *(0.63, 0.04) and* $\tau(t) = 30 + 10 + 10sin(\frac{2\pi}{200}t)$

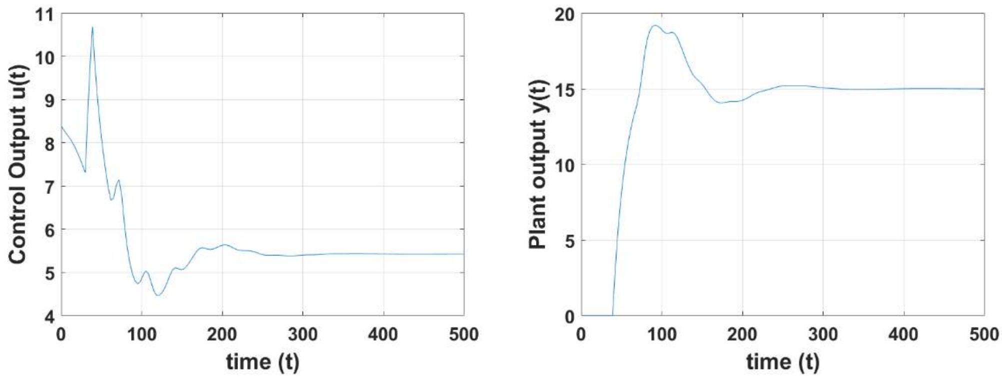

Figure 4.32. *Simulation result for* (K_p, K_i) = *(0.63, 0.04) and* $\tau(t) = 30 + 10 + 10sin(\frac{2\pi}{10}t)$

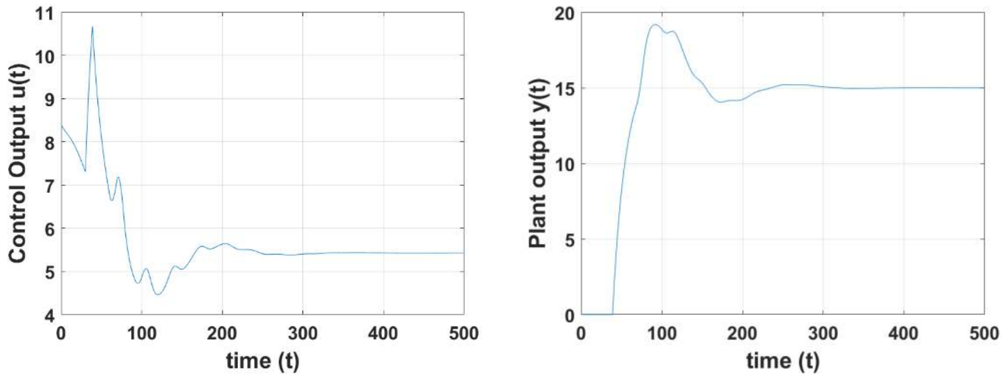

Figure 4.33. *Simulation result for (*K_p*,* K_i*) = (0.63, 0.04) and* $\tau(t) = 30 + 10 + 10sin(\frac{2\pi}{1}t)$

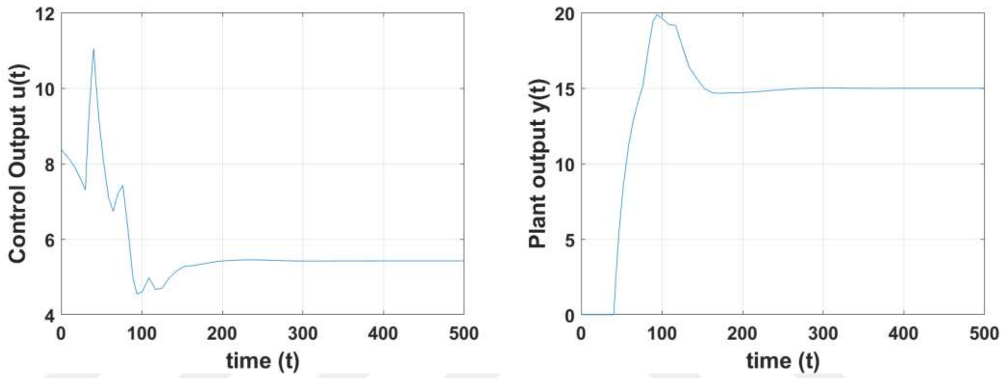

Figure 4.34. *Simulation result for (*K_p*,* K_i*) = (0.63, 0.04) and* $\tau(t) = 30 + 5 + 10sin(\frac{2\pi}{200}t)$

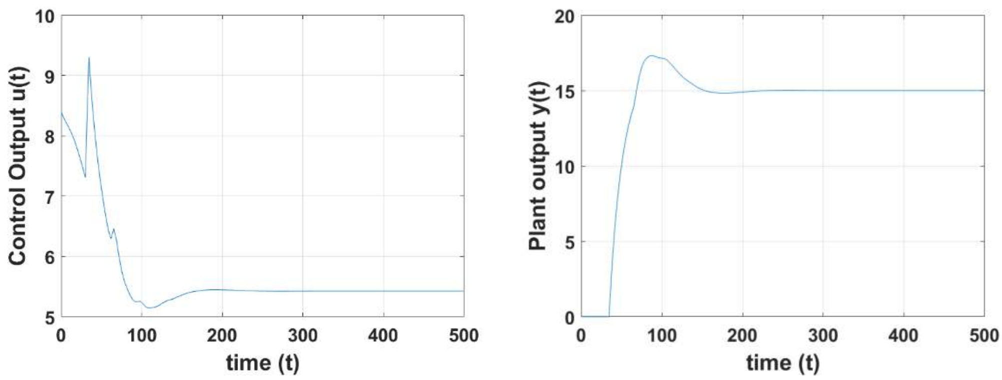

Figure 4.35. *Simulation result for (*K_p*,* K_i*) = (0.63, 0.04) and* $\tau(t) = 30 + 5 + 10sin(\frac{2\pi}{10}t)$

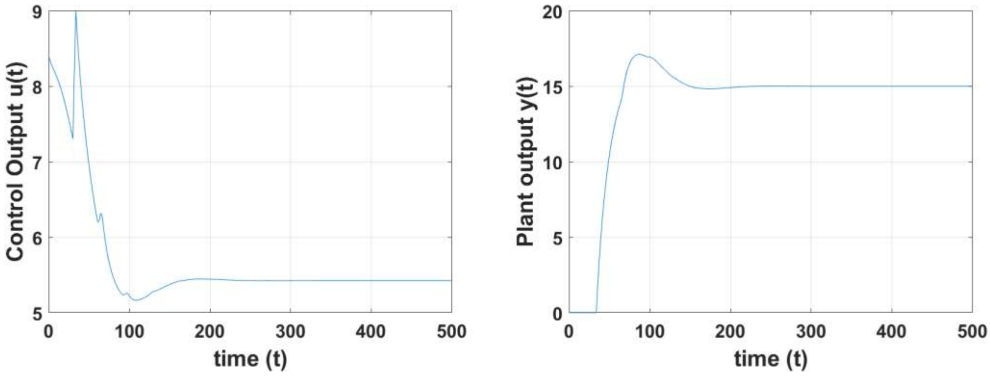

Figure 4.36. *Simulation result for (*K_p*,* K_i*) = (0.63, 0.04) and* $\tau(t) = 30 + 5 + 10sin(\frac{2\pi}{1}t)$

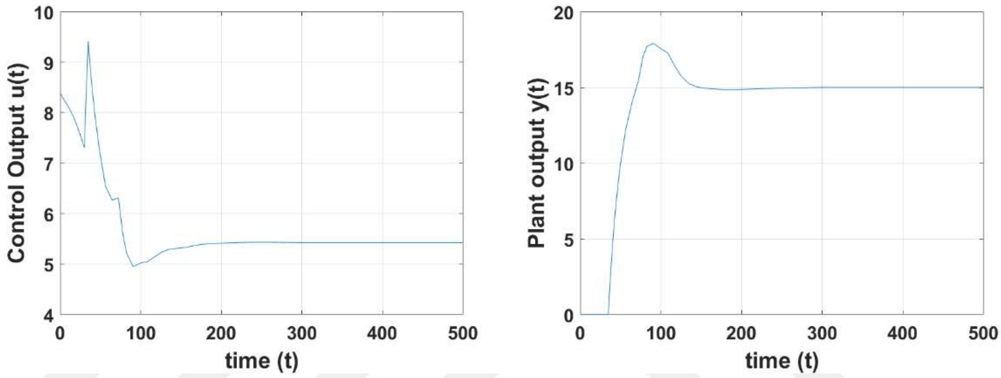

Figure 4.37. *Simulation result for (*K_p*,* K_i*) = (0.63, 0.04) and* $\tau(t) = 30 + 10\ sin(\frac{2\pi}{200}t)$

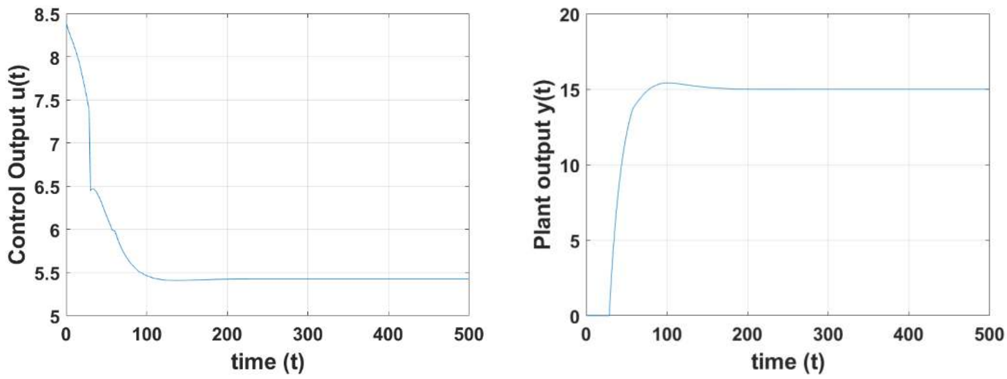

Figure 4.38. *Simulation result for (*K_p*,* K_i*) = (0.63, 0.04) and* $\tau(t) = 30 + 10sin(\frac{2\pi}{10}t)$

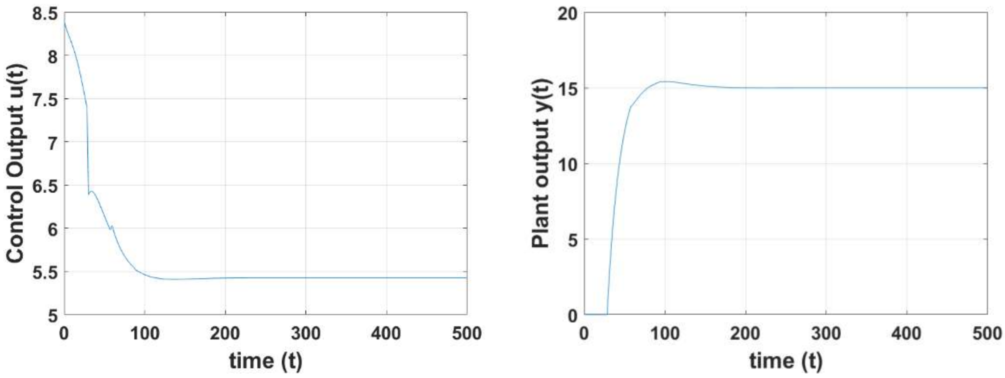

Figure 4.39. *Simulation result for (*K_p*,* K_i*) = (0.63, 0.04) and* $\tau(t) = 30 + 10\ sin(\frac{2\pi}{1}t)$

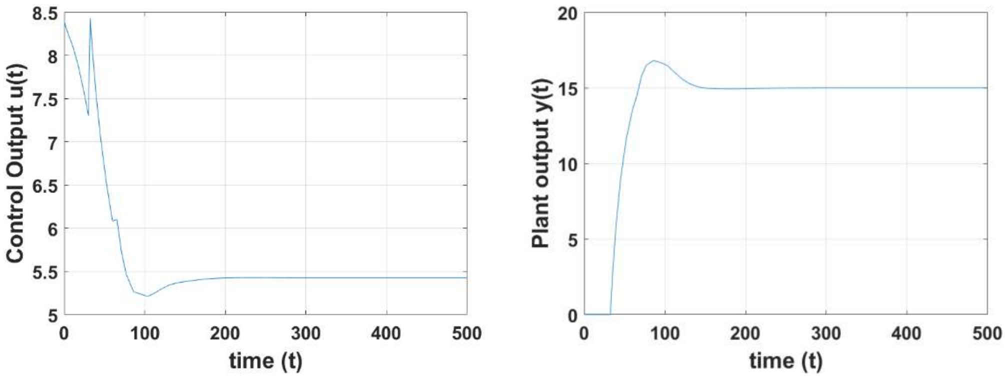

Figure 4.40. *Simulation result for (*K_p*,* K_i*) = (0.63, 0.04) and* $\tau(t) = 30 + 5in(\frac{2\pi}{200}t)$

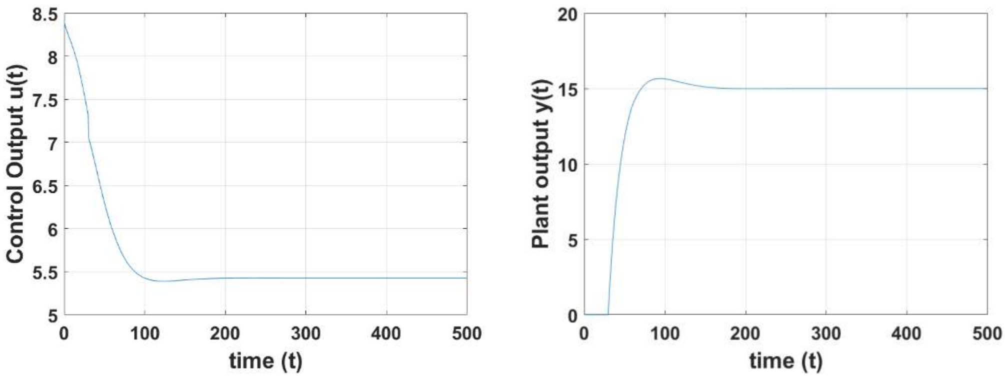

Figure 4.41. *Simulation result for (*K_p*,* K_i*) = (0.63, 0.04) and* $\tau(t) = 30 + 5sin(\frac{2\pi}{10}t)$

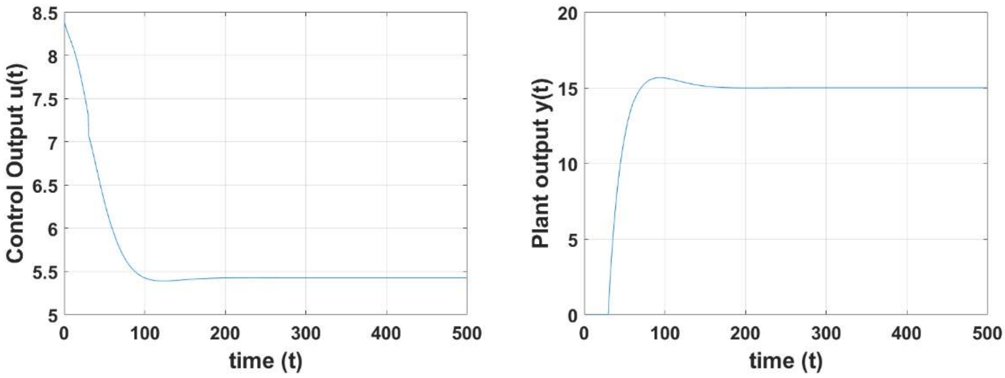

Figure 4.42. *Simulation result for (K_p, K_i) = (0.63, 0.04) and* $\tau(t) = 30 + 5sin(\frac{2\pi}{1}t)$

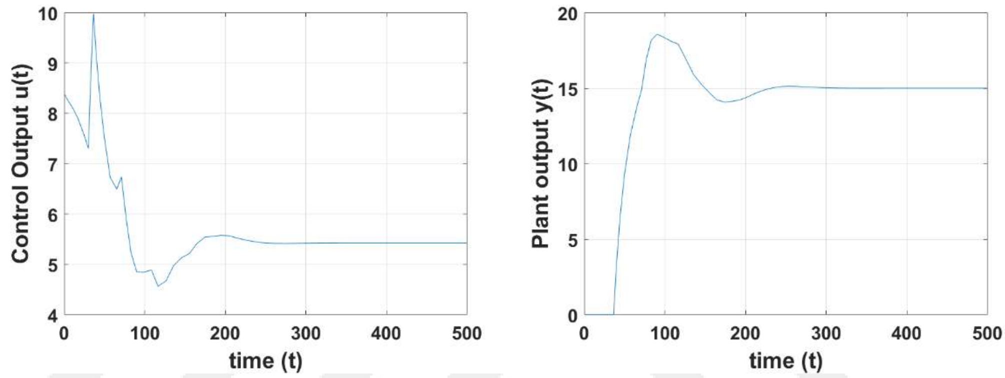

Figure 4.43. *Simulation result for (K_p, K_i) = (0.63, 0.04) and* $\tau(t) = 30 + 5 + 5\ sin(\frac{2\pi}{400}t)$

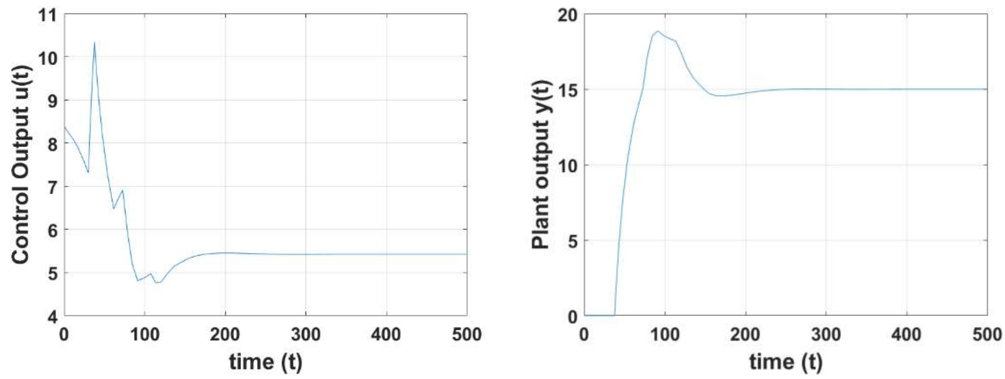

Figure 4.44. *Simulation result for (K_p, K_i) = (0.63, 0.04) and* $\tau(t) = 30 + 5 + 5sin(\frac{2\pi}{200}t)$

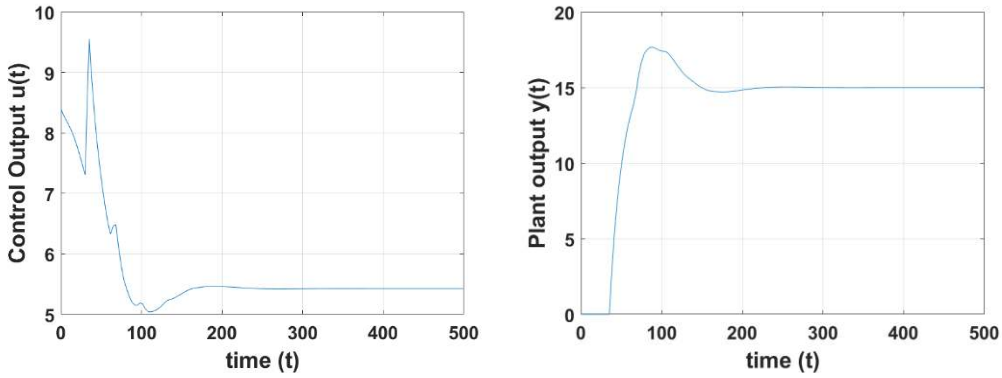

Figure 4.45. *Simulation result for (K_p, K_i) = (0.63, 0.04) and* $\tau(t) = 30 + 5 + 5sin(\frac{2\pi}{10}t)$

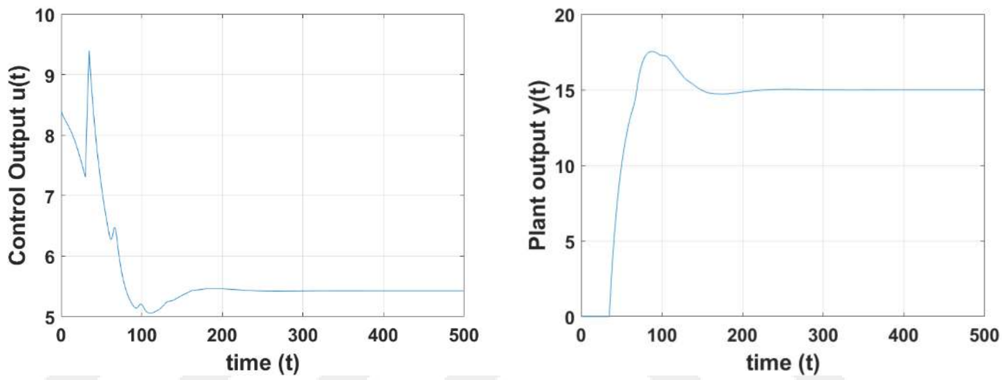

Figure 4.46. *Simulation result for (K_p, K_i) = (0.63, 0.04) and* $\tau(t) = 30 + 5 + 5sin(\frac{2\pi}{1}t)$.

As seen from Fig 4.14 to 4.46, SP-based PI controller robustly achieves the design objectives in presence of uncertain time-varying time-delays. It is observed from Figures 4.14, 4.18, 4.19, 4.20, 4.28, 4.29, presence time-invariant uncertain time-delays does not have noticable effect. In presence of uncertain time-varying time-delays, the controller output shows sharp variations whether the variation of delay is small or fast. If nominal delay increases, the controller becomes more sensitive for the variations of uncertain time-delay as seen by comparing Figure 4.21 and 4.22 with Figure 4.44 and 4.46. Note that it can be seen from Figures 4.24, 4.25, 4.38, 4.39, if uncertain delay is fast varying and $\delta(0) = 0$, the controller responses look like response of fixed nominal delay. Moreover, whenever the delay is slowly varying and $\delta(0)$ is constant, but non-zero, as seen by comparing Figure 4.21 and 4.22 with 4.30 and 4.36. SP controller is more sensitive in large nominal delays.

4.3 Delay-(nominal) based PI controller

In this part, delay-based PI controller design will be considered. The design approach is similar to the PI controller design for the delay-free plant $P_0(s)$. Note, in case of delay-free plant, the feedback system is stable for all non-negative K_p and K_i. In presence of "large delays", this does not hold. Therefore, a region in PI-parameter space, which ensures the stability of the feedback system given in Figure 3.1 with a plant $\Pi = P_0 e^{-hs}$ and achievement of the design objectives, is found for given nominal delay h. Once the region is determined for a choosen h, the corresponding controller parameters are found as mentioned before Section 4.1 as shown in Figures 4.47 and 4.48 (see Code 4.5). By using this approaches, several simulations are done for the free delay (nominal) plant $P_0(s)$ with time-varying time-delay which is the feedback system given in Figure 3.1 as presented in Figures 4.49 to 4.84 (see Code 4.6).

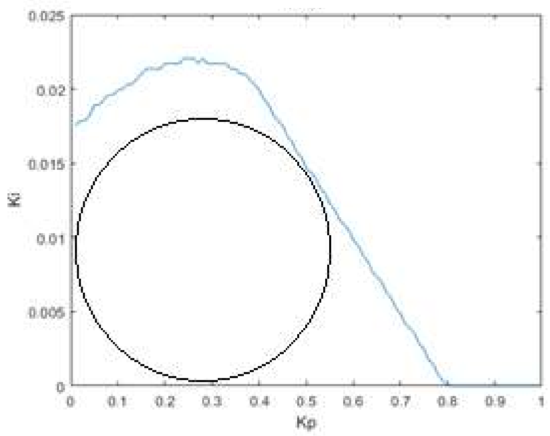

Figure 4.47. *The set of K_p and K_i ensuring design objectives for h=20.*

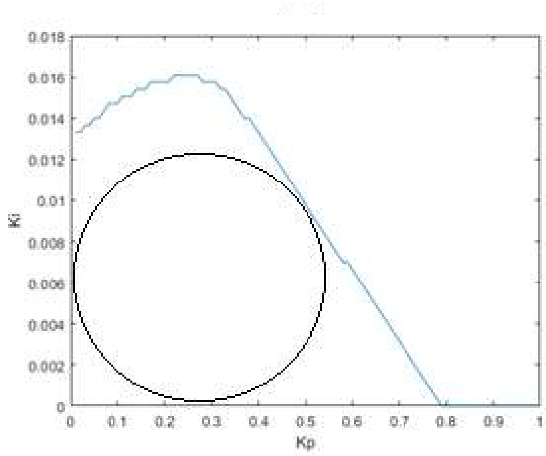

Figure 4.48. *The set of K_p and K_i ensuring design objectives for h=30.*

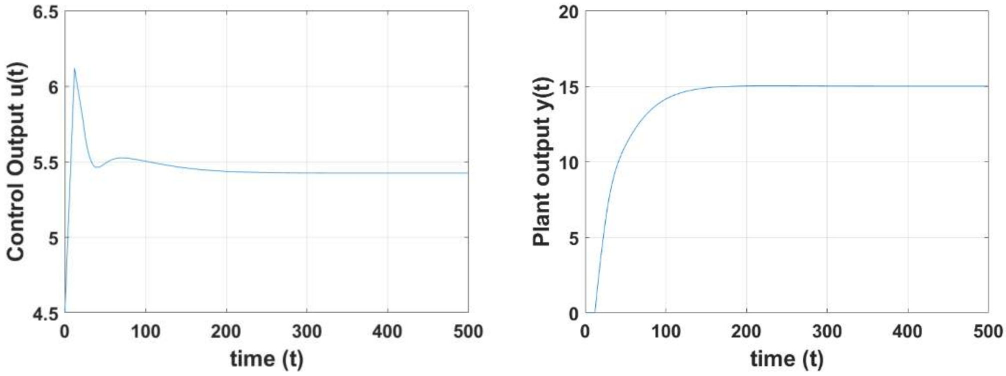

Figure 4.49. *Simulation results for (K_p, K_i) = (0.3, 0.009) and* $\tau(t) = 12$

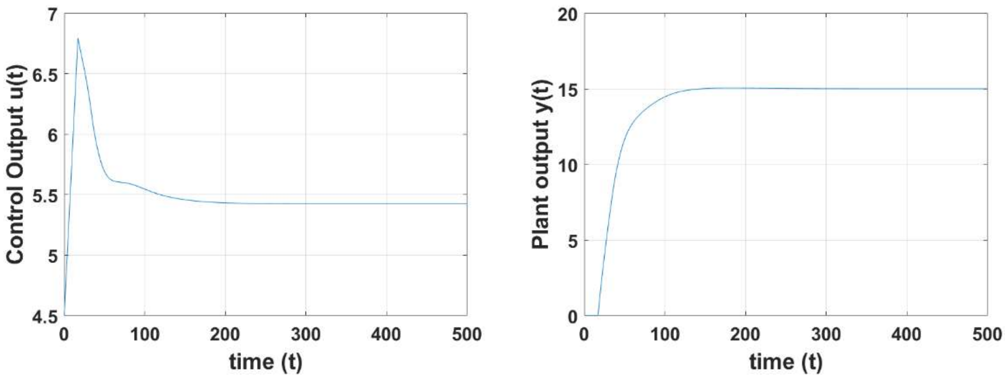

Figure 4.50. *Simulation results for (K_p, K_i) = (0.3, 0.009) and* $\tau(t) = 12 + 5$

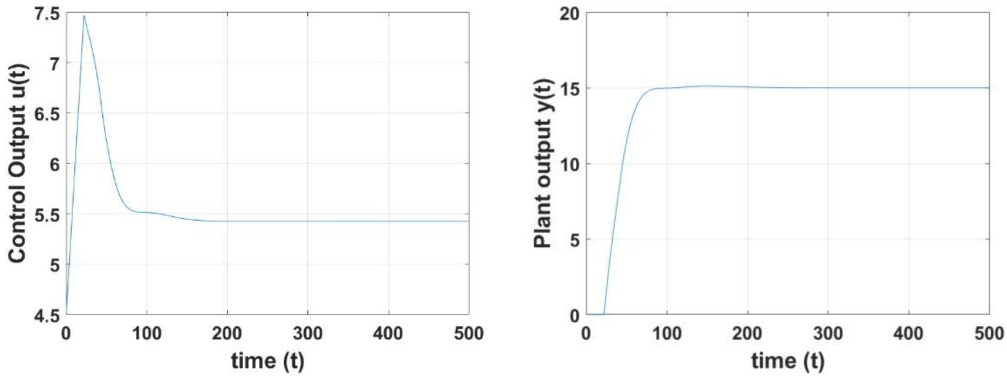

Figure 4.51. *Simulation results for* (K_p, K_i) = *(0.3, 0.009) and* $\tau(t) = 12 + 10$

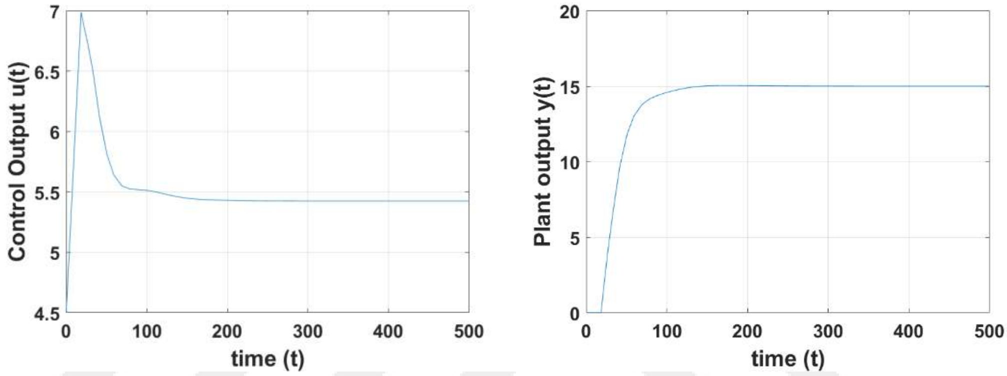

Figure 4.52. *Simulation results for* (K_p, K_i) = *(0.3, 0.009) and* $\tau(t) = 12 + 5 + 5\,sin(\frac{2\pi}{400}t)$

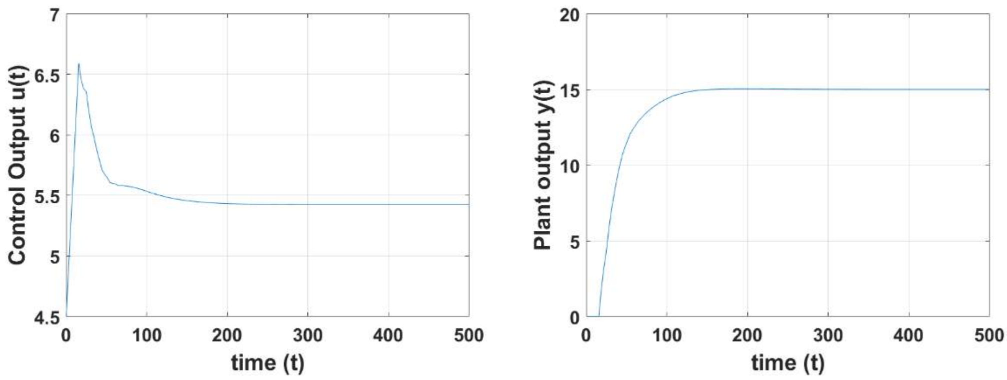

Figure 4.53. *Simulation results for* (K_p, K_i) = *(0.3, 0.009) and* $\tau(t) = 12 + 5 + 5\,sin(\frac{2\pi}{10}t)$

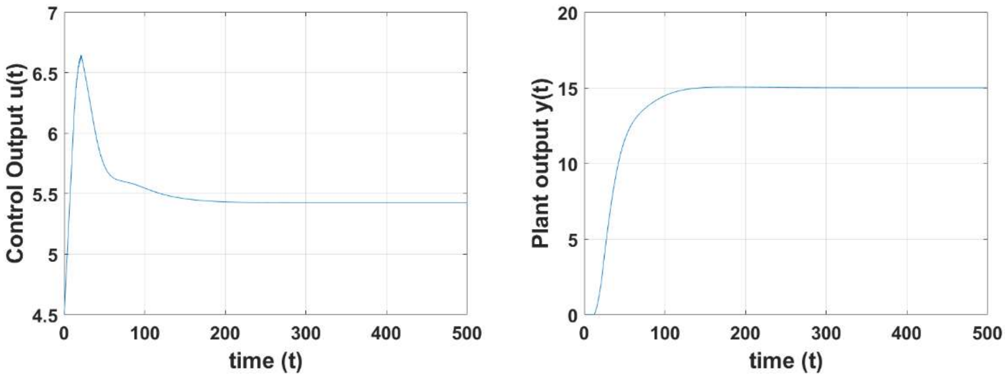

Figure 4.54. *Simulation results for* (K_p, K_i) *= (0.3, 0.009) and* $\tau(t) = 12 + 5 + 5\ sin(\frac{2\pi}{1}t)$

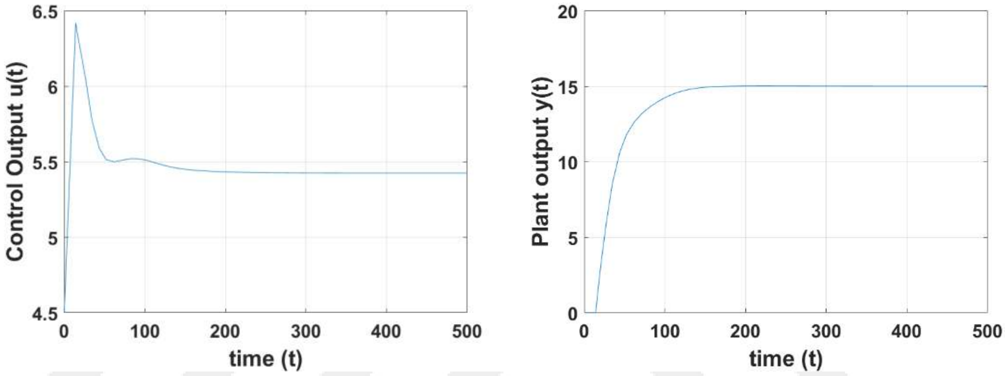

Figure 4.55. *Simulation results for* (K_p, K_i) *= (0.3, 0.009) and* $\tau(t) = 12 + 10sin(\frac{2\pi}{400}t)$

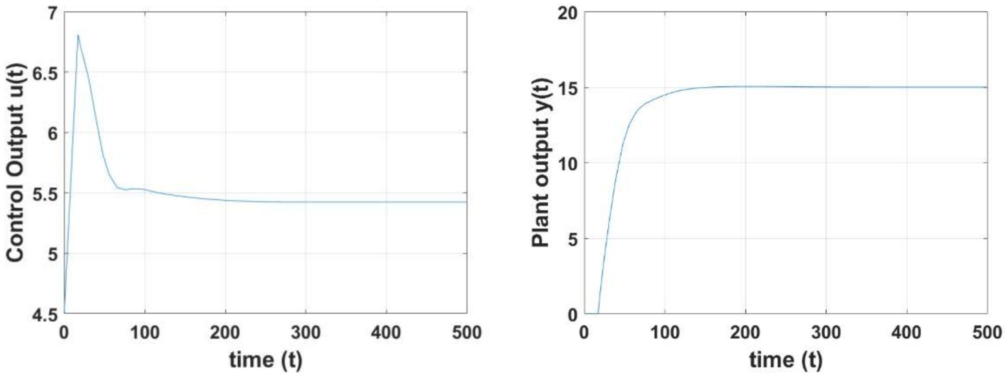

Figure 4.56. *Simulation results for* (K_p, K_i) *= (0.3, 0.009) and* $\tau(t) = 12 + 10sin(\frac{2\pi}{200}t)$

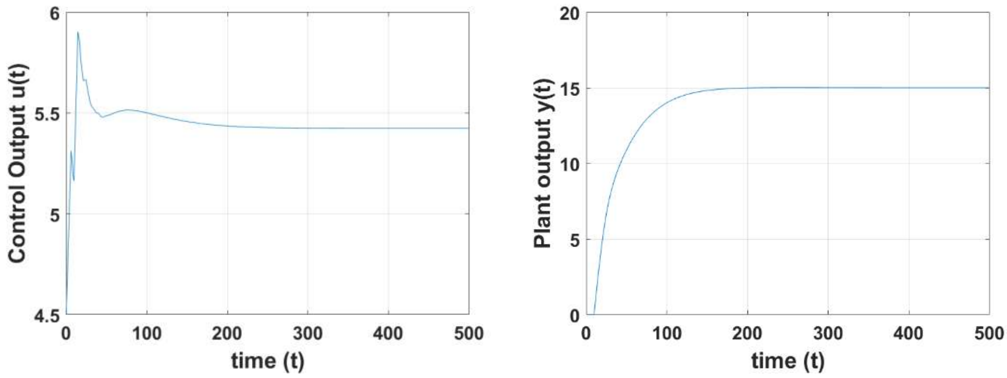

Figure 4.57. *Simulation results for (K_p, K_i) = (0.3, 0.009) and* $\tau(t) = 12 + 10sin(\frac{2\pi}{10}t)$

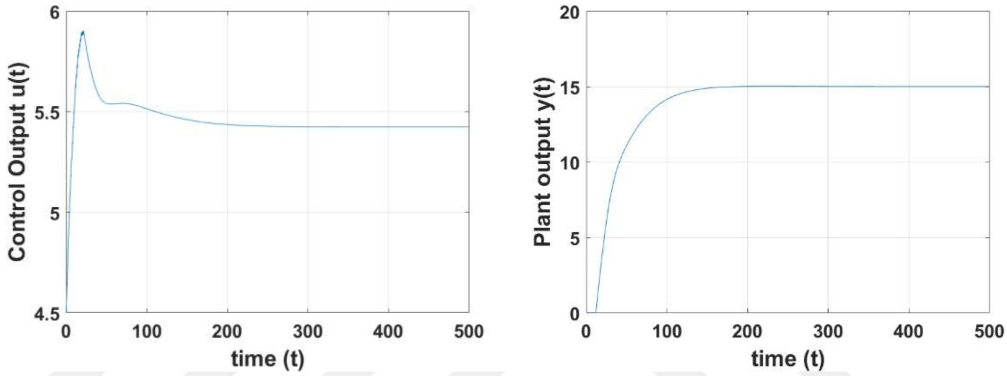

Figure 4.58. *Simulation results for (K_p, K_i) = (0.3, 0.009) and* $\tau(t) = 12 + 10sin(\frac{2\pi}{1}t)$

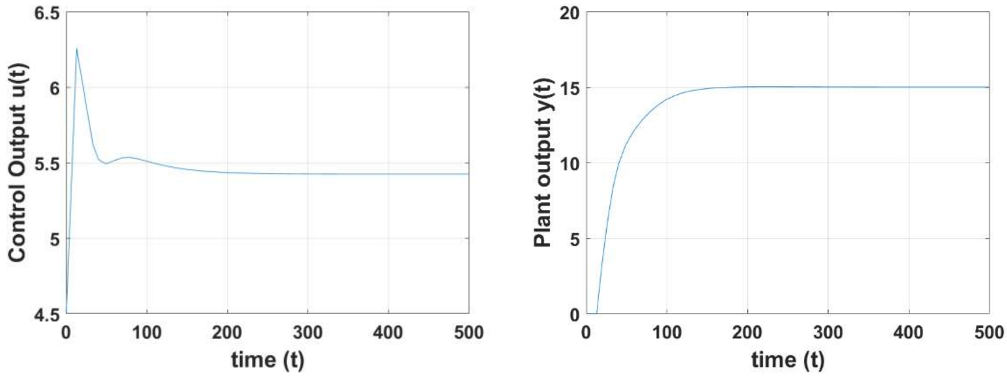

Figure 4.59. *Simulation results for (K_p, K_i) = (0.3, 0.009) and* $\tau(t) = 12 + 5\,sin(\frac{2\pi}{400}t)$

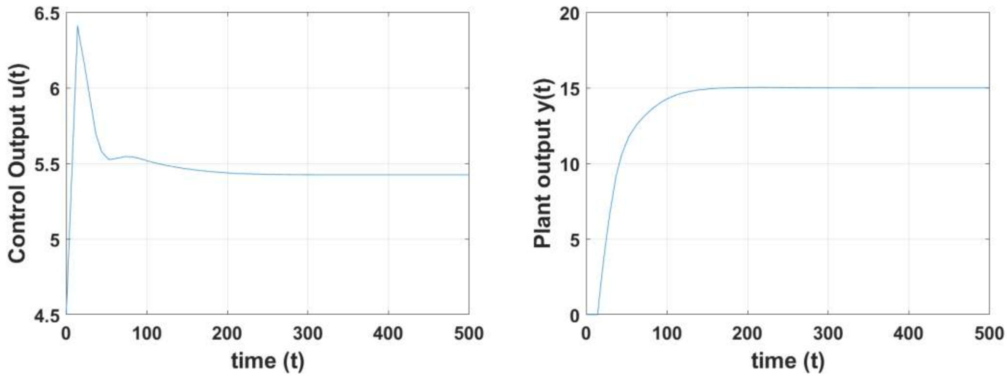

Figure 4.60. *Simulation results for* $(K_p, K_i) = (0.3, 0.009)$ *and* $\tau(t) = 12 + 5sin(\frac{2\pi}{200}t)$

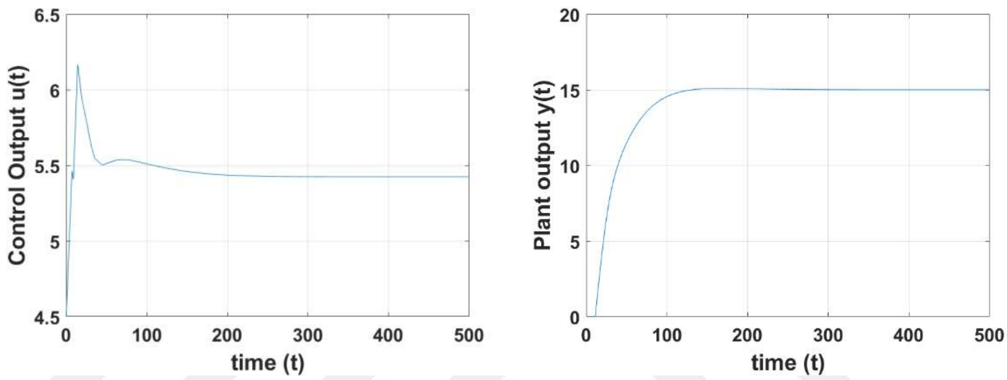

Figure 4.61. *Simulation results for* $(K_p, K_i) = (0.3, 0.009)$ *and* $\tau(t) = 12 + 5sin(\frac{2\pi}{10}t)$

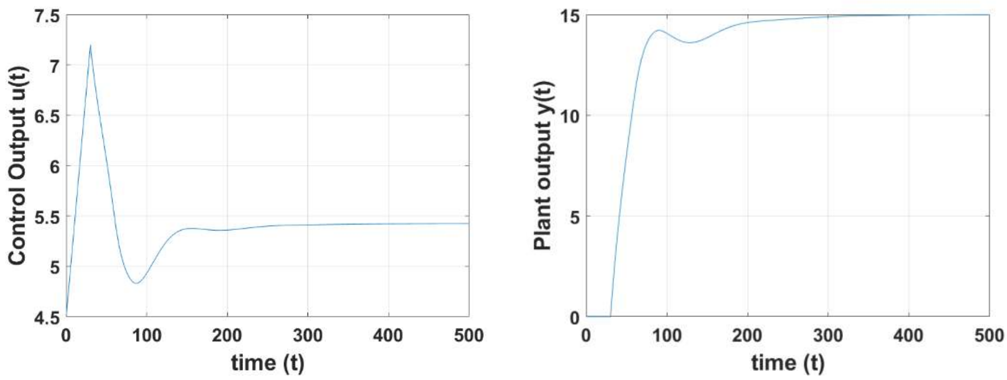

Figure 4.62. *Simulation results for* $(K_p, K_i) = (0.3, 0.006)$ *and* $\tau(t) = 30$

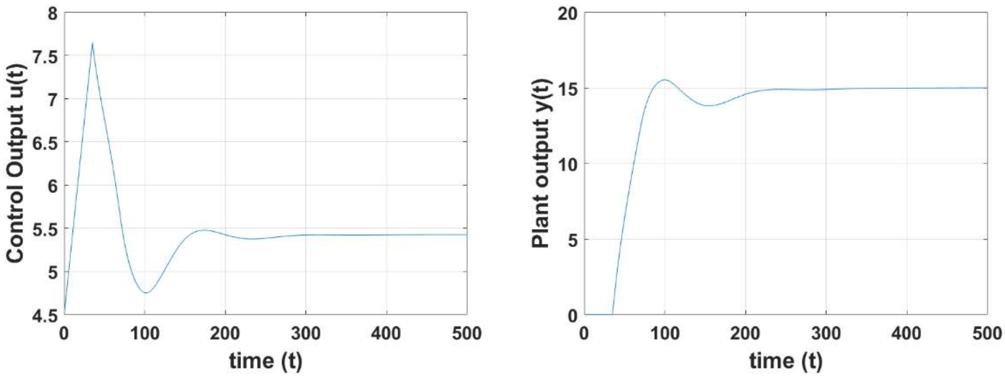

Figure 4.63. *Simulation results for* $(K_p, K_i) = 0.3, 0.006)$ *and* $\tau(t) = 30 + 5$

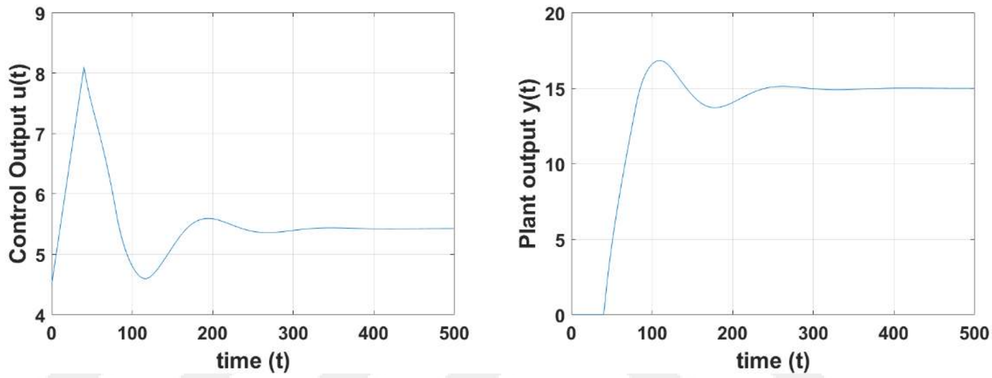

Figure 4.64. *Simulation results for* $(K_p,\ K_i) = (0.3, 0.006)$ *and* $\tau(t) = 30 + 10$

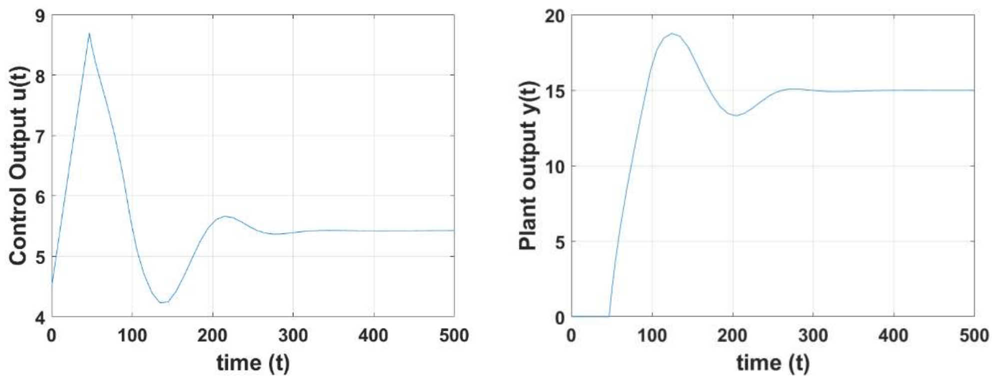

Figure 4.65. *Simulation results for* $(K_p, K_i) = (0.3, 0.006)$ *and* $\tau(t) = 30 + 10 + 10\ sin(\frac{2\pi}{400}t)$

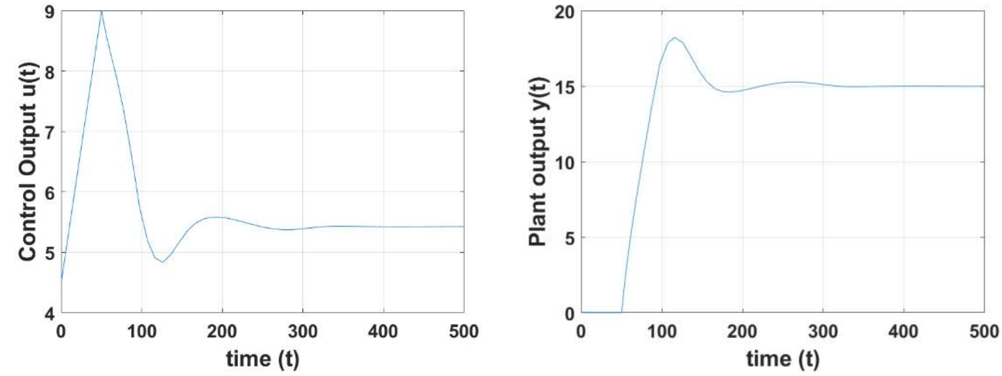

Figure 4.66. *Simulation results for* $(K_p, K_i) = (0.3, 0.006)$ *and* $\tau(t) = 30 + 10 + 10\, sin(\frac{2\pi}{200} t)$

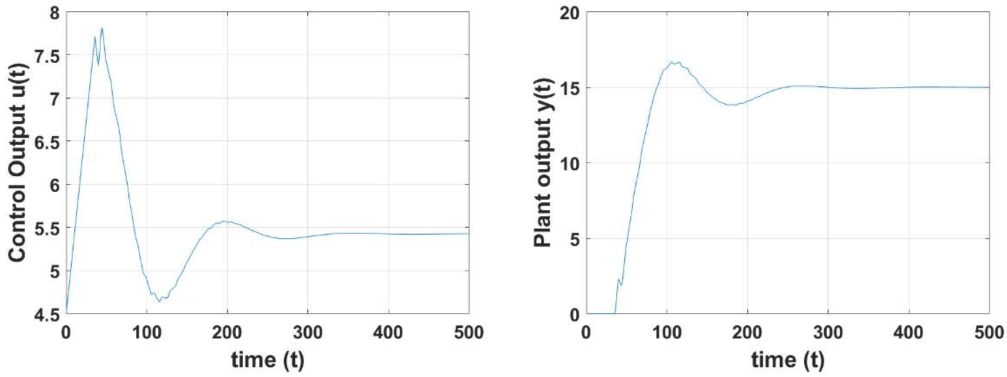

Figure 4.67. *Simulation results for* $(K_p, K_i) = (0.3, 0.006)$ *and* $\tau(t) = 30 + 10 + 10\, sin(\frac{2\pi}{10} t)$

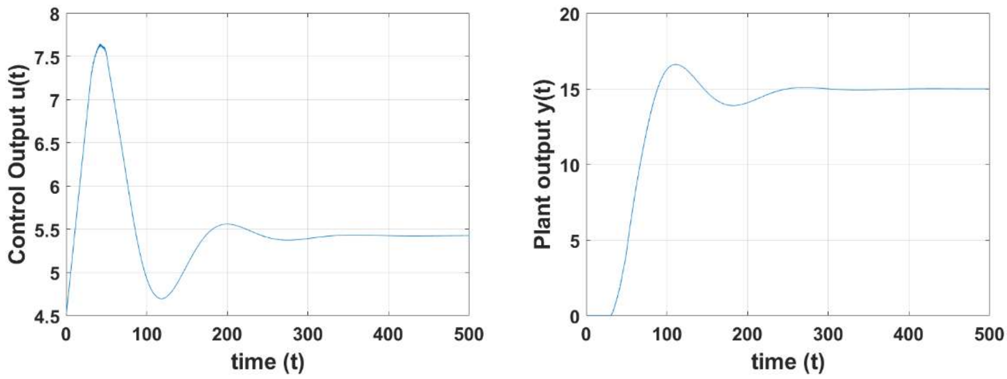

Figure 4.68. *Simulation results for* $(K_p, K_i) = (0.3, 0.006)$ *and* $\tau(t) = 30 + 10 + 10\, sin(\frac{2\pi}{1} t)$

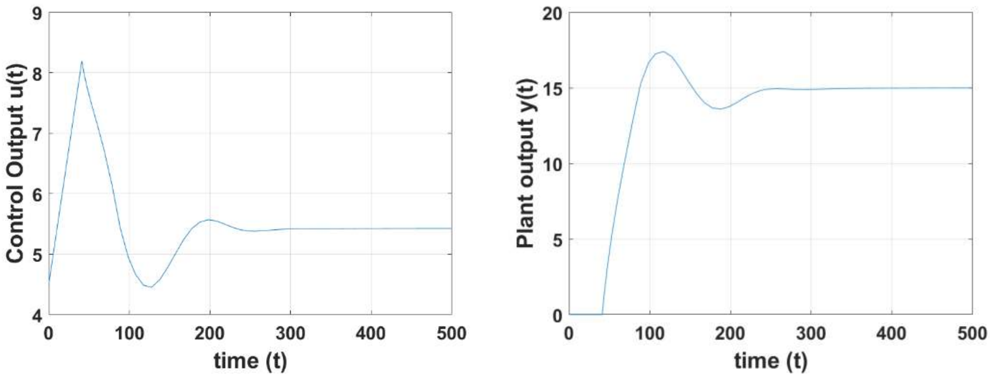

Figure 4.69. *Simulation results for* $(K_p, K_i) = (0.3, 0.006)$ *and* $\tau(t) = 30 + 5 + 10sin(\frac{2\pi}{400}t)$

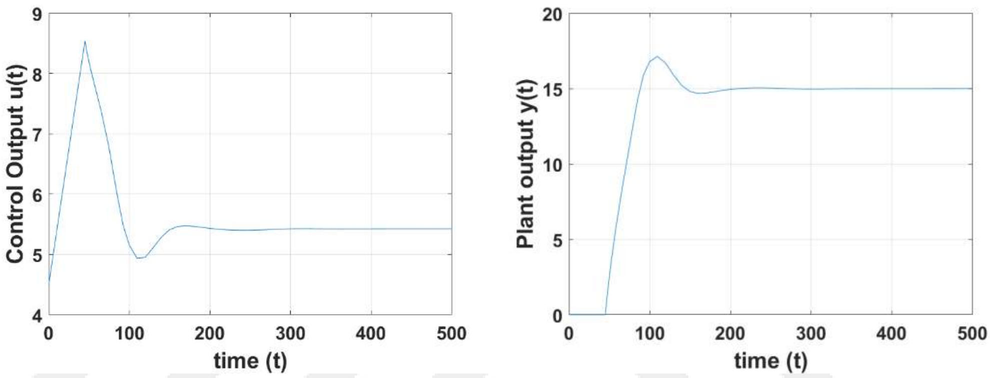

Figure 4.70. *Simulation results for* $(K_p, K_i) = (0.3, 0.006)$ *and* $\tau(t) = 30 + 5 + 10sin(\frac{2\pi}{200}t)$

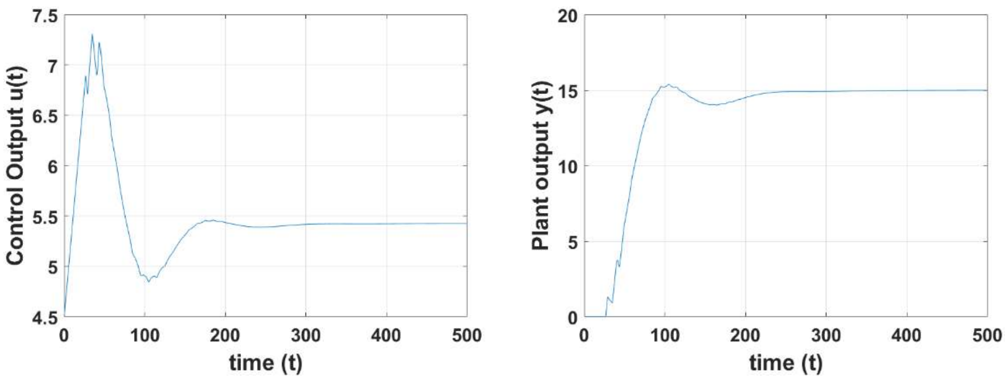

Figure 4.71. *Simulation results for* $(K_p, K_i) = (0.3, 0.006)$ *and* $\tau(t) = 30 + 5 + 10sin(\frac{2\pi}{10}t)$

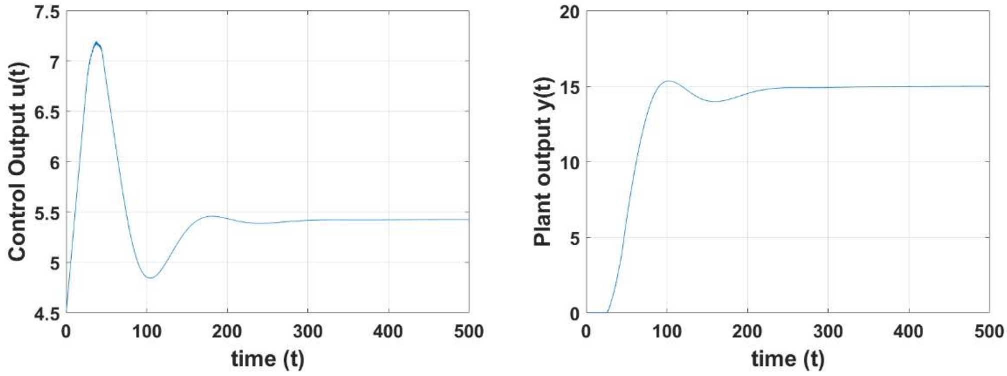

Figure 4.72. *Simulation results for* $(K_p, K_i) = (0.3, 0.006)$ *and* $\tau(t) = 30 + 5 + 10sin(\frac{2\pi}{1}t)$

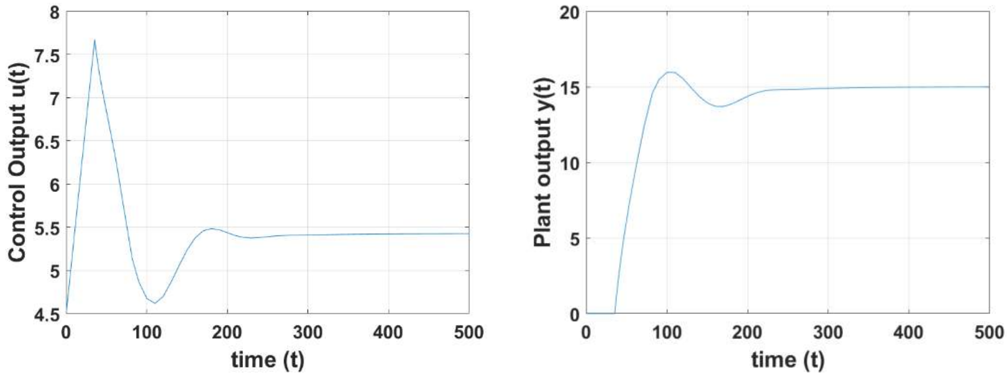

Figure 4.73. *Simulation results for* $(K_p, K_i) = (0.3, 0.006)$ *and* $\tau(t) = 30 + 10\ sin(\frac{2\pi}{400}t)$

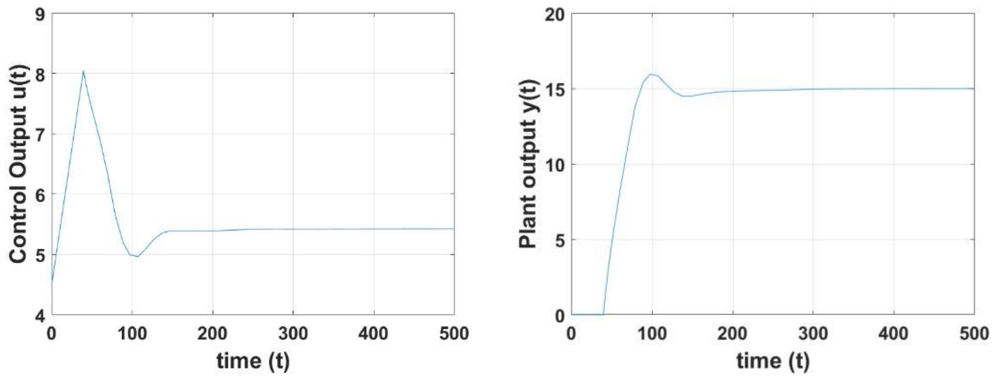

Figure 4.74. *Simulation results for* (K_p, K_i) $(0.3, 0.006)$ *and* $\tau(t) = 30 + 10sin(\frac{2\pi}{200}t)$

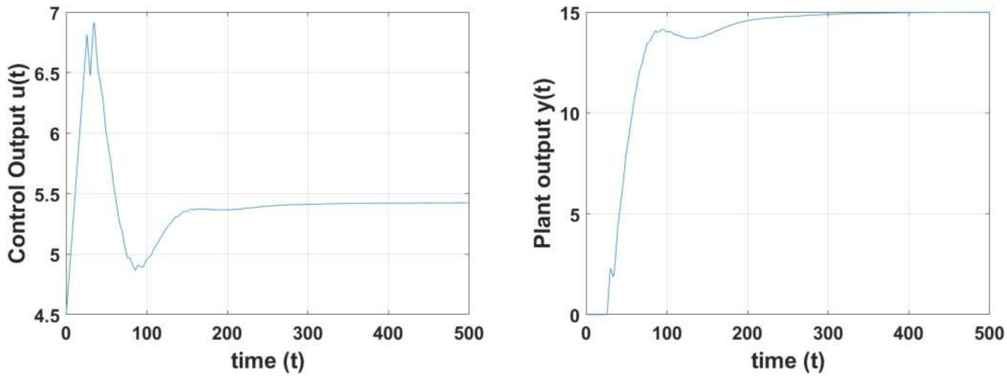

Figure 4.75. *Simulation results for (*K_p*,* K_i*)* $= (0.3, 0.006)$*and* $\tau(t) = 30 + 10sin(\frac{2\pi}{10}t)$

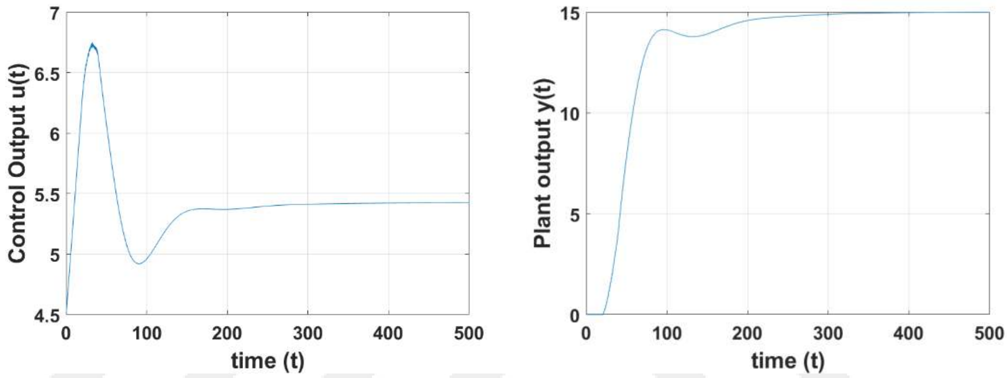

Figure 4.76. *Simulation results for (*K_p*,* K_i*)* $= (0.3, 0.006)$ *and* $\tau(t) = 30 + 10sin(\frac{2\pi}{1}t)$

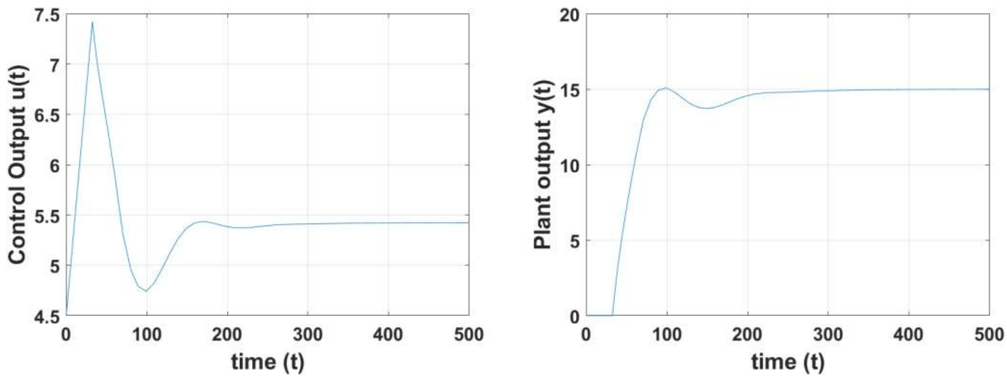

Figure 4.77. *Simulation results for (*K_p*,* K_i*)* $= (0.3, 0.006)$ *and* $\tau(t) = 30 + 5\ sin(\frac{2\pi}{400}t)$

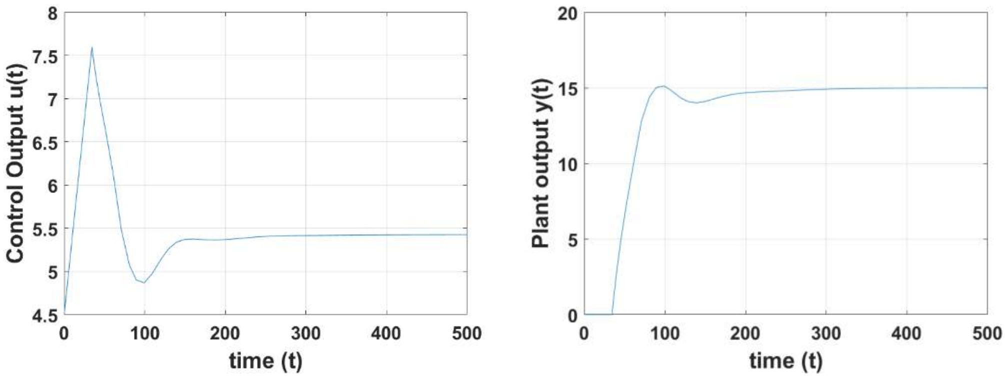

Figure 4.78. *Simulation results for* $(K_p,\ K_i) = (0.3, 0.006)$ *and* $\tau(t) = 30 + 5sin(\frac{2\pi}{200}t)$

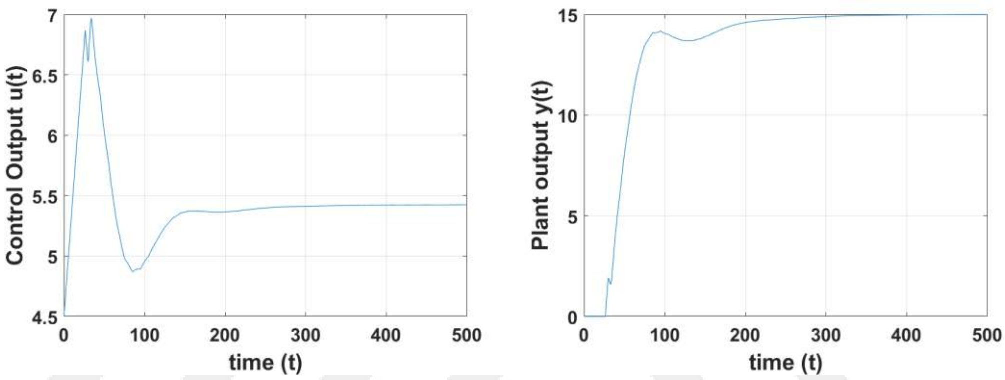

Figure 4.79. *Simulation results for* $(K_p,\ K_i) = (0.3, 0.006)$ *and* $\tau(t) = 30 + 5sin(\frac{2\pi}{10}t)$

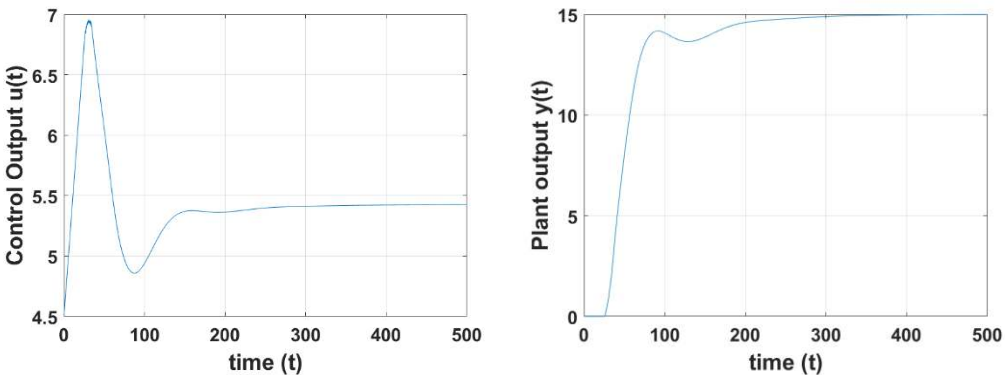

Figure 4.80. *Simulation results for* $(K_p,\ K_i) = (0.3, 0.006)$ *and* $\tau(t) = 30 + 5sin(\frac{2\pi}{1}t)$

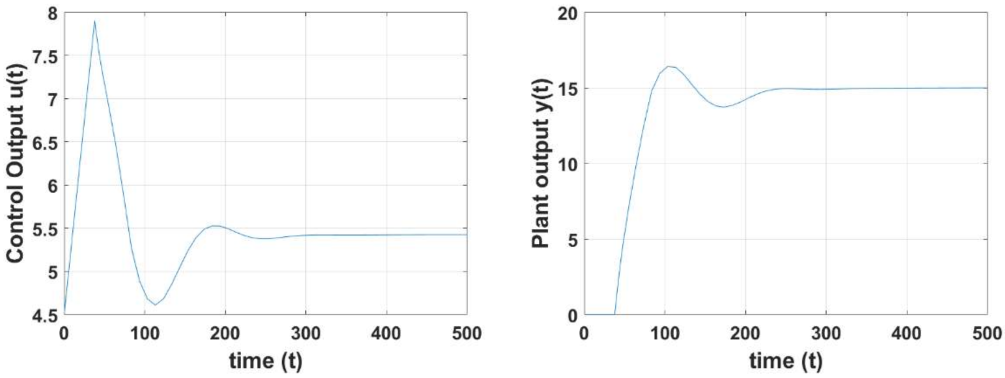

Figure 4.81. *Simulation results for* $(K_p,\ K_i) = (0.3, 0.006)$ *and* $\tau(t) = 30 + 5 + 5sin(\frac{2\pi}{400}t)$

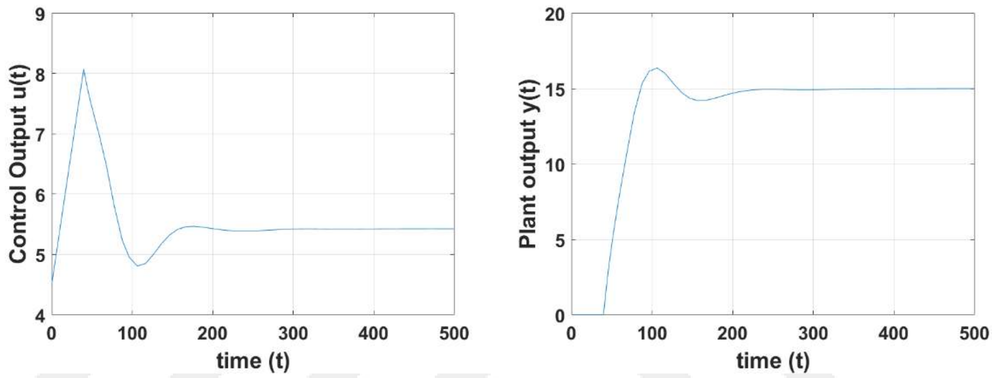

Figure 4.82. *Simulation results for* $(K_p,\ K_i) = (0.3, 0.006)$ *and* $\tau(t) = 30 + 5 + 5sin(\frac{2\pi}{200}t)$

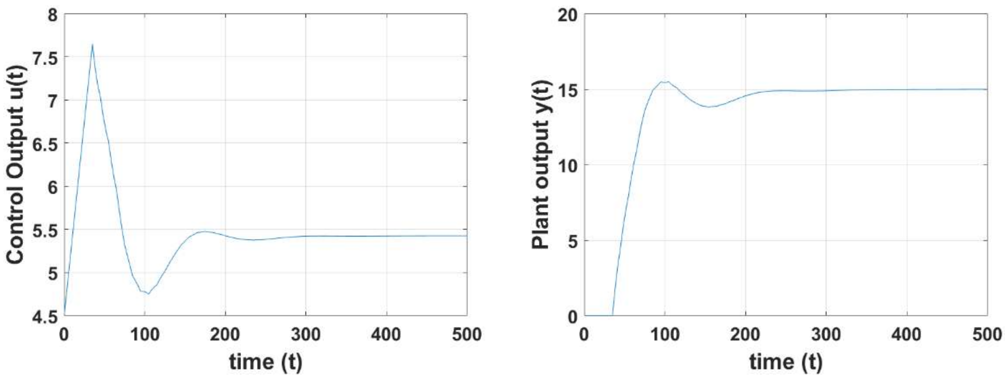

Figure 4.83. *Simulation results for* $(K_p,\ K_i) = (0.3, 0.006)$ *and* $\tau(t) = 30 + 5 + 5sin(\frac{2\pi}{10}t)$

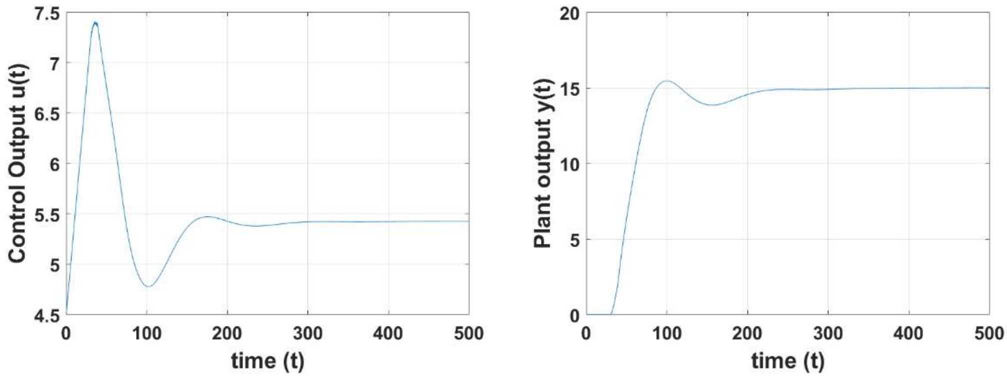

Figure 4.84. *Simulation results for* $(K_p, K_i) = (0.3, 0.006)$ *and* $\tau(t) = 30 + 5 + 5sin(\frac{2\pi}{1}t)$

As it is shown in the results of delay-based PI controller, the design objectives in presence of uncertain time-varying time-delays is satisfied. In presence of uncertain time-varying time-delays, the controller output has sharp variations whether the variation of delay is slow as it is seen from Figures 4.52, 4.54, 4.65 and 4.68. It is noticed that the overshoot in the plant output in presence of saml nominal delays is less than the large nominal delays as it is shown in Figures 4.55 and 4.73. Morever the maximum value of control output is larger when large nominal delay is presenced as it is presented in Figure 4.52, 4.55, 4.73 and 4.81. Note that in presence of large nominal delay the control output is less oscillated when variation of delay is fast as it is shown in Figures 4.73, 4.76, 4.77 and 4.80.

4.4 Robust PI controller

In order to design a robust PI controller which stabilizes the feedback system in presence of uncertain time-varying time-delay and achieves the design objectives, the approach proposed in Chapter 3 can be used. In order to design such a controller, first, a set of PI parameters, which stabilizes the feedback system in Figure 3.1 for $\Pi = P_0 e^{-hs}$ for a given h and ensuring the desired closed-loop requirements, is found in PI-parameter space. Then, for given weighting functions, where $W_1 := -\frac{s(b-ac)}{c(as+b)}$, and $W_2 := \frac{s+c}{as+b}$, where $a = \sqrt{\frac{1-\beta}{2}}$, $c = \frac{1}{\sqrt{2\delta}}$, and b is a positive free parameter, a set of PI parameters, which is in the above set and ensures the norm condition in (36), is found. Then, center of the biggest circle in later set is chosen as a desired PI controller. Then, robust PI controller parameters *Kp* and *Ki* for each case in Table 4.1 are obtained from the center of the circle given in Figures 4.85 to 4.87 (see Code 4.7).

For a realistic performance comparision of controllers, the feedback system in Figure 3.1 with Π, which corresponds to actual plant described at Chapter 2, is considered. By choosing the set point as 15, the pump input, corresponds to controller output, and, level output, correspods to level in Tank 2 in Figure 2.1, are presented in Figures 4.88 to 4.104 (see Codes 4.8, 4.9 and 4.10).

Table 4.1. *Design Parameter where b=2.*

Case	h	δ	β
1	10	1	0.3
2	10	5	0.8
3	25	5	0.8
4	40	10	0.8

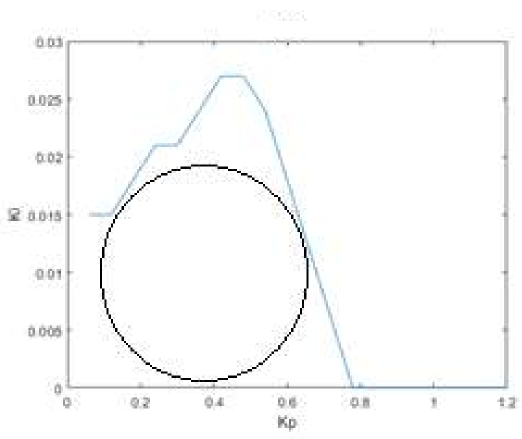

Figure 4.85. *The set of K_p and K_i ensuring design objectives for case 1 and case 2,*

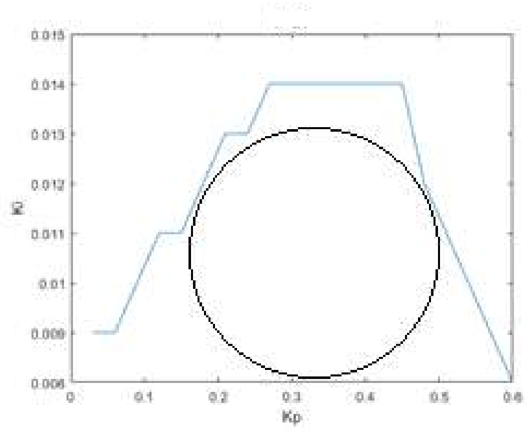

Figure 4.86. *The set of K_p and K_i ensuring design objectives for case 3,*

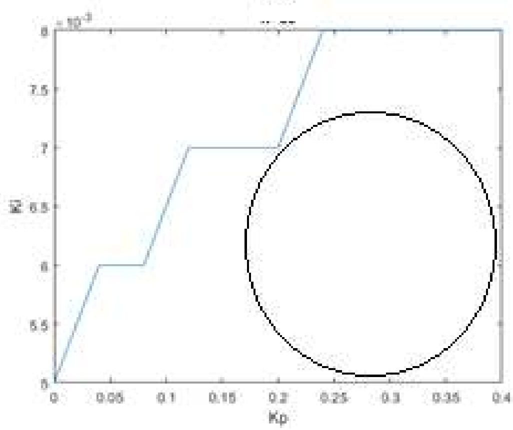

Figure 4.87. *The set of K_p and K_i ensuring design objectives* for case 4,

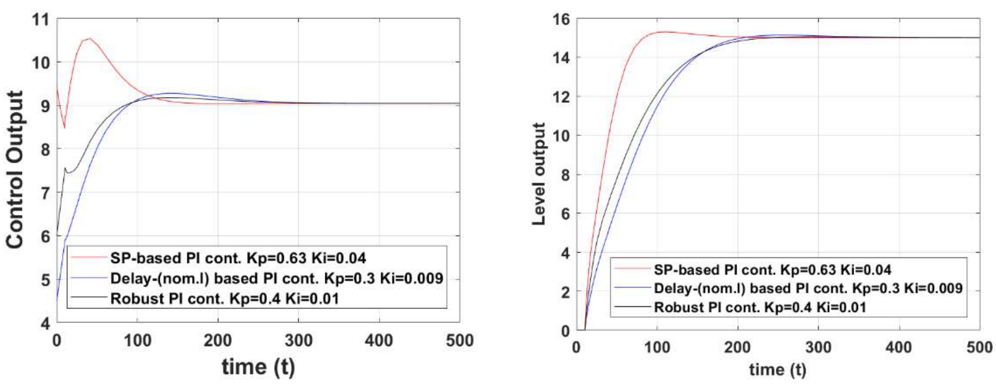

Figure 4.88. *Simulation results for* $\tau(t) = 10 + \frac{1}{8} + \frac{7}{8}\ sin(\frac{2\pi}{200}t)$

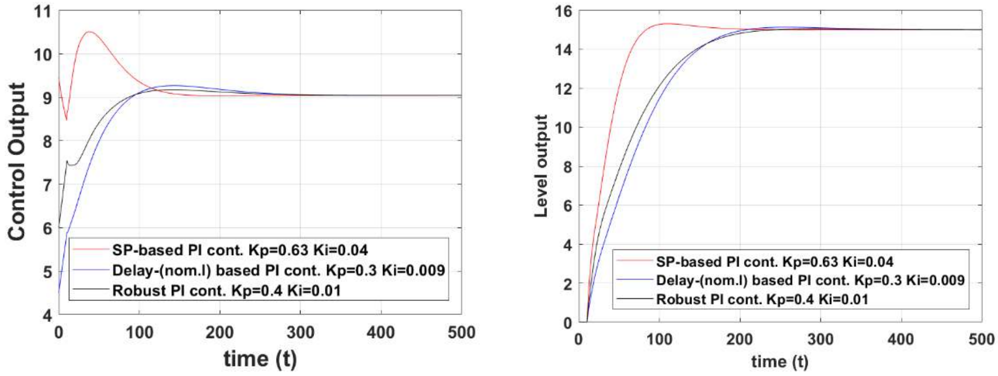

Figure 4.89. *Simulation results for* $\tau(t) = 10 + \frac{1}{8} + \frac{7}{8}\ sin\left(\frac{2\pi}{10}t\right)$

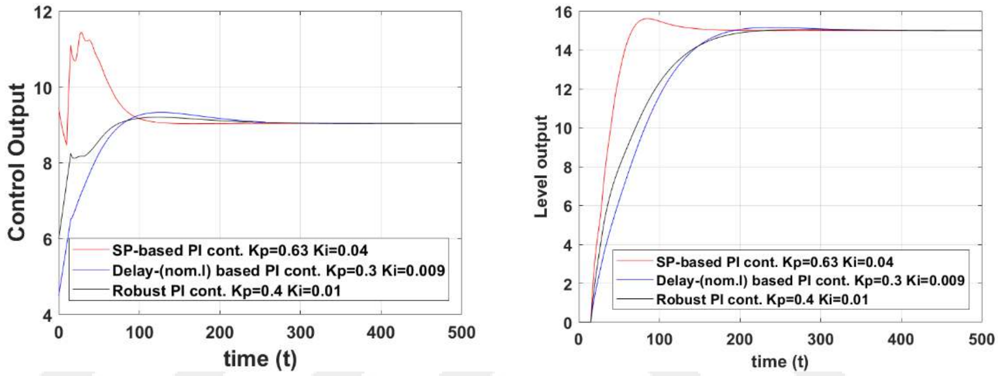

Figure 4.90. *Simulation results for* $\tau(t) = 10 + 5$

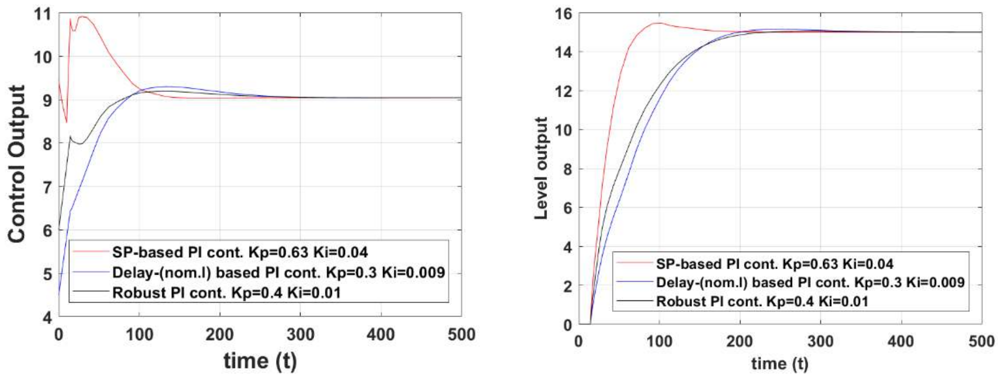

Figure 4.91. *Simulation results for* $\tau(t) = 10 + \frac{5}{2} + \frac{5}{2}\ sin(\frac{2\pi}{40}t)$

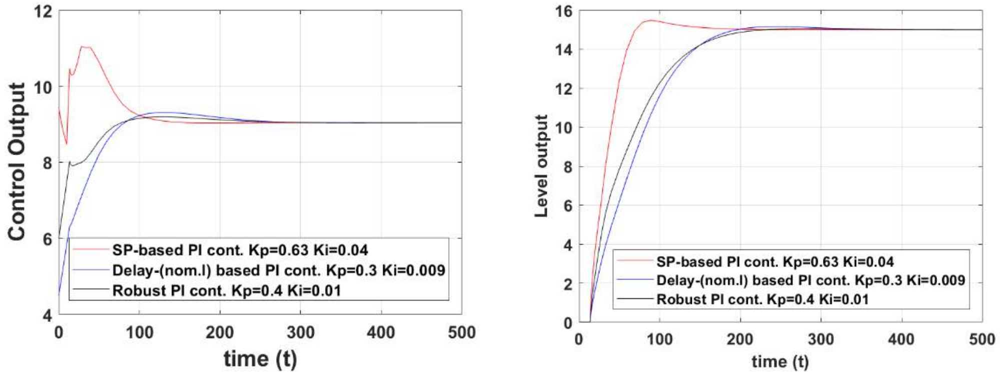

Figure 4.92. *Simulation results for* $\tau(t) = 10 + \frac{5}{2} + \frac{5}{2}\ sin(\frac{2\pi}{200}t)$

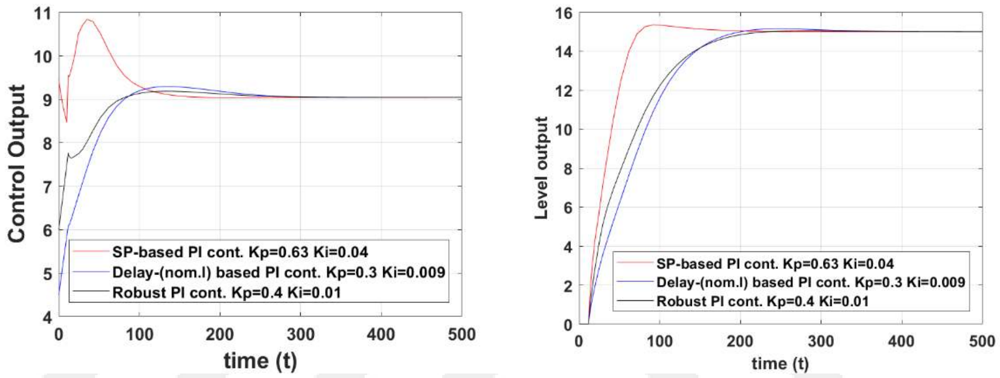

Figure 4.93. *Simulation results for* $\tau(t) = 10 + \frac{1}{8} + \frac{36}{8}\ sin(\frac{2\pi}{200}t)$

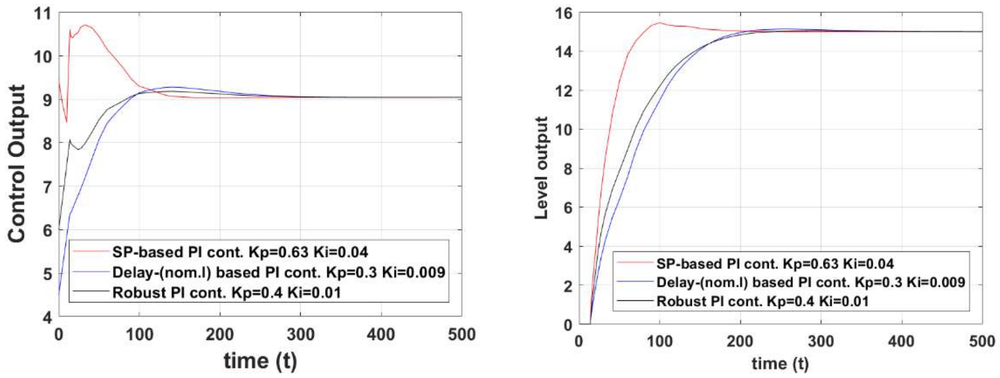

Figure 4.94. *Simulation results for* $\tau(t) = 10 + \frac{1}{8} + \frac{36}{8}\ sin(\frac{2\pi}{40}t)$

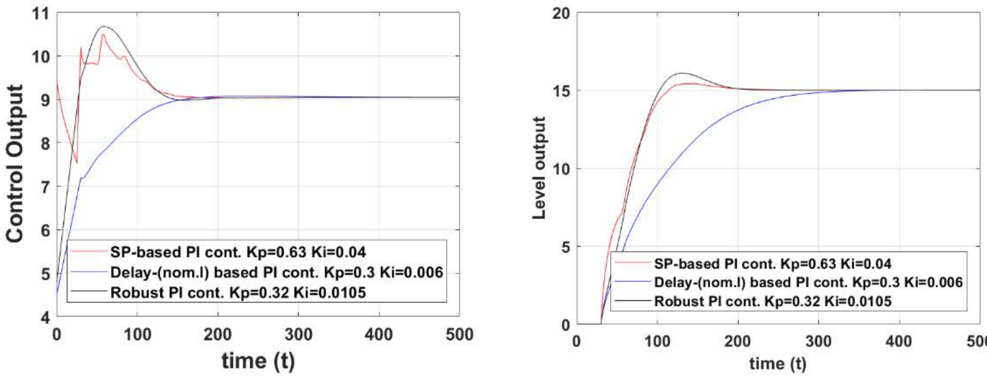

Figure 4.95. *Simulation results for* $\tau(t) = 25 + 5$

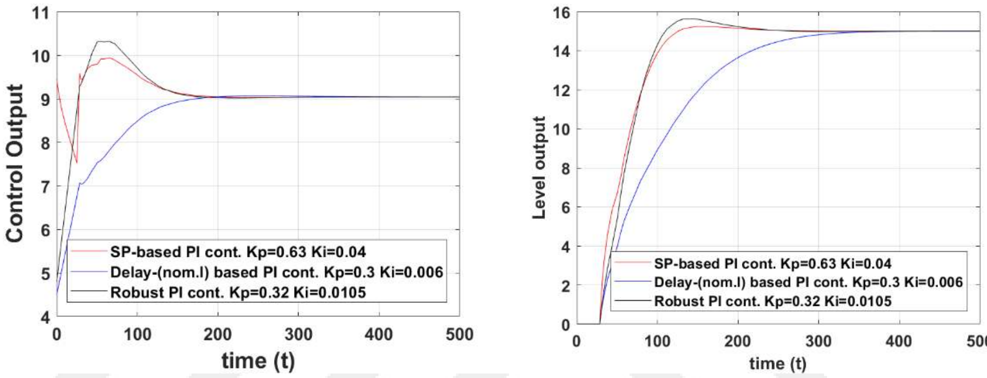

Figure 4.96. *Simulation results for* $\tau(t) = 25 + \frac{5}{2} + \frac{5}{2}\ sin(\frac{2\pi}{20}t)$

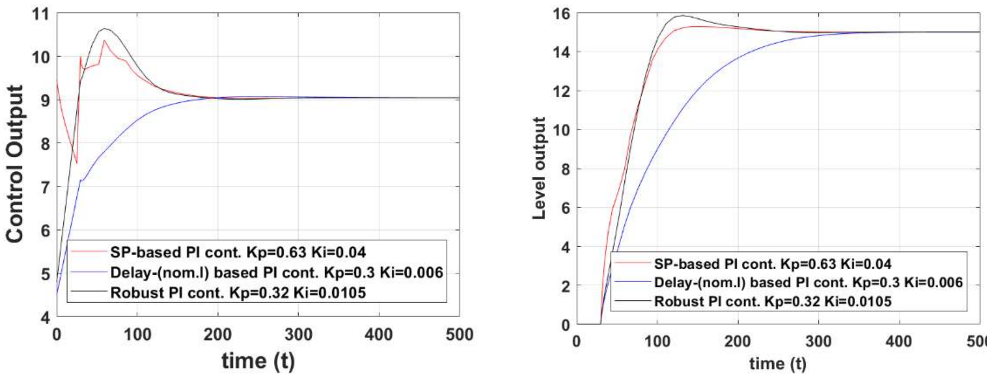

Figure 4.97. *Simulation results for* $\tau(t) = 25 + \frac{5}{2} + \frac{5}{2}\ sin(\frac{2\pi}{200}t)$

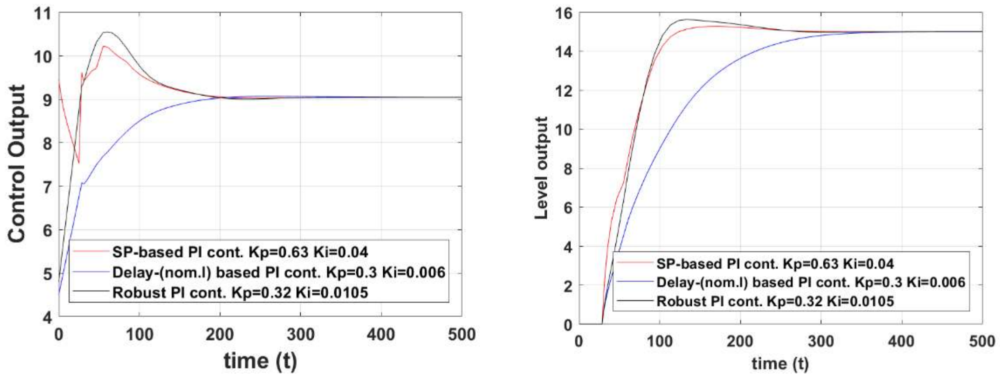

Figure 4.98. *Simulation results for* $\tau(t) = 25 + \frac{1}{8} + \frac{36}{8}\ sin(\frac{2\pi}{200}t)$

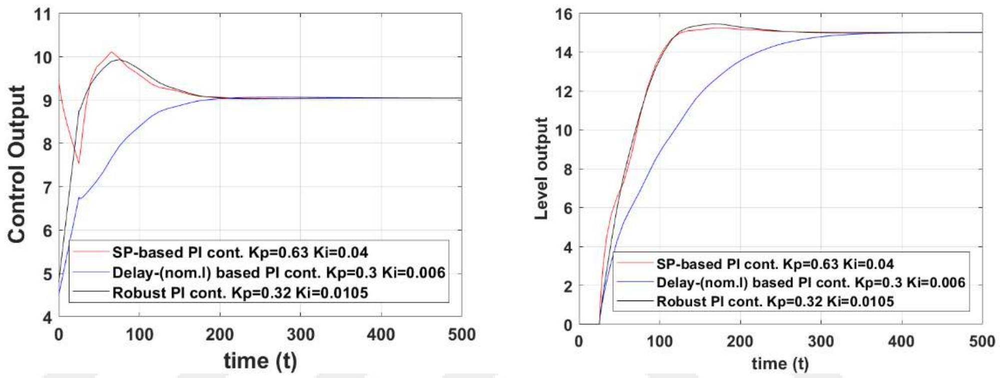

Figure 4.99. *Simulation results for* $\tau(t) = 25 + \frac{1}{8} + \frac{36}{8}\ sin(\frac{2\pi}{50}t)$

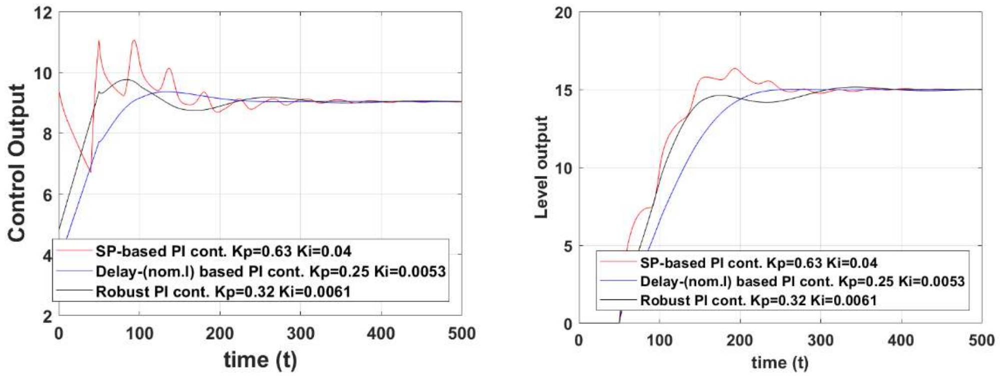

Figure 4.100. *Simulation results for* $\tau(t) = 40 + 10$

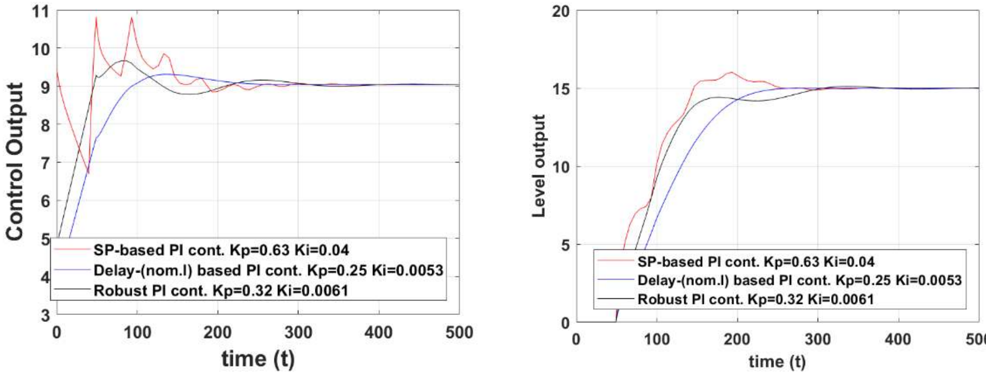

Figure 4.101. *Simulation results for* $\tau(t) = 40 + 9 + \frac{1}{2}\ sin(\frac{2\pi}{20}t)$

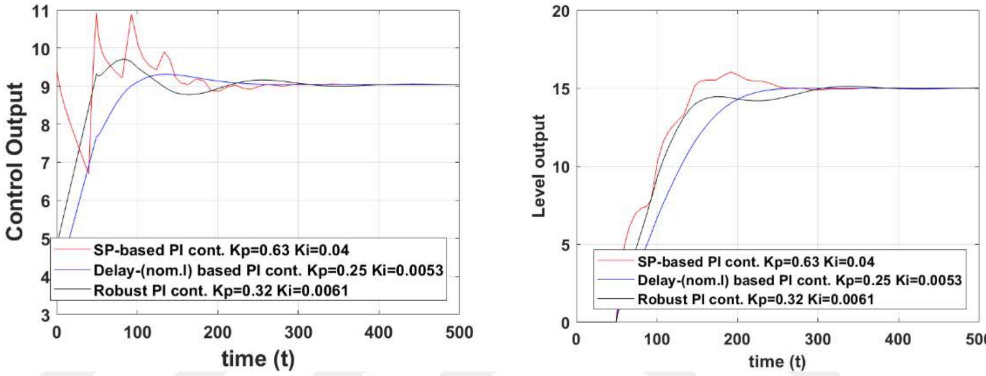

Figure 4.102. *Simulation results for* $\tau(t) = 40 + 9 + \frac{1}{2}\ sin(\frac{2\pi}{200}t)$

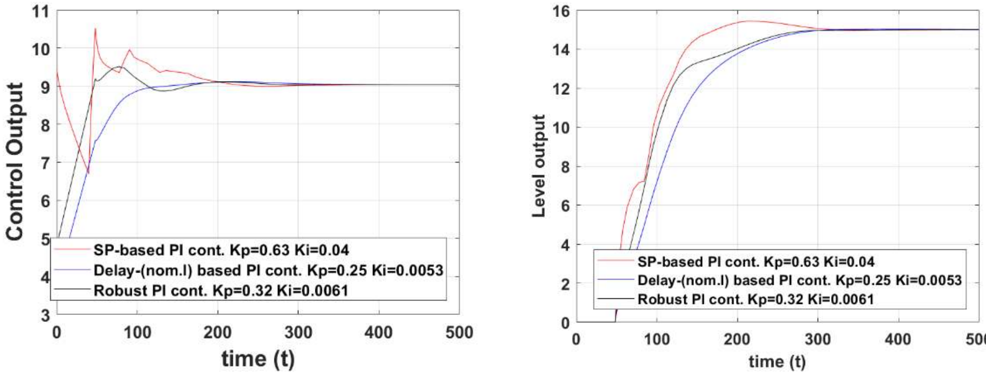

Figure 4.103. *Simulation results for* $\tau(t) = 40 + \frac{1}{8} + 8\ sin\left(\frac{2\pi}{200}t\right)$

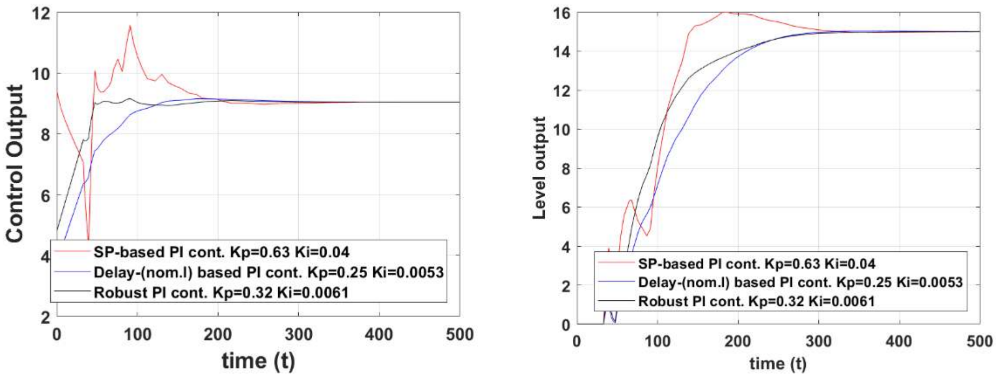

Figure 4.104. *Simulation results for* $\tau(t) = 40 + \frac{1}{8} + 8\, sin\left(\frac{2\pi}{40}t\right)$

As seen in the figures all controllers, the required level tanks are satisfied before the settling time constraint. Robust PI controller almost make more overshoot compared to other controllers, however for sufficiently large delay, SP based PI controllers result in large overshoot as it is seen in Figures 4.100 to 4.104. Furthermore, in presence of fast varying delays, the controller outputs may not be applicable in practice, since the actuator inputs look like having sharp behaviors. In addition, these behaviors are also observed for large nominal delays and is less effected of whatever the uncertain time-varying delay is fast of slow as it is shown in Figures 4.102 and 4.104. Moreover, the level output is faster and it has less settling time when small nominal delays are applied as seen by comparing Figures 4.91 and 4.101. However, in the robust control the level output has less rising time when large nominal delay is applied than small as it is presented in Figures 4.92 and 4.99.

Now the feedback system in Figure 3.1 with Π, which corresponds to the free delay (nominal plant) $P_o(s)$ given in (24), is considered. The simulation results are presented in Figures 4.105 to 4.121 (see Codes 4.11, 4.12 and 4.13).

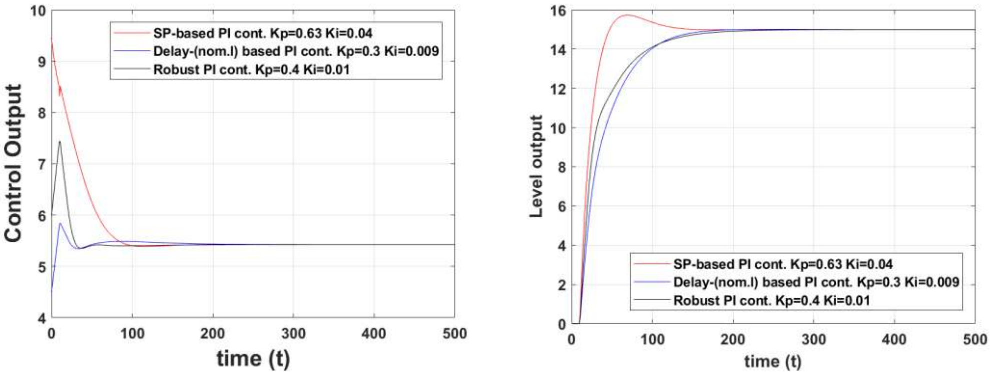

Figure 4.105. *Simulation results for* $\tau(t) = 10 + \frac{1}{8} + \frac{7}{8}\ sin(\frac{2\pi}{200}t)$

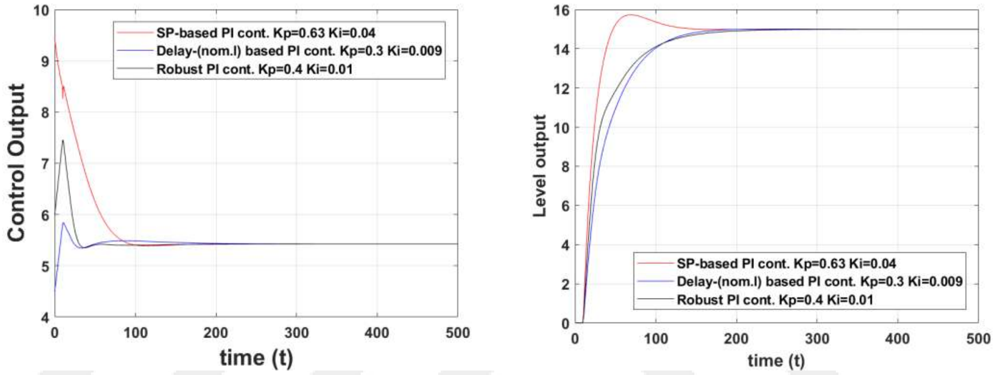

Figure 4.106. *Simulation results for* $\tau(t) = 10 + \frac{1}{8} + \frac{7}{8}\ sin\left(\frac{2\pi}{10}t\right)$

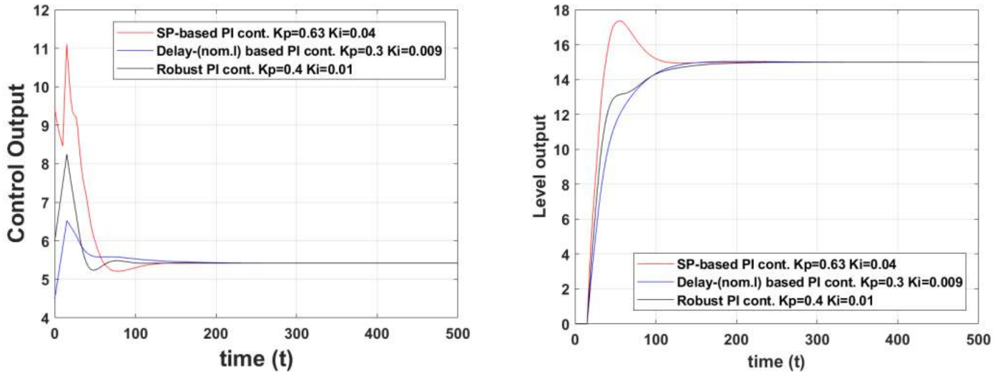

Figure 4.107. *Simulation results for* $\tau(t) = 10 + 5$

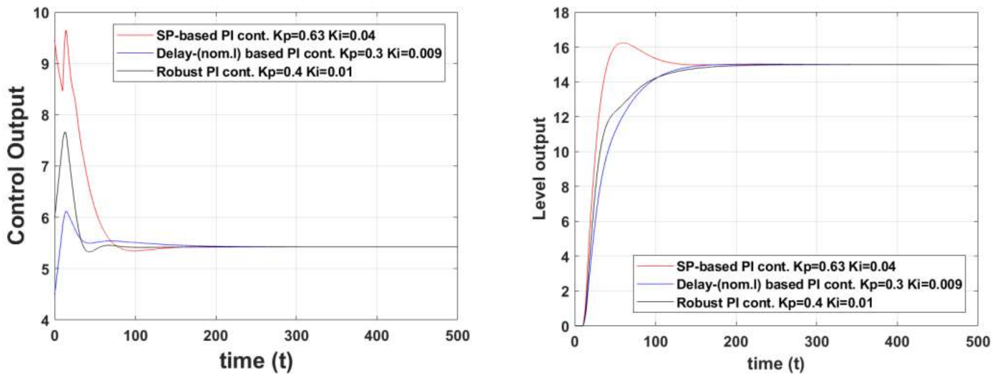

Figure 4.108. *Simulation results for* $\tau(t) = 10 + \frac{5}{2} + \frac{5}{2}\ sin(\frac{2\pi}{40}t)$

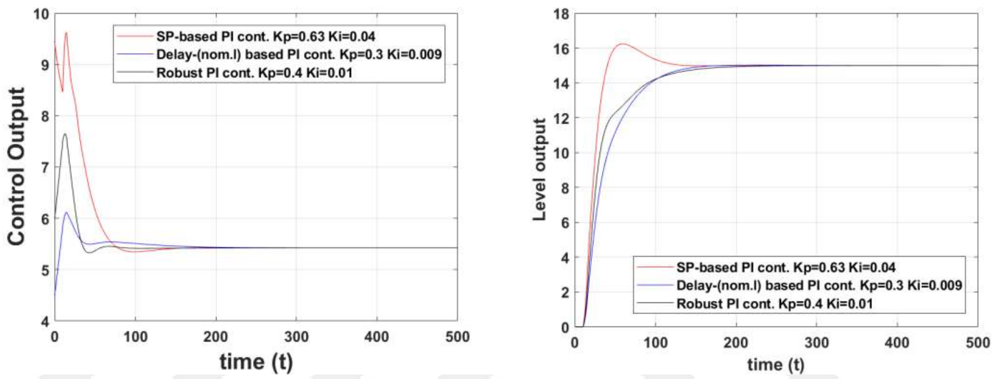

Figure 4.109. *Simulation results for* $\tau(t) = 10 + \frac{5}{2} + \frac{5}{2}\ sin(\frac{2\pi}{200}t)$

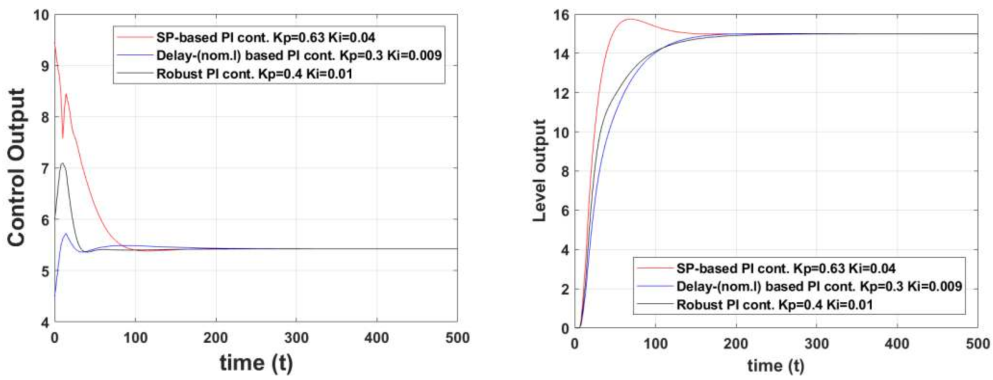

Figure 4.110. *Simulation results for* $\tau(t) = 10 + \frac{1}{8} + \frac{36}{8}\ sin(\frac{2\pi}{200}t)$

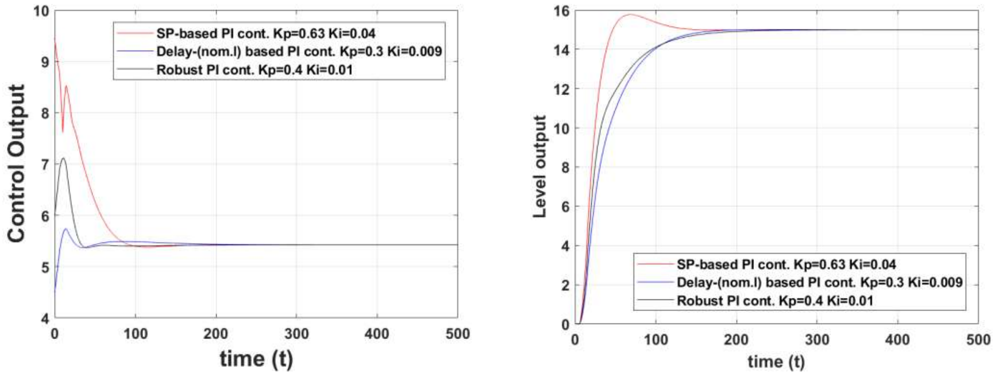

Figure 4.111. *Simulation results for* $\tau(t) = 10 + \frac{1}{8} + \frac{36}{8}\ sin(\frac{2\pi}{40}t)$

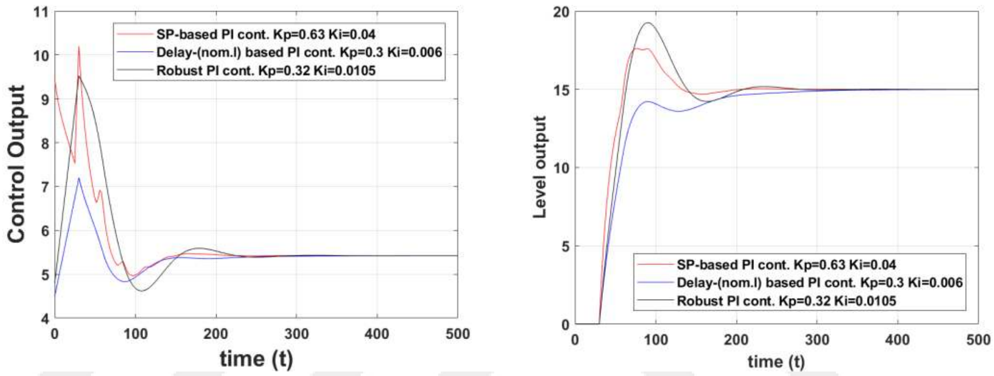

Figure 4.112. *Simulation results for* $\tau(t) = 25 + 5$

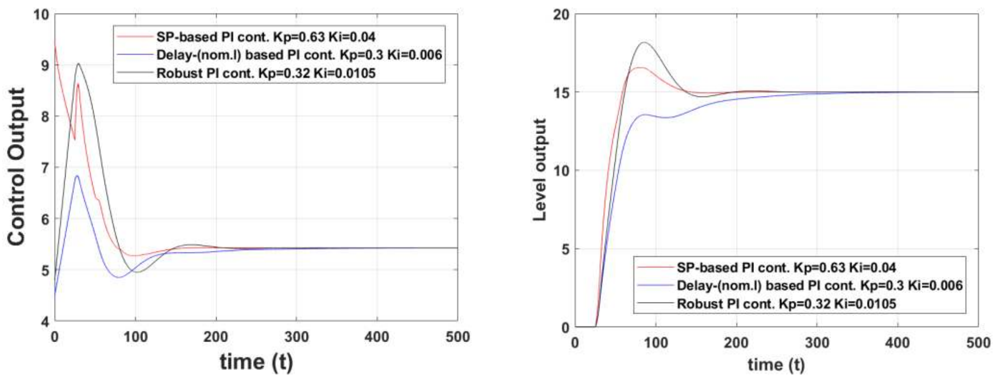

Figure 4.113. *Simulation results for* $\tau(t) = 25 + \frac{5}{2} + \frac{5}{2}\ sin(\frac{2\pi}{20}t)$

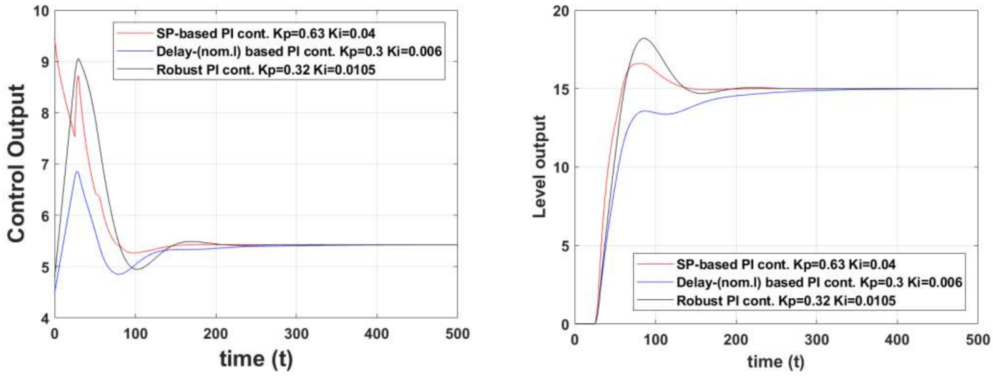

Figure 4.114. *Simulation results for* $\tau(t) = 25 + \frac{5}{2} + \frac{5}{2}\ sin(\frac{2\pi}{200}t)$

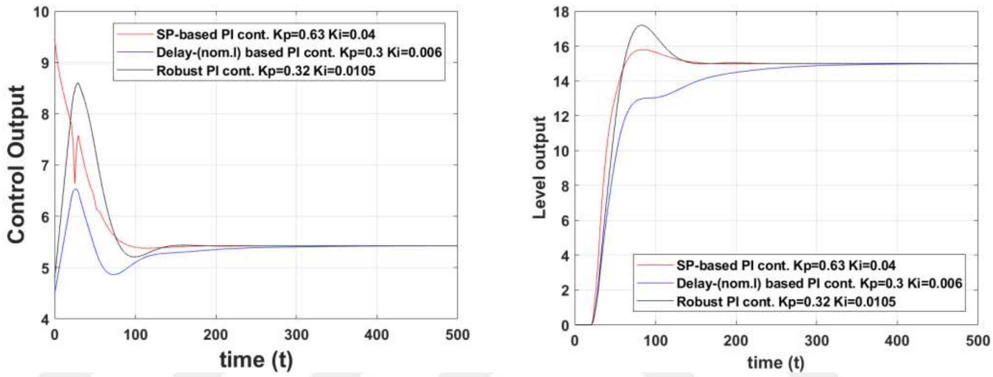

Figure 4.115. *Simulation results for* $\tau(t) = 25 + \frac{1}{8} + \frac{36}{8}\ sin(\frac{2\pi}{200}t)$

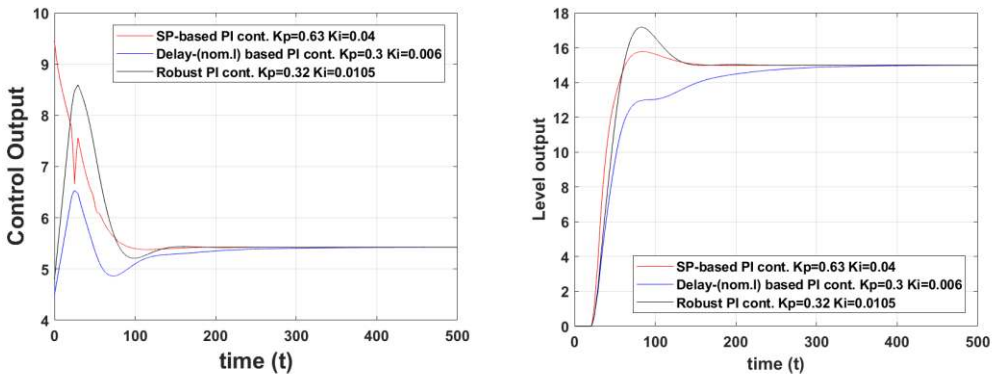

Figure 4.116. *Simulation results for* $\tau(t) = 25 + \frac{1}{8} + \frac{36}{8}\ sin(\frac{2\pi}{50}t)$

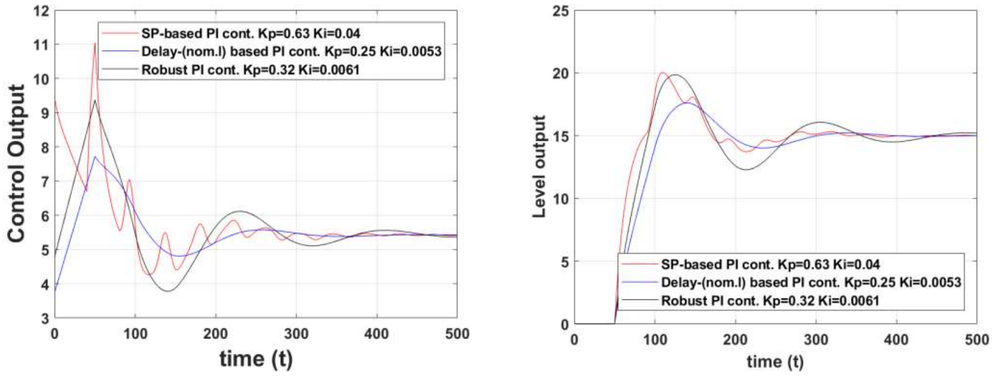

Figure 4.117. *Simulation results for* $\tau(t) = 40 + 10$

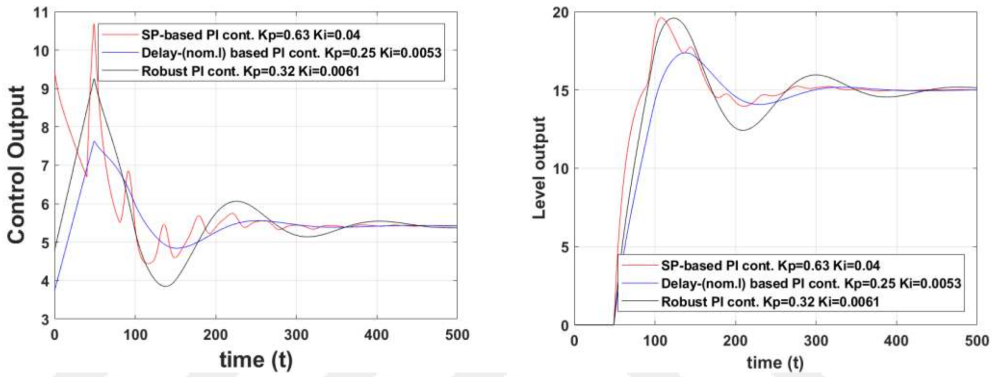

Figure 4.118. *Simulation results for* $\tau(t) = 40 + 9 + \frac{1}{2}\ sin(\frac{2\pi}{20}t)$

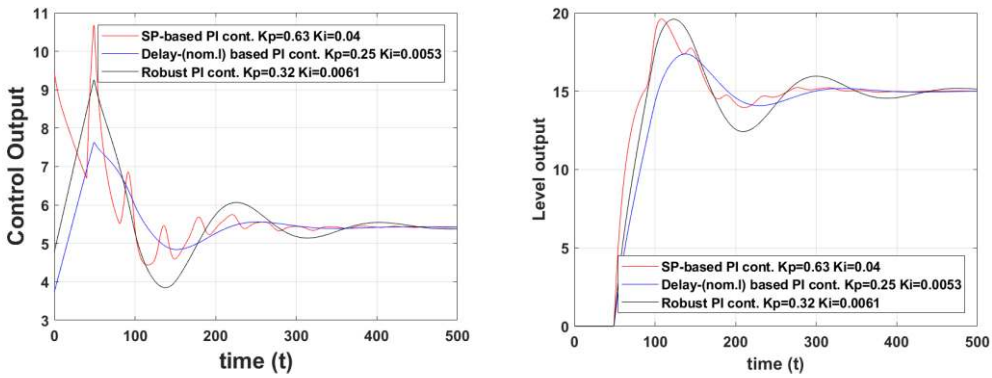

Figure 4.119. *Simulation results for* $\tau(t) = 40 + 9 + \frac{1}{2}\ sin(\frac{2\pi}{200}t)$

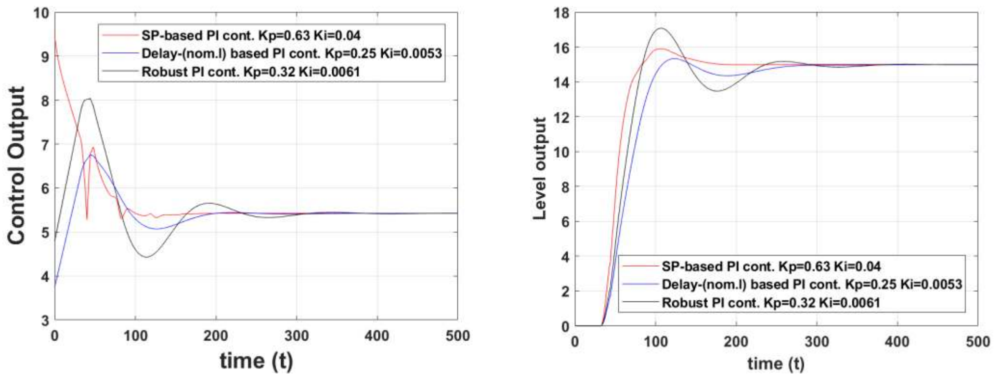

Figure 4.120. *Simulation results for* $\tau(t) = 40 + \frac{1}{8} + 8\,sin\left(\frac{2\pi}{200}t\right)$

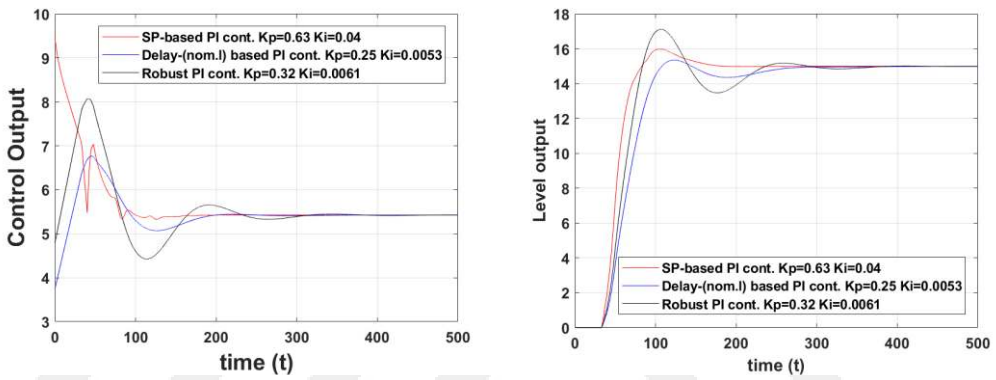

Figure 4.121. *Simulation results for* $\tau(t) = 40 + \frac{1}{8} + 8\,sin\left(\frac{2\pi}{40}t\right)$

As seen from Figure 4.105 to 4.121, all controllers robustly achieve the design objectives in presence of uncertain time-varying time-delays. It is observed from SP based PI controller, In presence of uncertain time-varying time-delays, while the delay variation is small or fast, the controller output shows sharp variations. As nominal delay increases, the overshoot becomes larger and the controller becomes more sensitive for the variations of uncertain time-delay. In comparison to other controllers, robust PI controllers almost always have more overshoot, but, for sufficiently high delays, SP-based PI controllers yield large overshoot, as seen in Figures 4.117 to 4.119. Furthermore, the controller outputs appear to have sharp behaviors in the presence of fast varying delays. Furthermore, as shown in Figures 4.117 to 4.121, same behaviors are also found for high nominal delays and are less affected by whether the uncertain time-varying delay is fast or slow. Moreover, the level output is faster and it has less settling time when small nominal delays are applied as seen by comparing Figures 4.05 and 4.121.

5. CONCLUSION

The performance of various PI controllers constructed for level control of coupled tanks system with uncertain time delays is investigated in this thesis. The Coupled Tanks system is a "Two-Tank" module consisting of a pump with a water basin and two tanks. Due to the transportation phenomena, the pump does not provide water to the tanks whenever a voltage is applied to it. Therefore, there exists a dead-time in the dynamics of the coupled tanks which affects the system behavior, so the $\mathscr{H}\infty$ controller design is considered for our SISO system with uncertain-time-varying-delay through analyzing the dead time in the input. By explaining the mathematical model of the coupled tanks system and linearized the non-linear equations of motion that describe the system, the free delay transfer function will be found which will be helpful in designing the controllers.

In this work, a sufficient condition for the existence of a controller is given, which can stabilize a given feedback system against uncertain time-varying delays. Then, using this condition, a robust PI controller design technique for coupled tanks is proposed, the input of which is affected by the uncertain time-varying time delay. In addition, Smith-Predictor and delay-based PI controller design techniques are proposed for the same system. Then, in order to examine the influence of the uncertain time-varying delay on the performance of these controllers, several simulation studies were carried out on the considered coupled tank system.

REFERENCES

[1] Alam, M. T., Khan, Z. H., Charan, P., & Ansari, M. A. (2015). Level control of coupled tanks system using feedback linearization control. *IJSRD - International Journal for Scientific Research & Development*, 60--63.

[2] Åström, K. J., & Hägglund, T. (2001). The future of PID control. *Control engineering practice*, 1163--1175.

[3] Åström, K. J., & Hägglund, T. (2004). Revisiting the Ziegler--Nichols step response method for PID control. *Journal of process control*, 635--650.

[4] Başar, T., & Bernhard, P. (2008). *H-infinity optimal control and related Minimax Design Problems.* Boston, Basel, Berlin: Springer Science and Business Media.

[5] Başçi, A., & Derdiyok, A. (20016). Implementation of an adaptive fuzzy compensator for coupled tank liquid level control system. *Measurement*, 12--18.

[6] Cengel, Y., & Cimbala, J. (2010). Mass, Bernolli, and Energy Equation. In *Fluid Mechanics: Fundamentals And Applications (Si Units)* (pp. 141-242). Tata McGraw Hill Education Private Limited.

[7] Chidambaram, M., & Sree, R. P. (2003). A simple method of tuning PID controllers for integrator/dead-time processes. *Computers and chemical engineering*, 211--215.

[8] Gu, K., & Niculescu, S.-I. (2003). Survey on recent results in the stability and control of time-delay systems. *Journal of Dynamic Systems Measurement and Control*, 158--165.

[9] Ho, L. N., Wahab, N. A., & Shehu, I. A. (2016, 05 30). Control of a coupled tank system using PI controller with advanced control methods. *Jurnal Teknologi*, 42-43.

[10] Kao, C.-Y., & Rantzer, A. (2007). Stability analysis of systems with uncertain time-varying delays. *Automatica*, 959--970.

[11] Lee, Y., Lee, J., & Park, S. (2000). PID controller tuning for integrating and unstable processes with time delay. *Chemical engineering science*, 3481--3493.

[12] Maxim, A. ; Ionescu, C.; Keyser, R. De. (2016). Modelling and identification of a coupled sextuple water tank system. *2016 IEEE International Conference on Automation, Quality and Testing, Robotics (AQTR)*, (pp. 1--6). Cluj-Napoca.

[13] Meinsma, G., & Mirkin, L. (2003). $\mathscr{H}\infty$ control of systems with multiple i/o delays. *IFAC Proceedings Volumes*, 191-196.

[14] Meinsma, G., Mirkin, L., & Zhong, Q.-C. (2002). Control of systems with {I/O} delay via reduction to a one-block problem. *IEEE Transactions on Automatic Control*, 1890 - 1895.

[15] Michiels, W., Fridman, E., & Niculescu, S.-I. (2009). Robustness assessment via stability radii in delay parameters. *International Journal of Robust and Nonlinear Control*, 1405--1426.

[16] O'Dwyer, A. (2000). A summary of PI and PID controller tuning rules for processes with time delay. Part 1: PI controller tuning rules. *IFAC Proceedings Volumes*, 159--164.

[17] Özbay, H., & Gündeş, A. N. (2007). Resilient PI and PD controller designs for a class of unstable plants with I/O delay. *Applied and Computational Mathematics: an international journal*, 18--26.

[18] Pan, H., Wong, H., Kapila, V., & de Queiroz, M. S. (2005). Experimental validation of a nonlinear backstepping liquid level controller for a state coupled two tank system. *Control Engineering Practice*, 27--40.

[19] Shehu, I. A., & Wahab, N. A. (2016). Applications of MPC and PI controls for liquid level control in coupled-tank systems. *2016 IEEE International Conference on Automatic Control and Intelligent Systems (I2CACIS)* (pp. 119--124). IEEE.

[20] Skogestad, S. (2003). Simple analytic rules for model reduction and PID controller tuning. *Journal of process control*, 291--309.

[21] Tandoh, H., Cao, Y., & Awoyomi, A. (2017). Smith predictor for slug control with large valve stroke time. *Computer Aided Chemical Engineering* (pp. 1531--1536). Elsevier.

[22] Tijjani, A. S., Shehu, A. M., Alsabari, A. M., & Sambo, Y. A. (2017). Performance Analysis for Coupled-Tank System Liquid Level Control using MPC, PI and PI-plus-Feedforward Control Scheme. *Journal of Robotics and Automation*, 42--53.

[23] Ünal , H., & İftar, A. (2008). A small gain theorem for systems with non-causal subsystems. *Automatica*, 2950-2953.

[24] Ünal, H. U. (2010). H_inf controller design for uncertain multiple-time-delay systems. *Ph.D. dissertation.* Eskişehir, Turkey: Anadolu University.

[25] Ünal, H. U., & Iftar, A. (2008). Utilization of non-causal uncertainty blocks in the robust flow controller design problem for data-communication networks. *2008 IEEE International Conference on Control Applications*, (pp. 61-66).

[26] Ünal, H. U., Melchor-Aguilar, M., Üstebay, D., Niculescu, S.-I., & Özbay, H. (2000). Comparison of PI controllers designed for the delay model of TCP/AQM networks. *Chemical engineering science*, 3481--3493.

[27] Warrad, S. B., Boubaker, O., Lungu, M., & Zhu, Q. M. (2019). On Unknown Input Observer Design for Linear Systems With Delays in States and Inputs. *New Trends in Observer-Based Control* (pp. 119-139).

[28] Vyhlídal T., Zítek P. (2014). QPmR - Quasi-Polynomial Root-Finder: Algorithm Update and Examples. *New Trends in Observer-Based Control* (pp. 119-139). In: Vyhlídal T., Lafay JF., Sipahi R. (eds) Delay Systems. Advances in Delays and Dynamics, Springer, Cham. https://doi.org/10.1007/978-3-319-01695-5_22.

[29] Quanser Coupled Tanks Modeling and Parameters, User manual.

[30] Niculescu, S.-I. (2001). *Delay Effects on Stability, a Robust Control Approach, Lecture Notes in Control and Information Sciences* (vol. 269). London: Springer Science and Business Media.

[31] Curtain, R., & Zwart, H. (2012). *Introduction to infinite-dimensional systems theory: a state-space approach* (vol. 21). New York: Springer Science and Business Media.

[32] Niculescu, S.-I., & Gu, K. (2012). *Advances in time-delay systems* (vol. 38). Springer Science and Business Media.

[33] Zhou, K., Doyle, J. C., & Glover, K. (1996). *Robust and optimal control.* Prentice Hall, Englewood Cliffs, . U.S.A.

APPENDIX

In the following, we will present the m-files which are used to design the controllers and present the time domain responses. In the codes, sim('A_B_ C') corresponds to model name A_B_C.

Code 4.1

```
clear all
close all

Kpm = [];
Kim = [];
Kp=1;
while Kp>=0
    Ki=0;
    Kimm=[0];

    while Ki>=0 && Ki<1

Tf=500;                          % the period of simulation
sim('free_delay_plant',Tf);
Yout=simout.signals.values;   % a code which import the results from Simullink
t=simout.time;
uc=Yout(:,1);
M=max(uc);
        if M < 12
            Kimm=[Kimm Ki];
            Ki=Ki+0.01;
        else
            Ki=-1;
        end
    end
    Kim=[Kim max(Kimm)];
    Kp=Kp-0.01
end
Kpint=[1:-0.01:0.01];
plot(Kpint,Kim)
xlabel('Kp')
ylabel('Ki')

 grid on
 hold on
%%%%%%%%%%%%%%%%%%%%%%%%%%%%%%%%%%%%%%%%%%%%%%%%%%%%%%%%%%
```

```
Kpm = [];
Kim = [];

s = tf('s');
Kp=1;
while Kp>=0
    Ki=0;
    Kimm=[0];

    while Ki>=0 && Ki<1

C = Kp + Ki/s;
P = tf([0 0.127 0.0080109],[1 0.1359 0.0029]);  % The free delay transfer function
H = P*C*(1+P*C)^(-1);  % The closed loop transfer function

t = [0:1000];
u = max(0,min(15*t,15));  % the input signal ( step function ).

Y =lsim(H,u,t);           % The function which find the responce.

S1 = lsiminfo(Y);
S2 = S1.Max;              % The overshoot values

if (S2<17.25) % The overshoot less than 15%

            Kimm=[Kimm Ki];
            Ki=Ki+0.01;
        else
            Ki=-1;
        end
    end
    Kim=[Kim max(Kimm)];
    Kp=Kp-0.01
end


Kpint=[1:-0.01:0.01];
plot(Kpint,Kim)
xlabel('Kp')
ylabel('Ki')

hold on

legend({'Q4','Q2'},'Location','southeast')
```

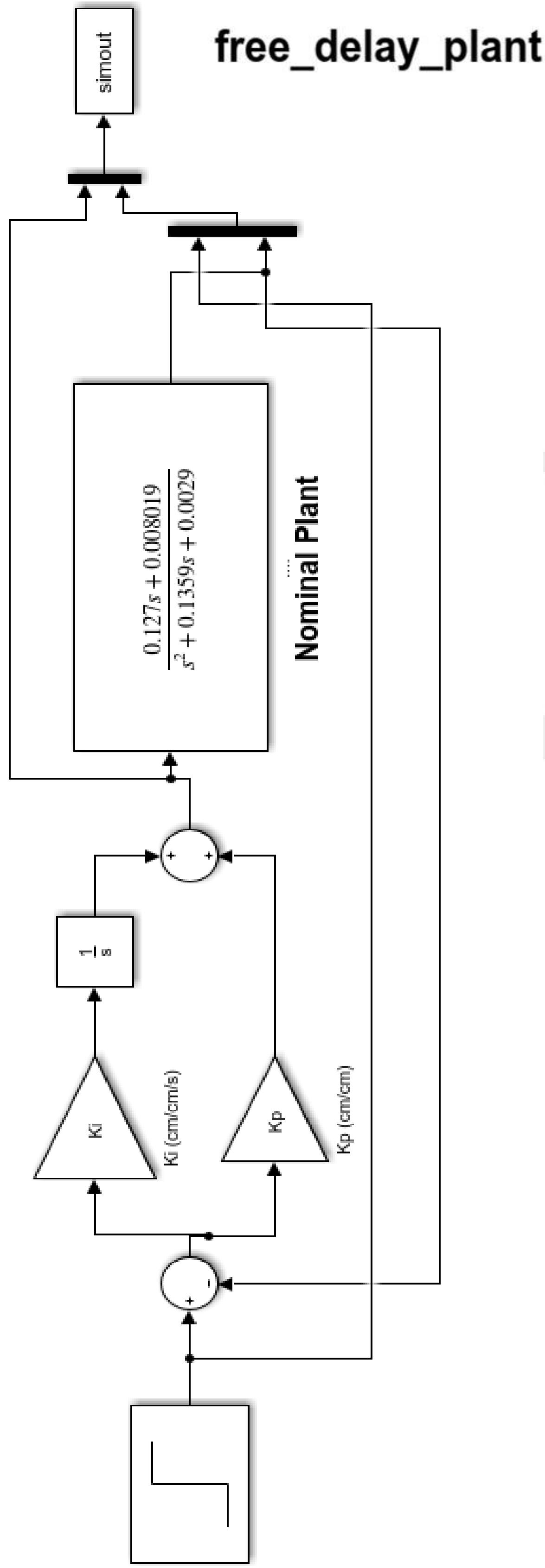

free_delay_plant
simout
$\frac{0.127s+0.008019}{s^2+0.1359s+0.0029}$
Nominal Plant
$\frac{1}{s}$
Ki
Ki (cm/cm/s)
Kp
Kp (cm/cm)

Code 4.2

```
%tau(t)=h+a+b*sin(freq*t)

Kp=0.63;
Ki=0.04;

h=12;
a=0 ;
b=10;
freq=2*pi/400;

Tf=500;

sim('Actual_and_Nominal_Plant_time_variant_delay',Tf);

Yout1=simout1.signals.values;
t=simout1.time;
uc1=Yout1(:,1);
y1=Yout1(:,3);

Yout2=simout2.signals.values;
t=simout2.time;
uc2=Yout2(:,1);
y2=Yout2(:,3);

figure(1)
plot(t,y,'r',t,y1,'b',t,y2,'k' );
set(gca,'FontName','Helvetica','FontSize',13,'FontWeight','Bold')
xlabel('time (t)','FontName','Helvetica','FontSize',14,'FontWeight','Bold');
ylabel('Level output','FontName','Helvetica','FontSize',14,'FontWeight','Bold');
grid on
legend({'Nominal Plant with time variant delay','Actual Plant with time variant delay'})
saveas(gcf,['Lvel_hs' num2str(k)],'png');

figure(2)
plot(t,uc,'r',t,uc1,'b',t,uc2,'k' );
set(gca,'FontName','Helvetica','FontSize',14,'FontWeight','Bold')
xlabel('time (t)','FontName','Helvetica','FontSize',18,'FontWeight','Bold');
ylabel('Control Output','FontName','Helvetica','FontSize',18,'FontWeight','Bold');
grid on
legend({'Nominal Plant with time variant delay','Actual Plant with time variant delay'})
saveas(gcf,['control_hs' num2str(k)],'png');
```

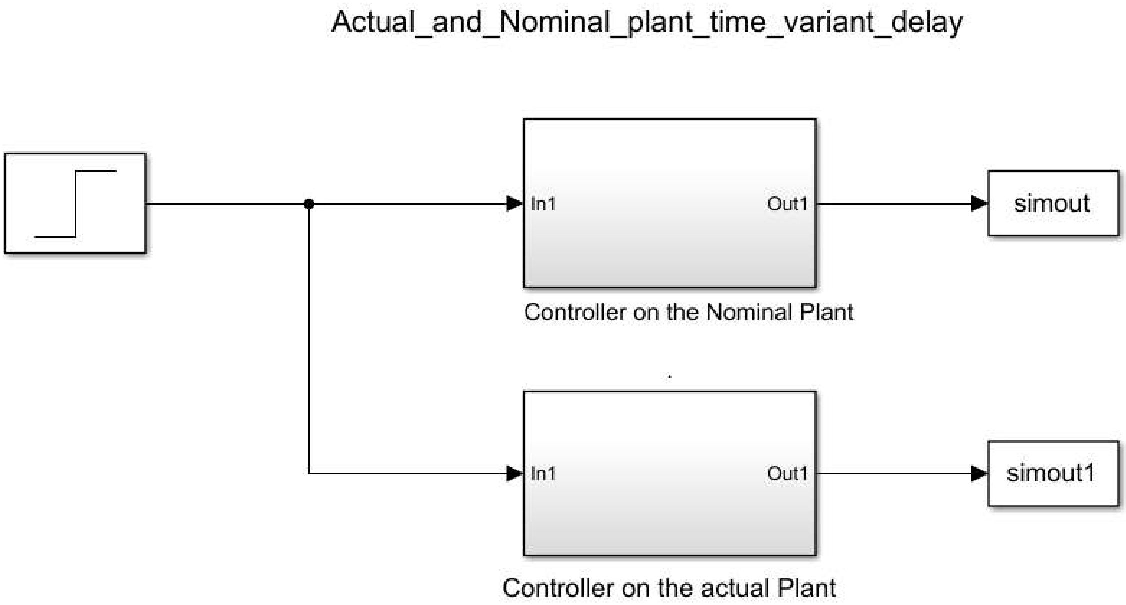
Actual_and_Nominal_plant_time_variant_delay
In1
Out1
simout
Controller on the Nominal Plant
In1
Out1
simout1
Controller on the actual Plant

Controller on the Nominal Plant

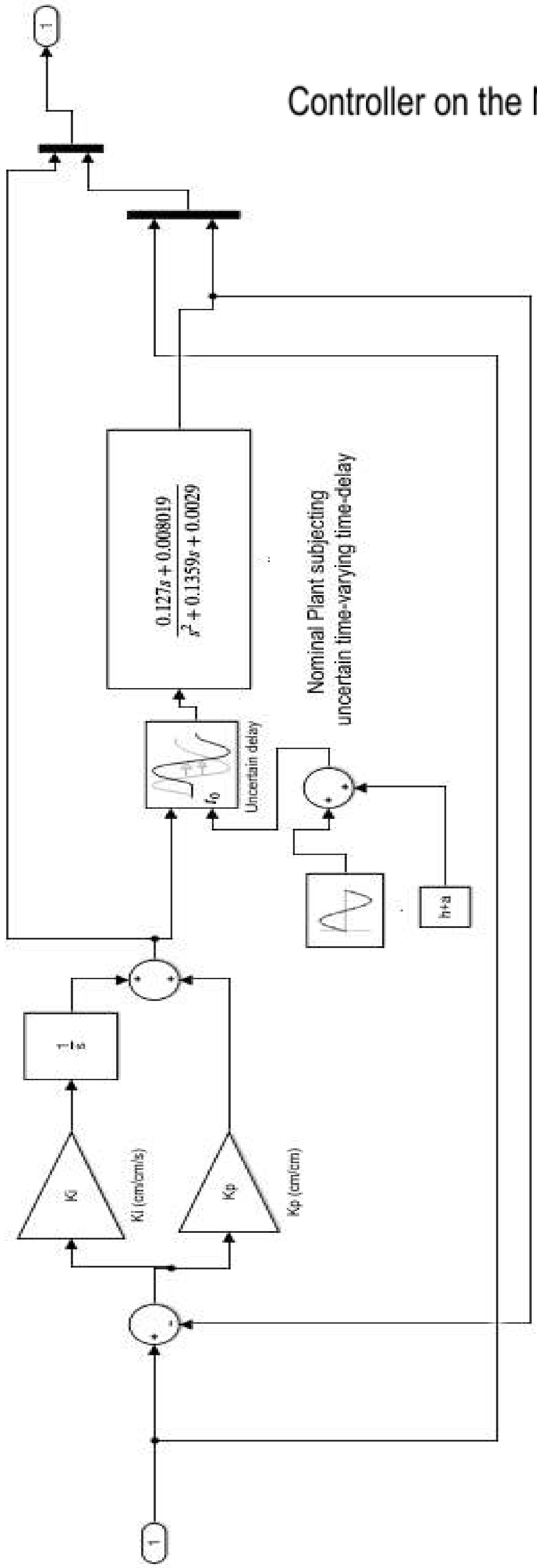

Controller on the actual Plant

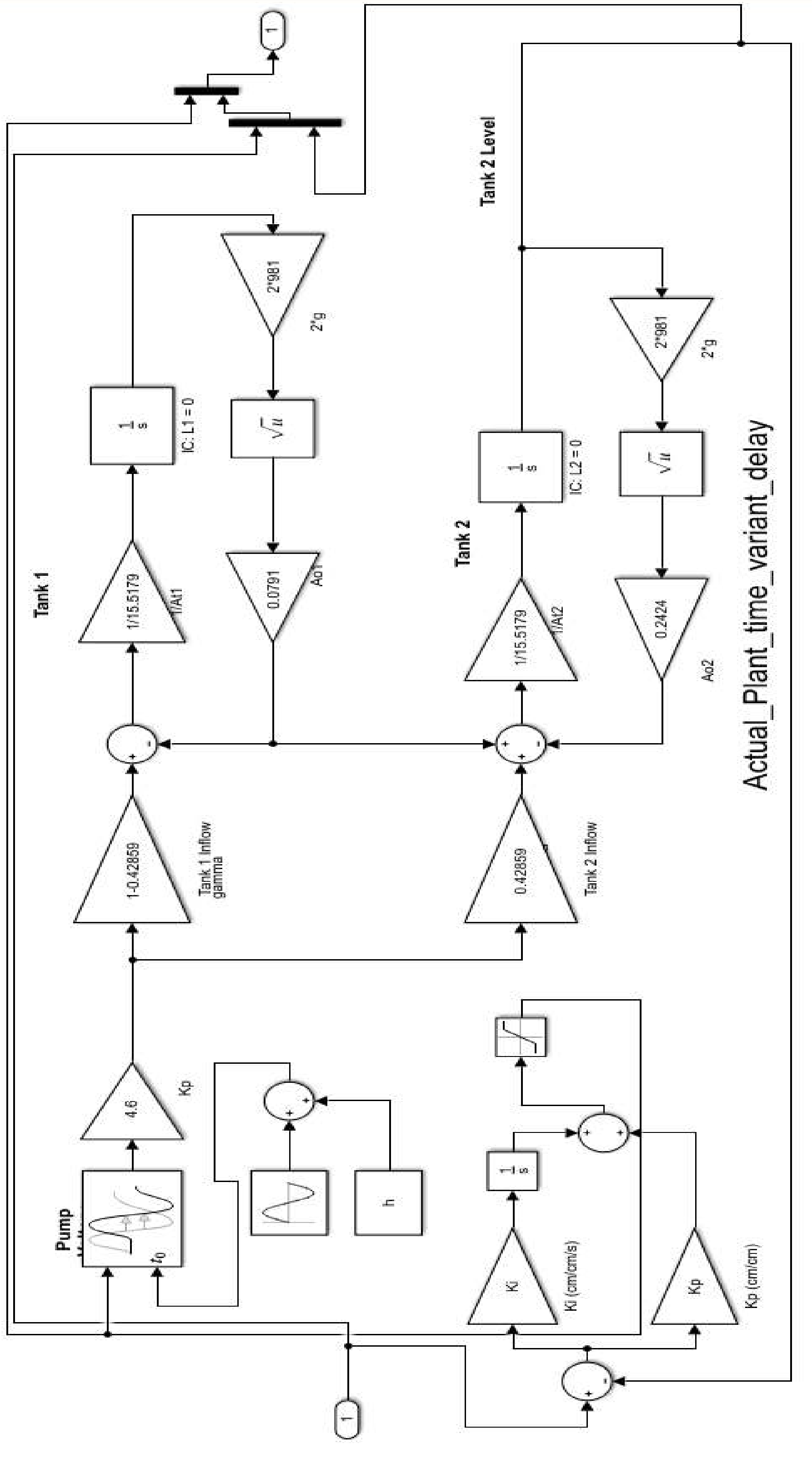

Code 4.3

```
%tau(t)=h+a+b*sin(freq*t)

Kp=0.56;
Ki=0.037;

h=50;
a=0 ;
b=0;
freq=1;

Tf=500;                      % the period of simulation
sim('Smith_Predictor_based_PI_controller',Tf);
Yout=simout.signals.values;  % a code which import the results from Simullink
t=simout.time;
uc=Yout(:,1);                % The control signal
y=Yout(:,3);                 % The Level signal

figure(1)
plot(t,uc);
set(gca,'FontName','Helvetica','FontSize',15,'FontWeight','Bold')
xlabel('time (t)','FontName','Helvetica','FontSize',18,'FontWeight','Bold');
ylabel('Control Output u(t)','FontName','Helvetica','FontSize',18,'FontWeight','Bold');
grid on
saveas(gcf,['control_P0tau' num2str(k)],'png');

figure(2)
plot(t,y);
set(gca,'FontName','Helvetica','FontSize',15,'FontWeight','Bold')
xlabel('time (t)','FontName','Helvetica','FontSize',18,'FontWeight','Bold');
ylabel('Plant output y(t)','FontName','Helvetica','FontSize',18,'FontWeight','Bold');
grid on
saveas(gcf,['Lvel_P0tau' num2str(k)],'png');
```

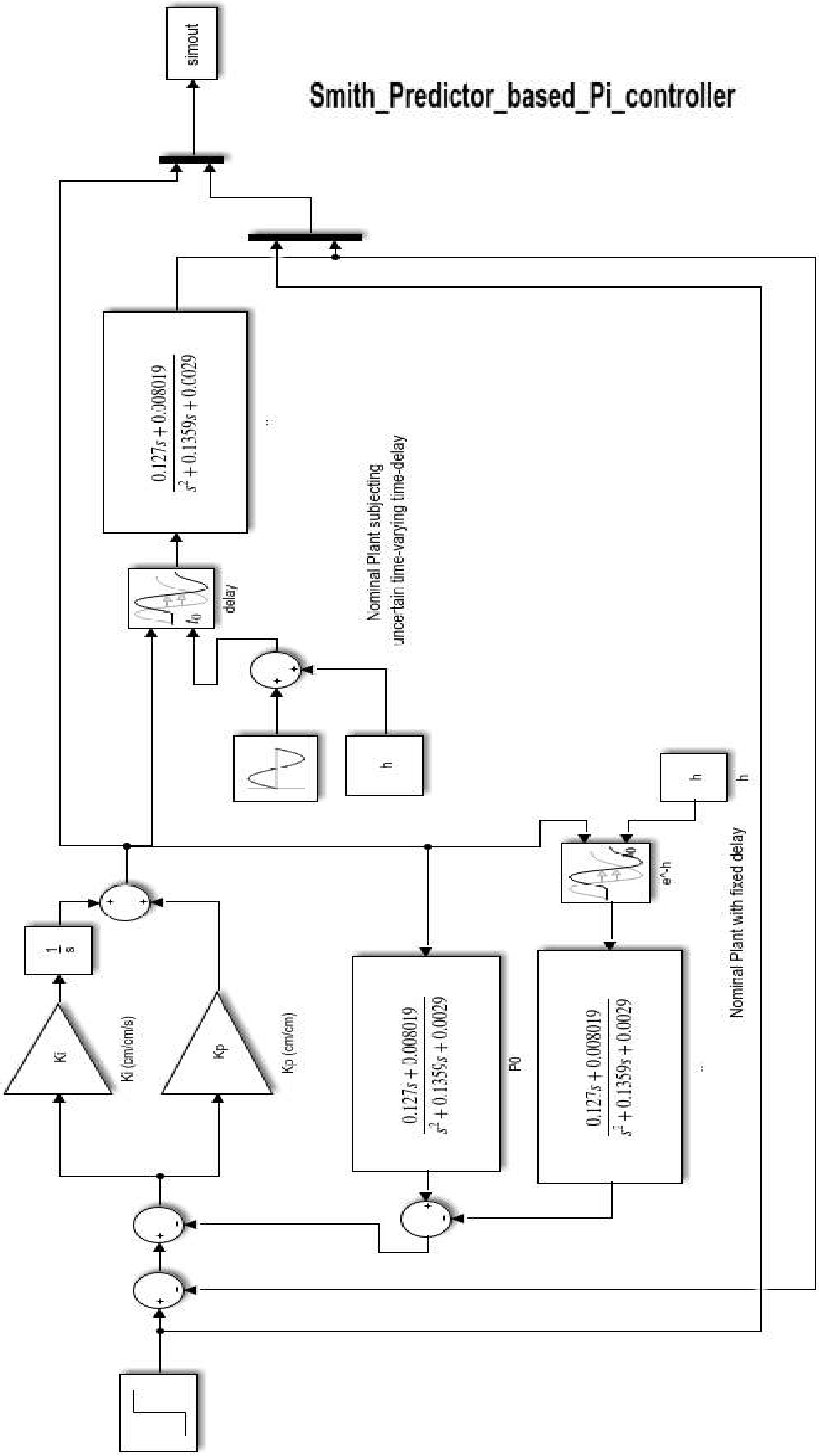
Smith_Predictor_based_Pi_controller
simout
Ki
Ki (cm/cm/s)
Kp
Kp (cm/cm)
1/s
0.127s + 0.008019 / s^2 + 0.1359s + 0.0029
delay
h
Nominal Plant subjecting uncertain time-varying time-delay
P0
e^-h
Nominal Plant with fixed delay

Code 4.4

```
%tau(t)=h+a+b*sin(freq*t)

Kp=0.56;
Ki=0.037;

h=12;
a=0 ;
b=10;
freq=400;

Tf=500;                        % the period of simulation
sim('Smith_Predictor_based_PI_controller',Tf);
Yout=simout.signals.values;    % a code which import the results from Simullink
t=simout.time;
uc=Yout(:,1);                  % The control signal
y=Yout(:,3);                   % The Level signal

figure(1)
plot(t,uc);
set(gca,'FontName','Helvetica','FontSize',15,'FontWeight','Bold')
xlabel('time (t)','FontName','Helvetica','FontSize',18,'FontWeight','Bold');
ylabel('Control Output u(t)','FontName','Helvetica','FontSize',18,'FontWeight','Bold');
grid on
saveas(gcf,['control_P0tau' num2str(k)],'png');

figure(2)
plot(t,y);
set(gca,'FontName','Helvetica','FontSize',15,'FontWeight','Bold')
xlabel('time (t)','FontName','Helvetica','FontSize',18,'FontWeight','Bold');
ylabel('Plant output y(t)','FontName','Helvetica','FontSize',18,'FontWeight','Bold');
grid on
saveas(gcf,['Lvel_P0tau' num2str(k)],'png');
```

Code 4.5

```
clear all
close all

Kpm = [];
Kim = [];
h=50;
Kp=0.7;

while Kp>=0
    Ki=0;
    Kimm=[0];

    while Ki>=0 && Ki<0.7

      Fun=@(s)((s.^2 + 0.1359*s + 0.0029).*s+...
    exp(-h*s).*(0.127*s + 0.0080109).*(Kp*s+Ki));
    [R Y]=QPmR(2*[-1 1 -1 1],Fun,-1,-1,0);

  if( max(real(Y.zeros))<= 0 )
            Kimm=[Kimm Ki];
            Ki=Ki+0.007;
        else
            Ki=-1;
        end
    end
    Kim=[Kim max(Kimm)];
    Kp=Kp-0.007
end
Kpint=[0.7:-0.007:0.007];
plot(Kpint,Kim)
xlabel('Kp')
title(['h=50'])
ylabel('Ki')
```

Code 4.6

```
%tau(t)=h+a+b*sin(freq*t)

Kp=0.25;   Ki=0.0053;

h=30;
a=0 ;
b=10;
freq=2*pi/400;

Tf=500;
sim('Delay_based_PI_controller_linear_plant',Tf);

Yout=simout.signals.values;
t=simout.time;
uc=Yout(:,1);
y=Yout(:,3);

figure(1)
plot(t,y);
set(gca,'FontName','Helvetica','FontSize',13,'FontWeight','Bold')
xlabel('time (t)','FontName','Helvetica','FontSize',14,'FontWeight','Bold');
ylabel('Level output','FontName','Helvetica','FontSize',14,'FontWeight','Bold');
grid on
saveas(gcf,['Lvel_hs' num2str(1)],'png');

figure(2)
plot(t,uc);
set(gca,'FontName','Helvetica','FontSize',14,'FontWeight','Bold')
xlabel('time (t)','FontName','Helvetica','FontSize',18,'FontWeight','Bold');
ylabel('Control Output','FontName','Helvetica','FontSize',18,'FontWeight','Bold');
grid on
saveas(gcf,['control_hs' num2str(2)],'png');
```

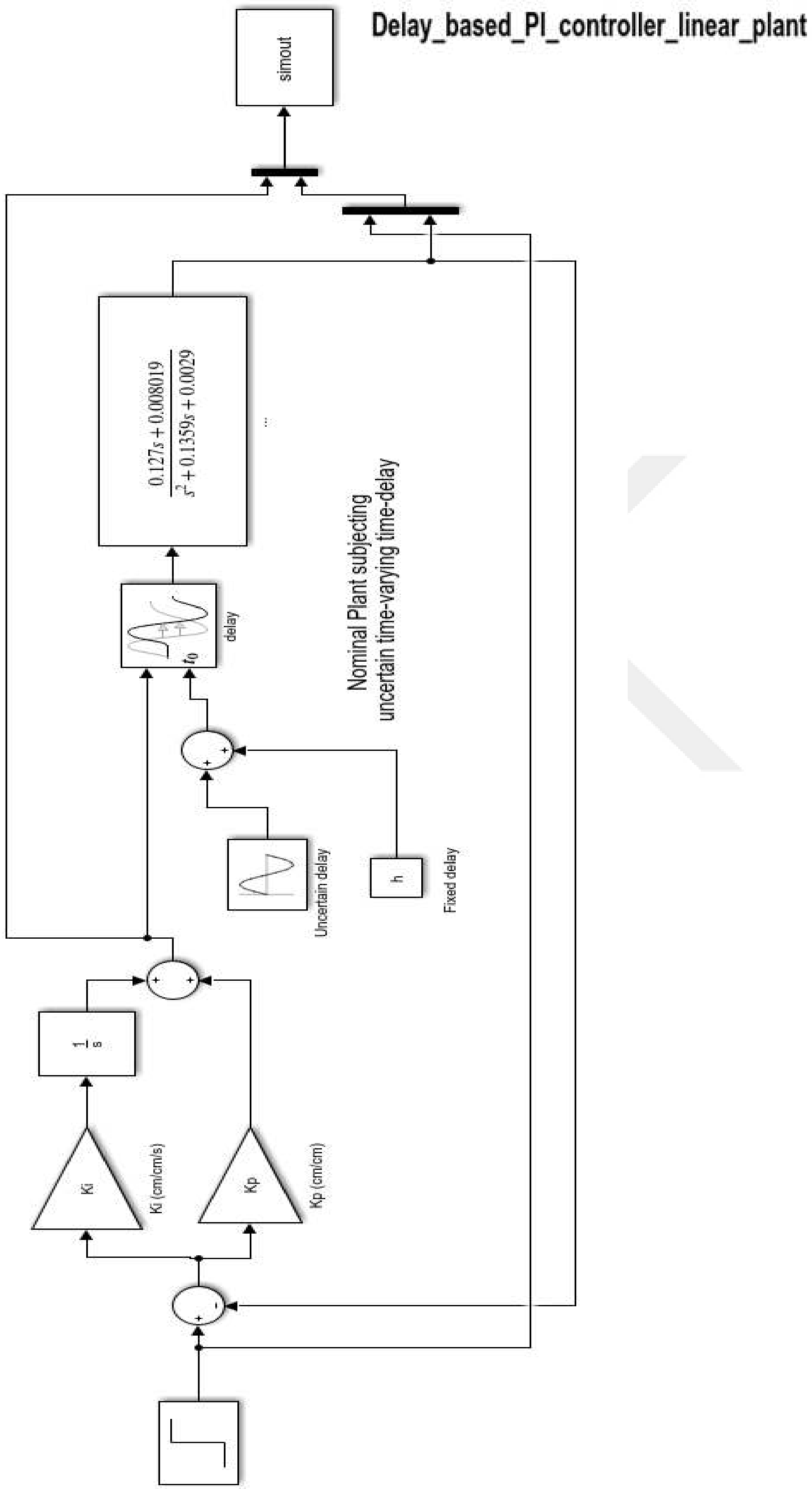
Delay_based_PI_controller_linear_plant
simout
$\frac{0.127s + 0.008019}{s^2 + 0.1359s + 0.0029}$
Nominal Plant subjecting
uncertain time-varying time-delay
delay
Uncertain delay
h
Fixed delay
$\frac{1}{s}$
Ki
Ki (cm/cm/s)
Kp
Kp (cm/cm)

Code 4.7

```
clear all
clc

Kpm = [];
Kim = [];
beta = 0.3;
segma = 1;
c = 1/(sqrt(2)*segma);
a = sqrt((1-beta)/2);
b=2;

h=10;
Kp=1.1;
while Kp>=0
    Ki=0;
    Kimm=[0];

    while Ki>=0 && Ki<0.08
        M = mynorm(a,b,c,Kp,Ki,h); % the condition through mynorm function

        if M < 1
            Kimm=[Kimm Ki];
            Ki=Ki+1e-3;
        else
            Ki=-1;
        end
    end
    Kim=[Kim max(Kimm)];
    Kp=Kp-1e-3
end
Kpint=[1.1:-1e-3:0];
plot(Kpint,Kim)
xlabel('Kp')
title(['h=10 sigama= 1 Beta = 0.3'])
ylabel('Ki')
```

Code 4.8

```
%tau(t)=h+a+b*sin(freq*t)

Kp=0.56;   Ki=0.037;   % For SP based PI controller

h=10;
a=1 ;
b=0;
freq=2*pi/1;

Tf=500;
sim('Smith_Predictor_based_Pi_controller_actual_plant',Tf);

Yout=simout.signals.values;
t=simout.time;
uc=Yout(:,1);
y=Yout(:,3);

figure(1)
plot(t,y);
set(gca,'FontName','Helvetica','FontSize',13,'FontWeight','Bold')
xlabel('time (t)','FontName','Helvetica','FontSize',14,'FontWeight','Bold');
ylabel('Level output','FontName','Helvetica','FontSize',14,'FontWeight','Bold');
grid on
saveas(gcf,['Lvel_hs' num2str(k)],'png');

figure(2)
plot(t,uc);
set(gca,'FontName','Helvetica','FontSize',14,'FontWeight','Bold')
xlabel('time (t)','FontName','Helvetica','FontSize',18,'FontWeight','Bold');
ylabel('Control Output','FontName','Helvetica','FontSize',18,'FontWeight','Bold');
grid on
saveas(gcf,['control_hs' num2str(k)],'png');
```

Smith_Predictor_based_Pi_controller_actual_plant

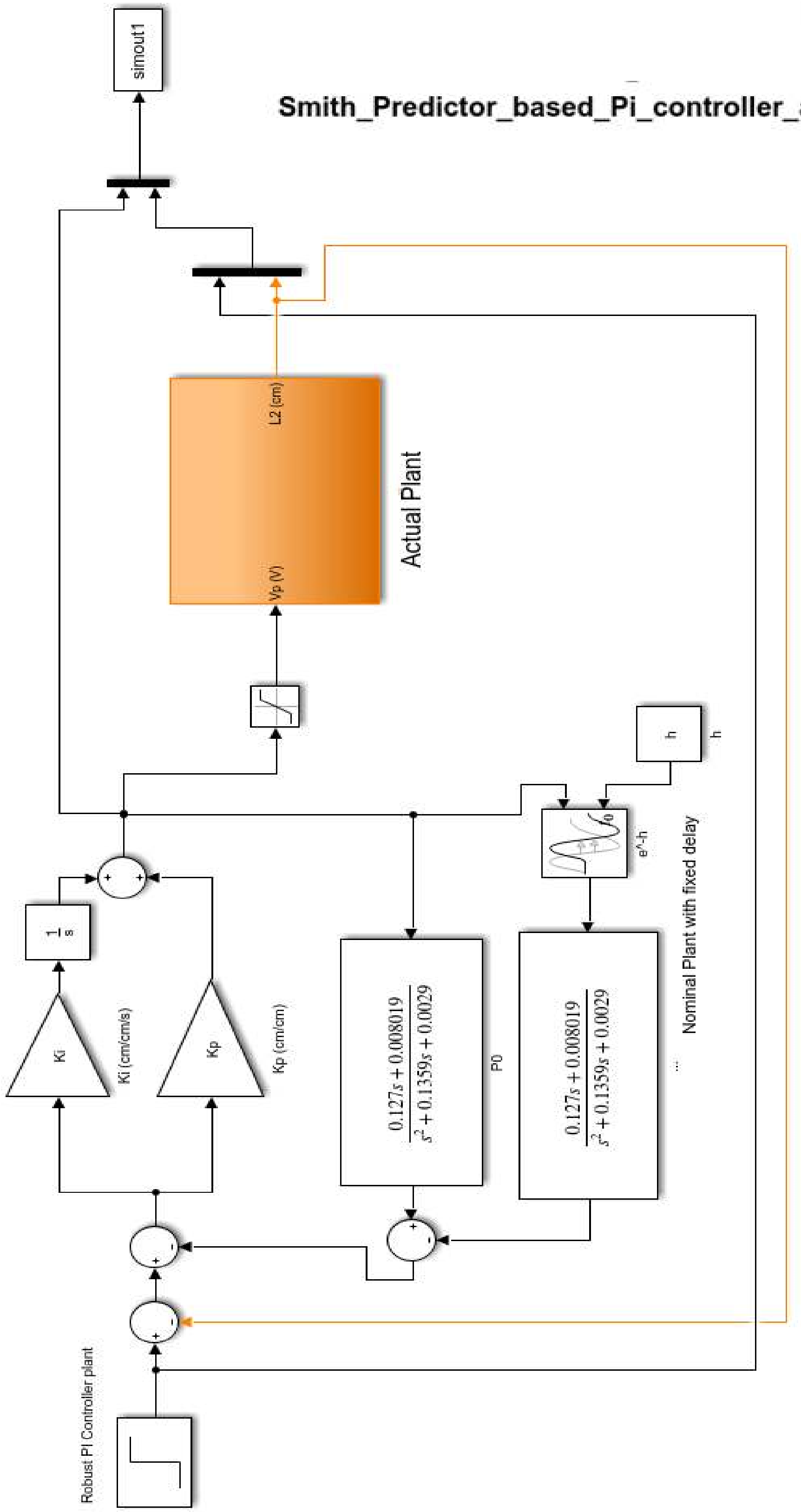

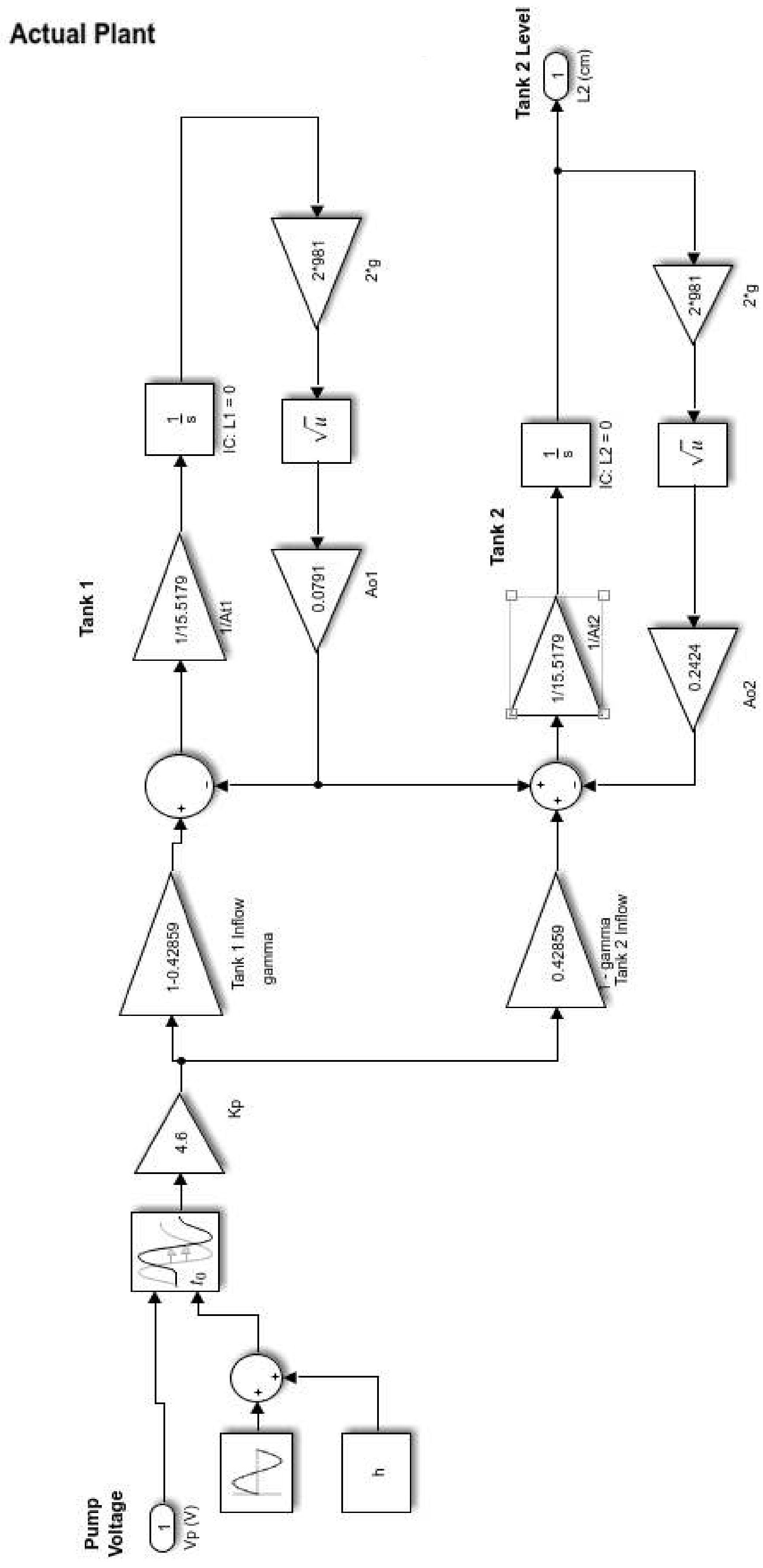
Actual Plant
Tank 1
Tank 2
Tank 2 Level
L2 (cm)
1
1/s
IC: L1 = 0
IC: L2 = 0
2*981
2*g
√u
0.0791
Ao1
1/15.5179
1/At1
1/At2
0.2424
Ao2
1-0.42859
Tank 1 Inflow
gamma
0.42859
1 - gamma
Tank 2 Inflow
4.6
Kp
h
Pump
Voltage
Vp (V)

Code 4.9

```
%tau(t)=h+a+b*sin(freq*t)

Kp=0.25;   Ki=0.0053;

h=10;
a=1 ;
b=0;
freq=2*pi/1;

Tf=500;
sim('Delay_based_PI_controller_actual_Plant',Tf);

Yout=simout.signals.values;
t=simout.time;
uc=Yout(:,1);
y=Yout(:,3);

figure(1)
plot(t,y);
set(gca,'FontName','Helvetica','FontSize',13,'FontWeight','Bold')
xlabel('time (t)','FontName','Helvetica','FontSize',14,'FontWeight','Bold');
ylabel('Level output','FontName','Helvetica','FontSize',14,'FontWeight','Bold');
grid on
saveas(gcf,['Lvel_hs' num2str(k)],'png');

figure(2)
plot(t,uc);
set(gca,'FontName','Helvetica','FontSize',14,'FontWeight','Bold')
xlabel('time (t)','FontName','Helvetica','FontSize',18,'FontWeight','Bold');
ylabel('Control Output','FontName','Helvetica','FontSize',18,'FontWeight','Bold');
grid on
saveas(gcf,['control_hs' num2str(k)],'png');
```

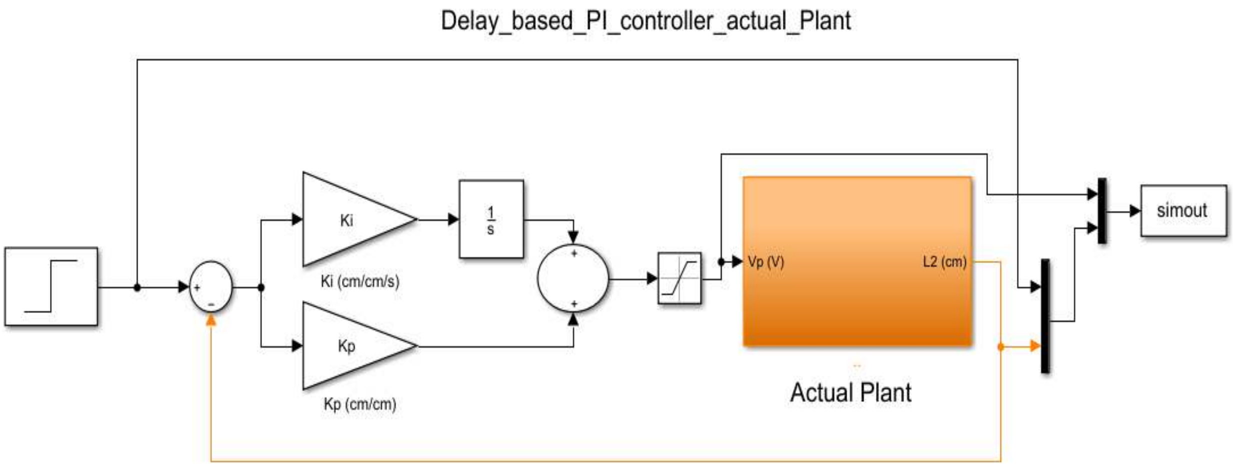

Code 4.10

```
%tau(t)=h+a+b*sin(freq*t)

Kp=0.29;    Ki=0.0061;

h=10;
a=1 ;
b=0;
freq=2*pi/1;

Tf=500;
sim('Robust_PI_controller_actual_Plant',Tf);

Yout=simout.signals.values;
t=simout.time;
uc=Yout(:,1);
y=Yout(:,3);

figure(1)
plot(t,y);
set(gca,'FontName','Helvetica','FontSize',13,'FontWeight','Bold')
xlabel('time (t)','FontName','Helvetica','FontSize',14,'FontWeight','Bold');
ylabel('Level output','FontName','Helvetica','FontSize',14,'FontWeight','Bold');
grid on
saveas(gcf,['Lvel_hs' num2str(k)],'png');

figure(2)
plot(t,uc);
set(gca,'FontName','Helvetica','FontSize',14,'FontWeight','Bold')
xlabel('time (t)','FontName','Helvetica','FontSize',18,'FontWeight','Bold');
ylabel('Control Output','FontName','Helvetica','FontSize',18,'FontWeight','Bold');
grid on
saveas(gcf,['control_hs' num2str(k)],'png');
```

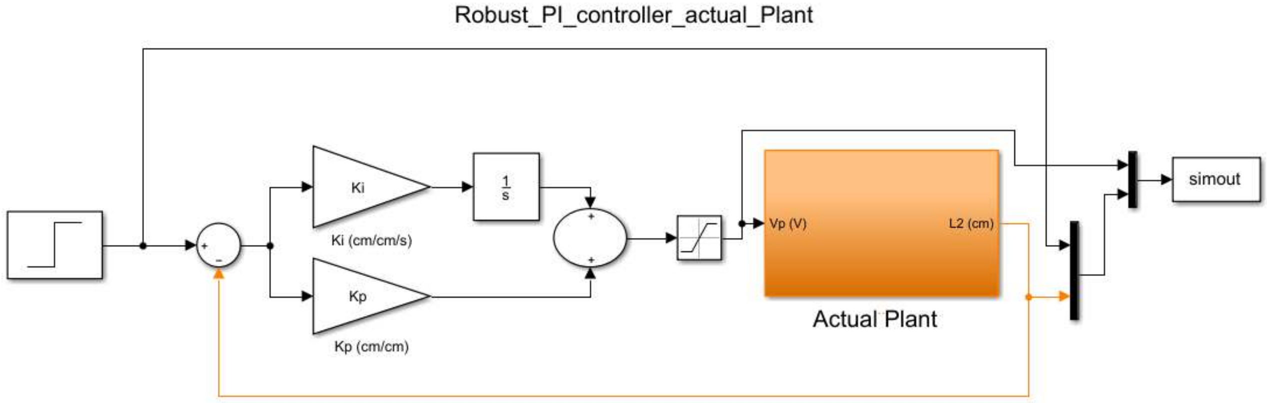

Code 4.11

```
%tau(t)=h+a+b*sin(freq*t)

Kp=0.56;   Ki=0.037;

h=10;
a=1 ;
b=0;
freq=2*pi/1;

Tf=500;
sim('Smith_Predictor_based_Pi_controller_linear_plant',Tf);

Yout=simout.signals.values;
t=simout.time;
uc=Yout(:,1);
y=Yout(:,3);

figure(1)
plot(t,y);
set(gca,'FontName','Helvetica','FontSize',13,'FontWeight','Bold')
xlabel('time (t)','FontName','Helvetica','FontSize',14,'FontWeight','Bold');
ylabel('Level output','FontName','Helvetica','FontSize',14,'FontWeight','Bold');
grid on
saveas(gcf,['Lvel_hs' num2str(1)],'png');

figure(2)
plot(t,uc);
set(gca,'FontName','Helvetica','FontSize',14,'FontWeight','Bold')
xlabel('time (t)','FontName','Helvetica','FontSize',18,'FontWeight','Bold');
ylabel('Control Output','FontName','Helvetica','FontSize',18,'FontWeight','Bold');
grid on
saveas(gcf,['control_hs' num2str(2)],'png');
```

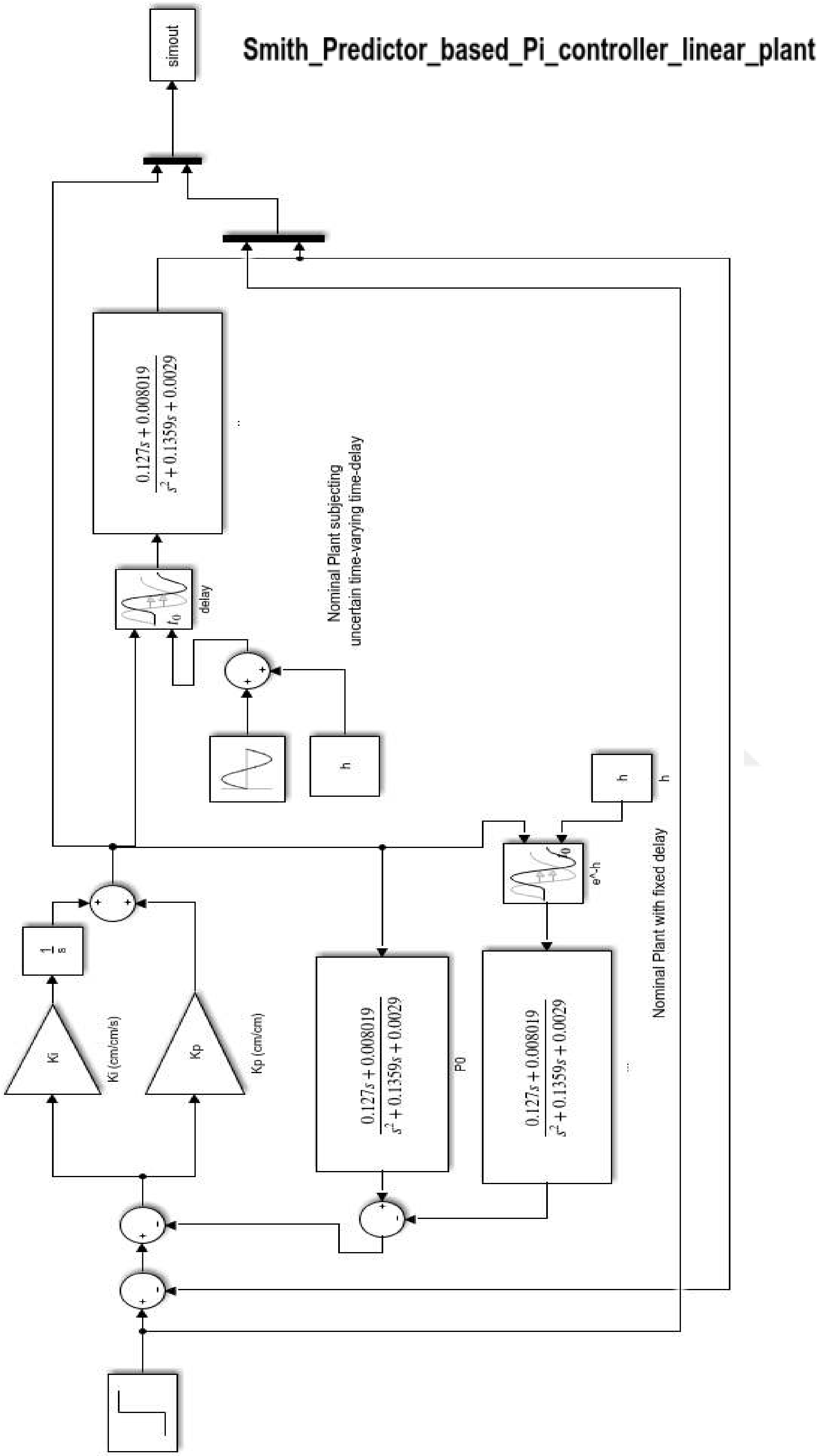
Smith_Predictor_based_Pi_controller_linear_plant
simout
0.127s + 0.008019 / s^2 + 0.1359s + 0.0029
delay
Nominal Plant subjecting uncertain time-varying time-delay
h
h
e^-h
Nominal Plant with fixed delay
1/s
Ki
Ki (cm/cm/s)
Kp
Kp (cm/cm)
P0

Code 4.12

```
%tau(t)=h+a+b*sin(freq*t)

Kp=0.25;   Ki=0.0053;

h=10;
a=1 ;
b=0;
freq=2*pi/1;

Tf=500;
sim('Delay_based_PI_controller_linear_plant',Tf);

Yout=simout.signals.values;
t=simout.time;
uc=Yout(:,1);
y=Yout(:,3);

figure(1)
plot(t,y);
set(gca,'FontName','Helvetica','FontSize',13,'FontWeight','Bold')
xlabel('time (t)','FontName','Helvetica','FontSize',14,'FontWeight','Bold');
ylabel('Level output','FontName','Helvetica','FontSize',14,'FontWeight','Bold');
grid on
saveas(gcf,['Lvel_hs' num2str(1)],'png');

figure(2)
plot(t,uc);
set(gca,'FontName','Helvetica','FontSize',14,'FontWeight','Bold')
xlabel('time (t)','FontName','Helvetica','FontSize',18,'FontWeight','Bold');
ylabel('Control Output','FontName','Helvetica','FontSize',18,'FontWeight','Bold');
grid on
saveas(gcf,['control_hs' num2str(2)],'png');
```

Delay_based_PI_controller_linear_plant

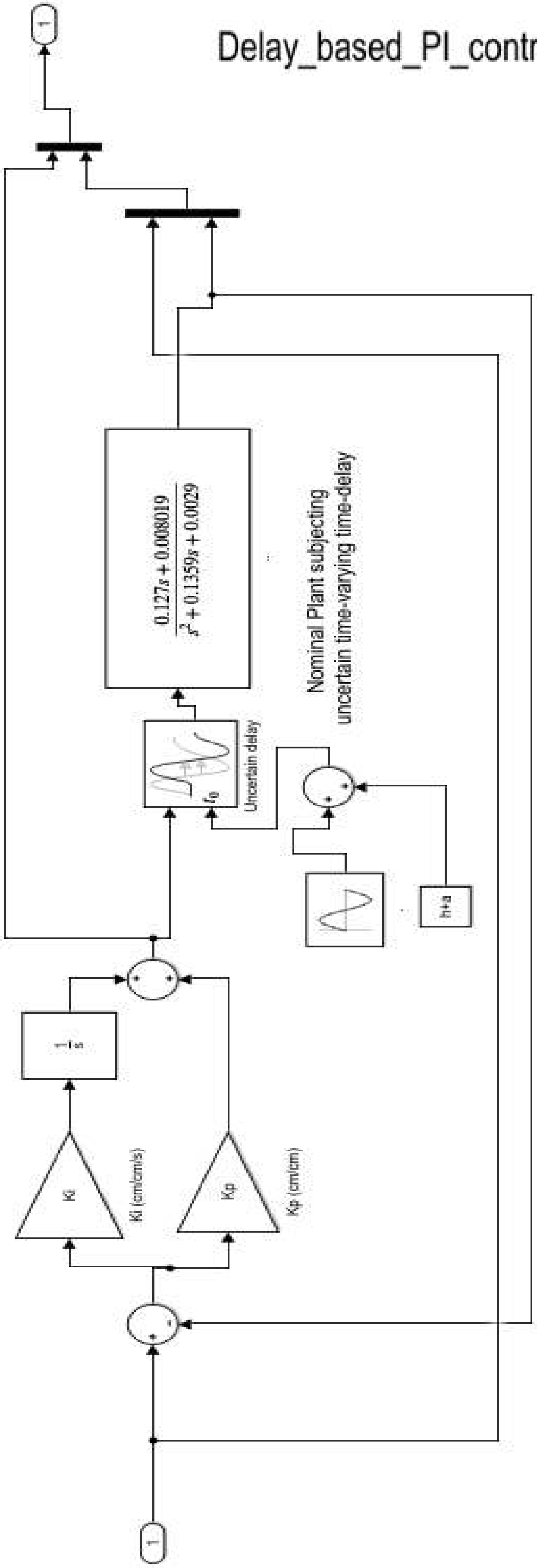

Code 4.13

```
%tau(t)=h+a+b*sin(freq*t)

Kp=0.29;   Ki=0.0061;

h=10;
a=1 ;
b=0;
freq=2*pi/1;

Tf=500;
sim('Robust_PI_controller_linear_plant',Tf);

Yout=simout.signals.values;
t=simout.time;
uc=Yout(:,1);
y=Yout(:,3);

figure(1)
plot(t,y);
set(gca,'FontName','Helvetica','FontSize',13,'FontWeight','Bold')
xlabel('time (t)','FontName','Helvetica','FontSize',14,'FontWeight','Bold');
ylabel('Level output','FontName','Helvetica','FontSize',14,'FontWeight','Bold');
grid on
saveas(gcf,['Lvel_hs' num2str(1)],'png');

figure(2)
plot(t,uc);
set(gca,'FontName','Helvetica','FontSize',14,'FontWeight','Bold')
xlabel('time (t)','FontName','Helvetica','FontSize',18,'FontWeight','Bold');
ylabel('Control Output','FontName','Helvetica','FontSize',18,'FontWeight','Bold');
grid on
saveas(gcf,['control_hs' num2str(2)],'png');
```

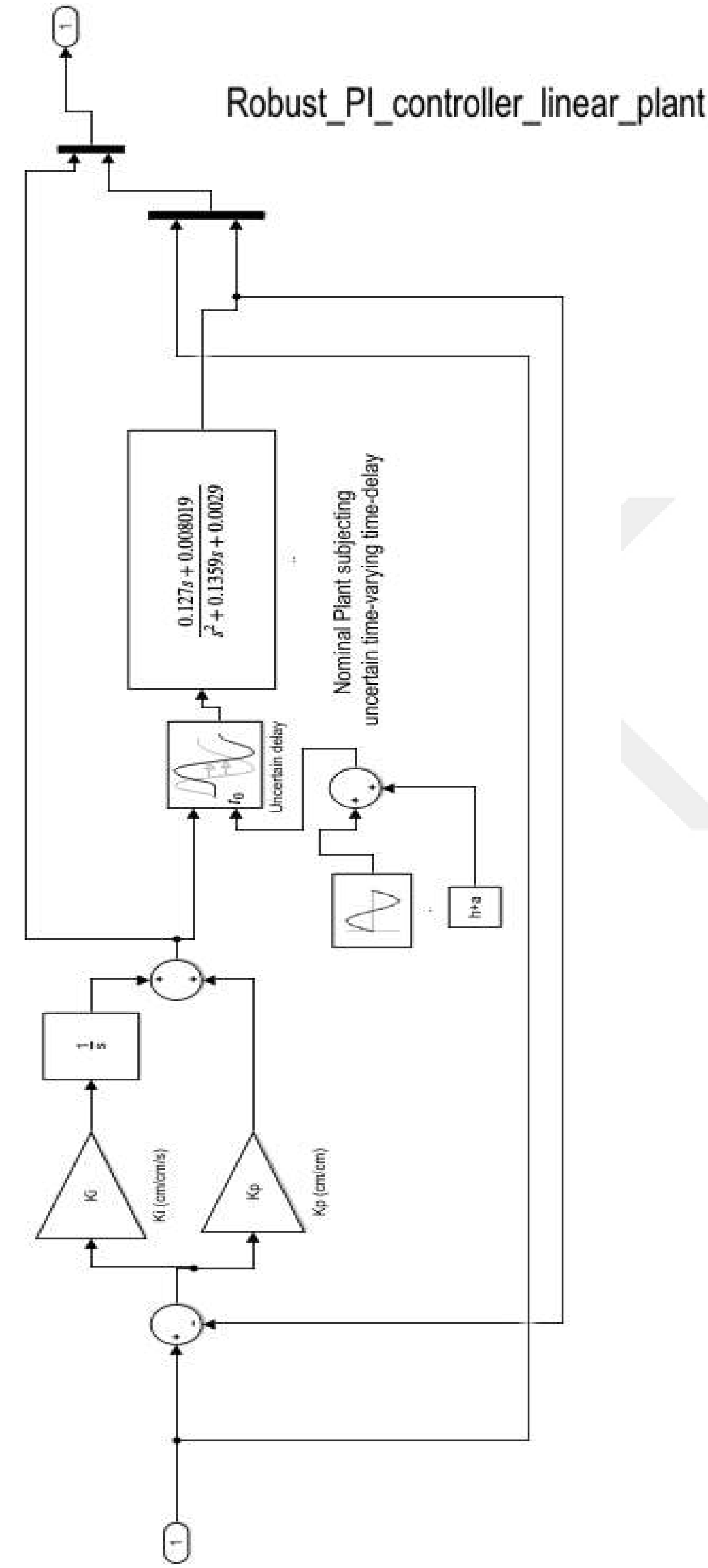

Robust_PI_controller_linear_plant
1
1
$\frac{0.127s + 0.008019}{s^2 + 0.1359s + 0.0029}$
Nominal Plant subjecting
uncertain time-varying time-delay
Uncertain delay
h+a
Ki
Ki (cm/cm/s)
Kp
Kp (cm/cm)